Elsevier Editorial System(tm) for Journal of Human Evolution

Manuscript Draft

Manuscript Number: HUMEV-E-17-00534R1

Title: Technological behaviour in the early Acheulean of EF-HR (Olduvai Gorge, Tanzania)

Article Type: SI: Oldowan-Acheulean

Keywords: Large cutting tools; handaxes; Acheulean origins; knapping skill; mental templates; lithic reduction sequences

Corresponding Author: Professor Ignacio de la Torre, PhD

Corresponding Author's Institution: University College London

First Author: Ignacio de la Torre, PhD

Order of Authors: Ignacio de la Torre, PhD; Rafael Mora

Abstract: Technological strategies of early humans are discussed in the light of a recently excavated stone tool assemblage from EF-HR, an archaeological site older than 1.33 Ma at Olduvai Gorge, Tanzania. Renewed fieldwork at EF-HR has unearthed a lithic collection containing over 2300 artefacts (including a hundred handaxes in stratigraphic position), which represents one of the largest assemblages for the early Acheulean in East Africa. Our technological study shows co-occurrence of two distinctive reduction sequences in the same assemblage, one aimed at obtaining small flakes and the other focused on the production of large, thick, heavy flakes which were then used as blanks for handaxe shaping. Flaking of small cores is expedient and low intensity, and knapping methods are similar to those observed in earlier Oldowan assemblages. Large cutting tools (LCTs)show no evidence of planform and biconvex symmetry, and shaping sequences are brief and discontinuous, indicating short use-lives for handaxes. Bifaces are rare and atypical. Recurrent morphotypes are knives, which are poorly-shaped, scraper-like, large-sized handaxes. Despite the apparent expediency of EF-HR handaxe production, a closer inspection of the interplay between debitage and façonnage stages reveals remarkably standardized procedural patterns. LCT blanks were produced following fixed knapping rules resulting in flakes with a specific morphology and mass distribution. Adapted to the idiosyncrasies of each blank, shaping was almost invariably imposed over the same areas in all LCTs, and sought to produce morphotypes that, technologically, are remarkably identical to each other. This strongly supports the existence of mental templates and technical rules that were systematically practiced in LCT production at EF-HR, and underscore the structured nature of technological behaviour at the onset of the Acheulean in East Africa.

Technological behaviour in the early Acheulean of EF-HR (Olduvai Gorge, Tanzania)

Ignacio de la Torre[1*] & Rafael Mora[2]

[1] Institute of Archaeology, University College London, 31-34 Gordon Square, WC1H 0PY London, United Kingdom

[2] Centre d'Estudis del Patrimoni Arqueologic de la Prehistoria, Facultat de Lletres, Universitat Autonoma de Barcelona, 08193 Bellaterra, Spain

* Corresponding author: i.torre@ucl.ac.uk

Abstract

Technological strategies of early humans are discussed in the light of a recently excavated stone tool assemblage from EF-HR, an archaeological site older than 1.33 Ma at Olduvai Gorge, Tanzania. Renewed fieldwork at EF-HR has unearthed a lithic collection containing over 2300 artefacts (including a hundred handaxes in stratigraphic position), which represents one of the largest assemblages for the early Acheulean in East Africa. Our technological study shows co-occurrence of two distinctive reduction sequences in the same assemblage, one aimed at obtaining small flakes and the other focused on the production of large, thick, heavy flakes which were then used as blanks for handaxe shaping. Flaking of small cores is expedient and low intensity, and knapping methods are similar to those observed in earlier Oldowan assemblages. Large cutting tools (LCTs) show no evidence of planform and biconvex symmetry, and shaping sequences are brief and discontinuous, indicating short use-lives for handaxes. Bifaces are rare and atypical. Recurrent morphotypes are knives, which are poorly-shaped, scraper-like, large-sized handaxes. Despite the apparent expediency of EF-HR handaxe production, a closer inspection of the interplay between debitage and façonnage stages reveals remarkably standardized procedural patterns. LCT blanks were produced following fixed knapping rules resulting in flakes with a specific morphology and mass distribution. Adapted to the idiosyncrasies of each blank, shaping was almost invariably imposed over the same areas in all LCTs, and sought to produce morphotypes that, technologically, are remarkably identical to each other. This strongly supports the existence of mental templates and technical rules that were systematically practiced in LCT production at EF-HR, and underscore the structured nature of technological behaviour at the onset of the Acheulean in East Africa.

Keywords: Large cutting tools; handaxes; Acheulean origins; knapping skill; mental templates; lithic reduction sequences

Introduction

The earliest handaxes are currently dated at ca. 1.76-1.74 Ma in West Turkana (Lepre et al., 2011) and Konso (Beyene et al., 2013). Slightly younger sites are found in Gona (Quade et al., 2008) and Olduvai (Diez-Martin et al., 2015), indicating the rapid spread of the Acheulean across East Africa. Although paleo-ecological factors and evolutionary implications of the Oldowan-Acheulean transition still need to be elucidated, stone tool assemblages suggest that important behavioural and cognitive changes were associated with the emergence of the Acheulean (see a discussion in de la Torre, 2016), and thus technological studies are crucial in order to understand this transition.

A pivotal assemblage in the characterization of the early Acheulean in Africa is the Evelyn Fuchs - Hans Reck (EF-HR) site (Olduvai Gorge, Tanzania), originally excavated by Mary Leakey (1971) in the 1960s. This assemblage became the main point of reference for all subsequent discussions on the origins of the Acheulean (e.g., Gowlett, 1979; Isaac, 1982) for two reasons. First, Leakey (1971) considered EF-HR to be the earliest handaxe-bearing site at Olduvai, and thus by default it became the world's first Acheulean site until older sites in Kenya and Ethiopia were discovered in the 1990s. Second, the assemblage excavated by Leakey contained a considerable number of handaxes, which enabled researchers to elaborate on comparisons between the Oldowan and the Acheulean (Stiles, 1977; Bower, 1977; Ludwig, 1999; Kimura, 2002; de la Torre and Mora, 2005). Despite the emblematic character and historiographic weight of EF-HR, the paucity of contextual details and ageing of original data –collected by Leakey (1971) more than half a century ago– evidenced the need to retrieve fresh information from the site.

Between 2009 and 2013, the Olduvai Gorge Geochronology Archaeology Project (OGAP) resumed fieldwork at EF-HR, which had not been conducted at the site since Leakey's original excavations. Renewed fieldwork has provided relevant information on the archaeo-stratigraphy and zooarchaeology (de la Torre et al., submitted), palaeontology (Bibi et al., submitted; Prassack et al., submitted), chrono-stratigraphy (McHenry, submitted), sedimentology (Stanistreet et al., submitted) and site formation processes (de la Torre and Wehr, submitted) of the assemblage. New tuff geochemical and stratigraphic correlations indicate that EF-HR sits above Tuff IIC, instead of below (McHenry, submitted; de la Torre et al., submitted). This locates the site in Upper Bed II, rather than Middle Bed II, and therefore EF-HR is younger than previously thought, with an age somewhere in between 1.66 and 1.33 Ma (see McHenry, submitted). Fieldwork by OGAP has also demonstrated that the EF-HR assemblage underwent post-depositional disturbance (de la Torre and Wehr, submitted), and therefore the original consideration of EF-HR as a living floor (Leakey, 1971) should be reconsidered.

In addition, OGAP excavations unearthed a large stone tool assemblage in mint condition and with abundant handaxes in stratigraphic position, representing one of the highest density concentrations of Acheulean artefacts > 1.3 Ma anywhere in East Africa. The large size of the new stone tool assemblage, variety of lithic categories preserved at the site, and high number of handaxes, enables a comprehensive picture of technological strategies at the onset of the Acheulean at Olduvai to be presented. Such is the overarching aim of this paper, whose specific research questions include: to explain stone artefact variability within the same assemblage in the light of differences in reduction sequences and raw material procurement;

evaluate knapping and cognitive skill levels shown by EF-HR handaxes, and assess mental templates involved in their production; compare Oldowan and Acheulean skill and overall productivity using EF-HR as a prime case study for early Acheulean technologies; to discuss EF-HR in the context of the early Acheulean record and the Oldowan/Acheulean transition at Olduvai Gorge.

Materials and methods

Materials

This paper presents the stone tool assemblage collected by OGAP during fieldwork in the EF-HR locality and nearby outcrops (de la Torre et al., submitted). OGAP fieldwork involved excavations in the main site –previously dug by Mary Leakey (1971) and named here as T2-Main Trench–, and 11 additional test trenches across the EF-HR paleo-landscape, which cover an area of nearly 1 km^2 (de la Torre et al., submitted) (Fig. 1). Archaeological material was found in two stratigraphic positions, Interval I and Interval 2. The main assemblage is in Interval 1 and includes fossil remains and stone tools associated with an incision surface on a claystone unit, which can be traced laterally across all trenches. With the exception of one trench (T16), all trenches yielded stone tools in Interval 1. The Interval 2 assemblage, which is slightly higher up in the local EF-HR sequence, is significantly smaller, and was documented only in some trenches in the main EF-HR locality (see details in de la Torre et al., submitted).

Taking into account only the stratified archaeological material (i.e., disregarding remains collected from outcrop surfaces), OGAP recovered 2317 stone tools during the EF-HR excavations. While the breakdown of artefacts per trench is presented elsewhere (de la Torre et al., submitted), here our analysis considers the entire assemblage in stratigraphic position. General accounts of the lithic collection include both Intervals, whereas presentation of specific technological results will focus on the main assemblage, which includes material from Interval 1 that is not severely abraded (n=2100). The discussion section will also consider the EF-HR artefacts excavated by Leakey (1971), from analyses conducted by de la Torre and Mora (2005, 2014).

Methods

All EF-HR artefacts were measured with callipers and weighed with 0.1 g-resolution scales. A diameter tape was used to measure cutting edges of flakes, flake fragments, retouched tools and handaxes. Length was measured along the major axis, rather than the technological axis. All stone tools were attributed to a raw material group following identification by McHenry and de la Torre (submitted). Refit analysis (de la Torre and Wehr, submitted) and detailed features of pounded artefacts (Arroyo and de la Torre, submitted) are presented elsewhere. Taphonomically-relevant features such as edge damage and artefact size distributions are also discussed separately (de la Torre and Wehr, submitted). The present study will report on the technological analysis, with an emphasis on the study of handaxe production.

Attribution of each artefact to a general technological group followed Isaac et al. (1997), and thus distinguished between detached, flaked and pounded tools. Artefact diversity observed in early Acheulean assemblages has led some (e.g., de la Torre, 2009, 2011; de la Torre and

Mora, 2005; de la Torre et al., 2008) to propose a separation between two reduction sequences, namely the chaînes opératoires of small debitage and Large Cutting Tool (LCT) production. Where possible, this division will be followed here, although a substantial part of the debitage lacks defining features thus preventing attribution to either reduction sequence.

Flake cortex follows Toth's (1982) types, technological attributes of flakes are based on Mora et al. (1991), and analysis of retouched tools follows a simplified version of Laplace (1972). Knapping schemes in free-hand core reduction consider the interaction between flaking surfaces, flaking angles and directionality of removals, as proposed by de la Torre et al. (2003), and expanded by de la Torre (2011) and de la Torre and Mora (submitted).

Attribute analysis of handaxes is summarized in Fig. 2, and draws upon proposals by Tixier (1956), Clark and Kleindienst (2001), McNabb et al. (2004), de la Torre (2011) and de la Torre and Mora (2005, 2014). Given the qualitative importance of Acheulean handaxes, the present study places great emphasis on a detailed account of individual features of representative LCTs. This draws upon recent attempts to create 'biographies' of handaxes (e.g., de la Torre et al., 2014; Bleed et al., 2017) where procedural patterns can be ascertained. Therefore, the following presentation pays considerable attention to imaging, and to the description of debitage and façonnage stages of handaxe production.

As a group of artefacts, debitage material is considered here as a synonym for detached pieces, and both terms are used interchangeably. In the LCT chaîne opératoire, debitage stage refers to the sequence of actions leading to the removal of a LCT blank, and the façonnage stage to the subsequent shaping of LCT blanks (and therefore the terms façonnage and shaping are also interchangeable). We follow Isaac's (1977) definition of LCT and use it as a synonym for handaxe (de la Torre, 2011); both terms are used without distinction (and without functional connotations) for those shaped objects generally larger than 10 cm (sensu Kleindienst, 1962). This aims to avoid including all handaxes within the general term of bifaces since, as shown below, bifacial pieces are not truly representative of EF-HR. Particular types of handaxes such as knives, cleavers, picks and bifaces follow definitions by Tixier (1956), Kleindienst (1962) and Isaac (1977).

Statistical comparisons of the EF-HR lithic assemblage include the Chi-squared, Levene's, Bartlett's, Kruskal Wallis', ANOVA and Student's *t* tests, and factorial and principal component analyses, of categorical variables and numerical data.

Results

Assemblage composition

The EF-HR assemblage excavated by OGAP includes 2317 stone tools in stratigraphic position, and weighs nearly 223 kg (Table 1) (Fig. 3). Lavas dominate numerically (*n*= 1245; 53.7%), followed closely by metamorphic rocks (*n*= 1047; 44%), whereas chert is only marginally (*n*= 25; 1.1%) represented (Table 2). Lava dominance is accentuated in terms of weight contribution (176 kg; 79%) in contrast to metamorphic artefacts (46.7 kg; 21%) (Table 3). Basalt is the most represented lava (*n*= 712; 85.8 kg), followed numerically by phonolite (*n*= 302) and trachyte-trachyandesite (T-Ta) (*n*= 229), and in weight by T-Ta (56

kg) and phonolite (34 kg) (Tables 2 and 3). The metamorphic stone tool assemblage is almost exclusively made of quartzite (*n*= 1020; 45.3 kg).

Detached pieces (*n*=1934; 83.5%) dominate the assemblage (Table 1) (Fig. 4a), with nearly equal frequencies of lava (*n*= 969) and metamorphic (*n*= 942) artefacts (Table 2). Flaked pieces (*n*= 333) contribute more than twice the weight of detached artefacts (~132 kg versus ~57 kg), and are dominated by cores (*n*= 144) and LCTs (*n*= 100) (Table 1). In contrast to detached artefacts, flaked pieces are heavily dominated by lava (*n*= 234; ~107 kg) over metamorphic (*n*= 97; ~24 kg) (Tables 2 and 3) (Fig. 4b). Pounded artefacts are less important numerically (*n*= 50) although they contribute substantially to the total weight of the assemblage (33.5 kg) (Table 1), and maintain the predominance of lava (*n*= 42; 29 kg) over metamorphic (*n*=8; 4 kg) rocks (Tables 2 and 3).

Chi-squared results (X^2 (56) = 445.5, $p< 0.0001$) indicate significant differences between technological categories per raw material. In particular, adjusted residuals (see Supplementary Online Material [SOM] S1) highlight the overabundance of quartzite and chert shatter <20 mm, phonolite cores, T-Ta LCTs and basalt flakes, in contrast to an underrepresentation of quartzite cores and flakes, and of basalt shatter <20 mm.

Interval 1 artefacts constitute the bulk of the EF-HR collection (*n*= 2153; 92.9%) numerically, and in their contribution to the overall weight (~217 kg; 97.3%) of the assemblage (Table 1). A small fraction (*n*= 53; 2.4%) of the Interval 1 artefacts are heavily rounded (see discussion in de la Torre and Wehr, submitted), and are not considered in the analysis of the main EF-HR assemblage from Table 4 and Fig. 4c onwards.

The Chi-squared test (X^2 (28) = 319.81, $p< 0.0001$) indicates an association between general raw materials and technological categories in the main assemblage. Adjusted residuals (SOM S2) confirm results of SOM S1, which are also supported by a factorial correspondence analysis (Fig. 4e), and which reiterates the lower-than-expected frequency of lava shatter, metamorphic cores and whole flakes. Statistical results also highlight comparatively higher proportions of lava LCTs and hammerstones, as opposed to proportionally higher frequencies of metamorphic retouched tools.

Table 4 shows that a minimum of 590 artefacts (28.1% of the main EF-HR assemblage) correspond to the chaîne opératoire of LCT production, whereas 415 stone tools (19.8%) can confidently be attributed to the small debitage reduction sequence. This does not take into account a large part of the EF-HR main assemblage (*n*= 1095), and may explain the apparent overrepresentation of LCT production flakes when compared to small debitage flakes (see Fig. 4c); while large flakes can be attributed unambiguously to LCT production, many small flakes may derive from either chaîne opératoire, thus biasing flake counts against the small debitage assemblage. In terms of weight (Table 5), the LCT production assemblage (~111 kg) is significantly more relevant (51.9%) than small debitage (64 kg; 29.8%) or indeterminable (18.3%; 39 kg) artefacts. Small debitage cores and LCTs contribute, by far, the greatest amount of kg to the main EF-HR assemblage (Fig. 4d).

The Chi-squared comparison of categories per chaîne opératoire in the main EF-HR assemblage indicates significant differences (X^2 (4) = 275.2, $p< 0.0001$). The highest scores of statistically significant adjusted residuals are due to the absence of cores in LCT production, and also underline the absence of LCTs in the small debitage reduction sequence

and overrepresentation of flake fragments in LCT production. While the lack of LCTs in the small debitage chaîne opératoire is a truism in itself, and the underrepresentation of small debitage flake fragments may again be due to identification bias (i.e., they may be contained within the indeterminable assemblage), the complete absence of LCT cores clearly reflects a technological pattern.

Raw material-chaîne opératoire patterning is also observed; Chi-squared results (X^2 (6) = 100.99, $p< 0.0001$) indicate significant differences in the distribution of lava, metamorphic and chert rocks in each reduction sequence. Adjusted residuals show statistically significant lower frequencies of lava small debitage, and of quartzite LCT production debitage. Chert is only present in the small debitage reduction sequence.

Debitage

The main EF-HR assemblage is dominated by detached pieces (n= 1739; 82.8%) (Table 4), although their weight contribution (54 kg) accounts for 25.1% of the collection only (Table 5). Shatter < 20 mm is not abundant (11.2%) and most probably indicates fluvial winnowing (see discussion in de la Torre and Wehr, submitted).

Flake fragments (42.8% of the total; see Table 4) predominate among detached pieces, and a sample (*n*=75) shows recognisable knapping accidents; split fractures (*n*=33) and step terminations (*n*=24) are documented, and some flake fragments from the LCT reduction sequence include both accidents. Siret (split) flakes are caused by an excess of striking force, whereas step fractures might result from insufficient force applied and/or too thick volumes in the flaking surface. Since flake splitting suggests the application of substantial striking force, it could be that these flake fragments are related to a stage of handaxe shaping where the thinning of thick volumes on the surfaces of LCT blanks was the priority, rather than the production of whole flakes.

Whole flake dimensions range from 16 to 1520 mm in length and 0.5 to 562 g in weight (Tables 6 and 7), with lava flakes usually larger and wider than metamorphic and (particularly) chert flakes (Fig. 5e). This dimensional pattern according to raw material is more clearly observed in small debitage flakes (Fig. 5a and Fig. 5c; Fig. 6a), whose length classes (Fig. 6b) show statistically significant differences (X^2 (8) = 18.27, $p< 0.0193$). Length and weight differences per raw material in small and intermediate flakes of the LCT production sequence are negligible (Table 7) (Fig. 5b and 5d), and not statistically significant (X^2 (6) = 5.20, $p= 0.5174$).

Small debitage flakes (n=137; 1.7 kg) are usually slightly longer than wider (Fig. 7a), average 34 mm in length, and have a mean weight of ~13 g (Table 6). A clear preference for phonolite (n=48) and quartzite (n=47) is observed over all other rock types (e.g., basalt, T-Ta, chert, and others, which together amount to 42 whole flakes). Striking platforms are predominantly unifaceted (77.6%) (Table 8) (Fig. 6c), most dorsal surfaces preserve no cortex (53.5%), and there is a predominance of Type VI flakes (see values in Table 8) (Fig. 6d). Neither striking platforms (X^2 (6) = 7.38, $p= 0.2870$) nor dorsal surface cortex (X^2 (6) = 11.38, $p= 0.0773$) present statistically significant differences per raw material. In contrast, there is an association between raw material and Toth's types (X^2 (10) = 21.54, $p< 0.0176$), with adjusted residuals highlighting the proportional abundance of Type I chert flakes and Type VI metamorphic flakes, as opposed to an underrepresentation of Type VI lava flakes.

Most small debitage flakes derive from freehand exploitation of core surfaces (84.7%), whilst a smaller sample (n=10.2%) are *éclats débordants* from core edges and could potentially correspond to rejuvenation processes. A small proportion (5.1%) of bipolar flakes, exclusively in quartzite, are documented (Table 8).

Flakes attributed to LCT production have similar proportions of unifaceted butts as small debitage flakes (74.1%) but higher percentages of bifaceted and multifaceted butts (see Table 8). Differences between the two chaînes opératoires are statistically significant (X^2 (3) = 9.52, p<0.0213). The proportion of cortex-free dorsal surfaces of LCT production flakes is also higher (64.4%) than on small debitage flakes, but overall differences are not statistically significant (X^2 (3) = 6.99, p= 0.0721). The same pattern is observed in the distribution of Toth's flake types –with a higher overall proportion of non-cortical flakes in the LCT production reduction sequence (Table 8)– which again is not statistically significant (X^2 (5) = 9.41, p= 0.0936). 4.8% of flakes are *éclats débordants* that therefore modify the outline of at least two edges of LCT cores or LCT blanks. No bipolar knapping is observed among LCT production flakes (Table 8). Whole flakes associated with LCT production are separated into three groups – small, intermediate and large (potential LCT blank) flakes.

Small flakes (n= 131; 4.9 kg) are shorter and wider than those from the small debitage chaîne opératoire (see Fig. 7a versus 7b), and have a mean length of 57 mm and weight of 37 g (Table 7) (Fig. 5b and 5d). Whilst small debitage flakes are mostly of phonolite and quartzite (see above), LCT production small flakes are largely dominated by T-Ta (n= 84), followed at a distance by basalt (n=20) and quartzite (n=19); phonolite small flakes are rare (n= 6). Small flakes from LCT production usually have wide butts running across the entire proximal side of the flake, and show an obtuse angle between the striking platform and the ventral face (Fig. 7b). All these features relate small flakes to the shaping/ retouching of LCT edges (Fig. 7e); their short, wide morphology indicates that such flakes were aimed at modified edges –rather than the central volume of LCTs–, and butt thickness and their obtuse angles suggest deep indentation in LCT edges. Some small flakes show evidence of previous scars on their dorsal surfaces, whereas others have none (see examples of both in Fig. 7b). Small flakes with previous removals are clearly associated with dorsal shaping of LCTs made on flake blanks (Fig. 7c). The positioning of those flakes without previous scars is less precise; some might derive from large dorsal scars on LCTs and thus do not remove any ridges, whereas others are Kombewa flakes from the ventral shaping of LCT flake blanks (Fig. 7d) (see extended discussion by Dag and Goren-Inbar, 2001). Overall, the techno-morphological features of these LCT production small flakes indicate that their role was the modification of handaxe edges –rather than their volume–, which is consistent with the "denticulate sidescraper" retouch observed on most knives (see below).

Intermediate flakes (n= 67; 11.6 kg) are on average 95 mm long and weigh 173 g, may be either elongated or wide (Fig. 8a), but are consistently thin (27 mm) (Table 7). As with small flakes from LCT production, T-Ta predominates (n= 35), followed by quartzite (n= 17) and basalt (n= 10), whereas intermediate phonolite flakes are scarce (n= 5). Whilst butt features unambiguously associate LCT production small flakes with shaping (or rather retouching) of handaxe blanks (see discussion in previous paragraph), intermediate flakes may belong either to core preparation (i.e., before removal of LCT blanks) or LCT shaping (which in this case would be aimed at volume thinning through elongated, invasive removals). Intermediate flakes from core preparation include edge-core flakes and flakes with thick butts. Features of

edge-core flakes are consistent with flaking patterns preserved in LCTs from the debitage stage (e.g., Fig. 8b; SOM S3), and were geared towards rejuvenating flaking platforms and knapping surfaces. Flakes with thick (and often prepared) striking platforms – which due to that thickness are unlikely to be removed from LCT blanks but rather from the original cores– served to prepare core convexities prior to the removal of LCT blanks. The attribution of intermediate flakes to the thinning of LCT blanks is less straightforward, as most of their features can be found also on flakes produced during core preparation. Furthermore, the majority of LCTs at EF-HR show little or no thinning, and thus it is expected that only a few intermediate flakes would correspond to such a process.

Large flakes (i.e., potential LCT blanks) are scarce (n= 12), but form a relevant group in terms of raw material investment (4.7 kg). Raw material patterns follow small and intermediate flakes in dominance of T-Ta (n= 6) and quartzite (n=4), although in this instance there are no basalt blanks, but phonolite (n=2) is represented. Averaging 122 mm in length and 398 g in weight (Table 7), these large unretouched flakes are within the range of LCT variation (Fig. 5b and 5d), have thick volumes making them suitable blanks for LCT shaping (Fig. 8c and 8d) and, in some instances (e.g., Fig. 8e), could be considered as LCTs despite the absence of any secondary retouch (see also SOM S4).

Cores

All cores (n= 130; ~58 kg) documented in the EF-HR main assemblage are associated with the small debitage chaîne opératoire. As discussed above, phonolite cores are proportionally overrepresented, whereas the frequency of quartzite cores is lower than expected (see counts in Table 2). As a whole, lava cores (n= 101; ~50 kg) are far more abundant than metamorphic (n= 28; 7.5 kg) cores (77.7% versus 21.5%), while chert is only nominally (n= 1) represented (see Tables 3 and 4). With an average length of 81 mm and weight of 448 g, there is considerable variation in core dimensions (Table 6) (Fig. 5a and 5g), particularly in lava cores (Fig. 5c). Statistically significant differences exist per raw material (X^2 (6) = 22.68, p<0.0009), with quartzite cores consistently smaller than lava cores. 69.2% of all cores range between 60 and 99 mm in length (Table 9) and despite the large dimensions of some lava cores (see length and weight classes in Table 9), none bears evidence of LCT blank production (all scars overlap with the size of small debitage flakes).

Cortex is present on 85.5% of cores, and dominant on 59.7% (Table 9). Most cores are on cobbles (79.4%) (see examples in Fig. 9), and there are statistically significant differences (X^2 (2) = 17.85, p<0.0001) between lava and metamorphic core blanks (see Table 9). Almost half the cores (49.2%) show signs of battering. Clustered impacts on the end opposite the flaked area (e.g., Fig. 9a) suggest a dual use of some cobbles as hammerstones and cores (see also Arroyo and de la Torre, submitted), whereas *esquillées* are indicative of bipolar flaking. A statistically significant association exists between raw material and presence/absence of battering (X^2 (2) = 11.42, p<0.0033), with overrepresentation of such traces on metamorphic cores (see also Table 9). 79.5% of cores have less than seven scars, and just 9.3% show evidence of more than nine removals (Table 9). No statistically significant association is found between raw material and number of removals (X^2 (3) = 5.90, p= 0.1161).

Overall, the prevalence of cortical surfaces and low number of removals show that small debitage cores were not intensively reduced. As seen mainly on phonolite cobble blanks, usually cores were only exploited (either unifacially or bifacially) at one end, leaving the

opposite cortical area intact, potentially as a handling area (see examples in Fig. 9 and SOM S5).

Flaking schemes (Table 9 and Fig. 10) support a model of low intensity reduction, with test cores (11.1%) only exceeded by BAP flaking schemes (Fig. 9a-d). Most other prevalent reduction schemes such as UAU1- UAU2 (SOM S6) and BSP (Fig. 9f) are also indicative of short flaking sequences, whereas structured methods (e.g., discoid) are almost absent in the assemblage (see Table 9). Freehand knapping methods predominate, although 9.5% of flaked pieces indicate bipolar technology (Table 9). There are statistically significant differences per raw material (X^2 (15) = 58.33, p<0.0001), with adjusted residuals pointing to overrepresentation of bipolar, UAUT, MLT and discoid metamorphic cores, and of BAP lava cores.

Pounded artefacts

In addition to cores with evidence of battering (previous section), the EF-HR main assemblage includes 50 pounded artefacts (Table 4), having a total weight of over 33 kg (Table 5). Pounded tools are mostly of lava (~26 kg versus ~4 kg of metamorphic rocks), with a predominance of T-Ta (~13 kg) and basalt (~10 kg), followed by phonolite (~6kg) (see also Table 3). Two large T-Ta hammerstones were probably associated with LCT production, as their size and weight are unlikely to have served for small debitage flaking. Generally, however, it was impossible to unambiguously link pounded tools with either of the two chaînes opératoires evident at EF-HR (Tables 4 and 5), as smaller hammerstones could have been used for both small debitage flaking and LCT shaping. Nonetheless, pitted stones are likely to be linked to bipolar flaking by serving as anvils (see discussion in Arroyo and de la Torre, submitted); as bipolar was identified only in the small debitage reduction sequence, potentially pitted stone artefacts could be attributed to that particular chaîne opératoire.

Pounded tools are dominated by knapping hammerstones (n=28) on rounded cobbles with smooth cortical surfaces showing concentrated pitting at the ends of the cobble (SOM S7). Other pounded artefacts in the EF-HR main assemblage include hammerstones with fracture angles (n=7) and hammerstones with active edges (n=3), which are unsuitable for flaking (see discussion in Mora and de la Torre, 2005), therefore suggesting that activities other than knapping also occurred at the site. Techno-typological and microscopic features of EF-HR battered tools are further discussed elsewhere (see Arroyo and de la Torre, submitted).

Retouched tools

Retouched artefacts other than LCTs are present in both the small debitage and LCT chaînes opératoires of the EF-HR main assemblage, in almost identical absolute frequencies (n= 25 and n= 24, respectively) (Table 4), although differing widely in their weight contribution (464 g versus 4.3 kg) (Table 5). Retouched tools attributed to the small debitage reduction sequence are on flakes, although blanks are slightly longer (37 mm) and heavier (19 g) than unretouched flakes from the same chaîne opératoire (Table 6).

As most retouched tools from the LCT production sequence are on intermediate-sized blanks, it is not surprising that they are consistently larger than those of the small debitage chaîne opératoire (Fig. 5h). Fig. 5h also shows that length/width proportions of small debitage retouched tools are more clustered than those of the LCT reduction sequence. With a mean length of ~93 mm, retouched tools fall in the range of variation of LCTs (Fig. 5b). However,

they are consistently thinner (average 29 mm) and, as a result, considerably lighter than LCTs (average 174 g; see details in Table 7), thus helping differentiate them from handaxes (Fig. 5d). As discussed above, there are statistically significant differences in the distribution of retouched tools per raw material, with a higher-than-expected frequency of metamorphic over lava artefacts (SOM S2), and a particular deficit of basalt retouched tools (SOM S1).

Denticulates and sidescrapers are present in similar percentages (47.5% and 42.5%, respectively), and tool type proportions are consistent per chaîne opératoire (see Table 10). Overall, retouch is non-systematic, affects limited parts of a single edge, is usually unifacial, non-invasive, and does not significantly alter the blank outline (Fig. 11). Some retouched tools of the LCT reduction sequence are on Siret flake blanks (e.g., Fig. 11d, Fig. 11i), with the split fracture opposite the retouched edge, and potentially acting as a handling area or 'backing'. The same 'backing' morphology opposite a retouched edge is also evident on retouched tools on block blanks (see Fig. 11h). Furthermore, the same pattern is consistently found on LCTs (below), therefore supporting an intentional design for this shaping template, and the techno-typological continuity between LCTs and smaller retouched artefacts.

Large Cutting Tools: attribute analysis

Numerically, LCTs (n= 100) are a relevant category in the EF-HR main assemblage, and in terms of overall weight (~56 kg) they are only exceeded by small debitage cores (Table 3) (Fig. 4d). Lava LCTs (n= 78; ~44 kg) are more common than quartzite (n= 22; ~12 kg), and dominated by basalt (n= 40; ~21 kg) and T-Ta (n= 31; ~19 kg) pieces, with only seven (~ 4kg) phonolite handaxes (Table 3 and Table 4). Most LCTs are between 120 and 160 mm long (average 142 mm) (Fig. 12a), are considerably thick (mean = 45 mm) and heavy (mean = 561g) (Table 7), and weigh between 400 and 800 g (Fig. 12b) (see also Table 11). Dimensions of lava and metamorphic LCTs are remarkably similar (Table 7) (Fig. 5b and 5d), with no statistically significant association between length patterns (Table 11) and raw material (X^2 (4) = 5.143, p= 0.2729).

Dorsal cortex is present on 67.7% of LCTs and in very similar proportions on both lava and metamorphic artefacts (Table 11). At least 90% of LCTs are on flakes, most of which (70%) are side-struck. LCTs were rarely made on cobble (4%) or block (2%) blanks (Table 11) (Fig. 12d). Of those handaxes made on flakes, 76.2% retain the butt, whereas 23.8% show evidence of intentional butt removal via thinning. Striking platforms are mostly unifaceted (36.9%), and prepared butts (bifaceted and multifaceted) are more common than cortical ones (see values in Table 11) (Fig. 12e). A statistically significant association exists between raw materials and type of butt (X^2 (4) = 12.54, p< 0.0137), with the adjusted residuals indicating significance in two associations (i.e., an underrepresentation of thinned butts and proportional abundance of cortical butts on metamorphic flake blanks). Removals attributed to the debitage stage –i.e., those occurring during core flaking before LCT blanks were obtained, and which are preserved on the dorsal side of LCTs– range mostly between 1 to 3 (63.3%) (Table 11) (Fig. 12f). There is a statistically significant association per raw material (X^2 (2) = 7.21, p< 0.0271), where metamorphic handaxes with 1-3 dorsal removals are overrepresented, and have lower-than- expected frequencies of more elaborated patterns.

Façonnage is mainly unifacial (70.2%), with just 27.3% of LCTs showing bifacial shaping (Table 11) (Fig. 12g). No statistical differences exist per raw material (X^2 (2) = 0.58, p= 0.7454). 78.7% of LCTs have four or more shaping removals, most (58.5%) having between

4-9 scars (Table 11) (Fig. 12h). Convergent façonnage (i.e., shaping of two edges that converge at one end of the blank) is present in half (50.5%) of the LCT sample, and a further 20% shows rhomboidal shaping –see description in Bar-Yosef and Goren-Inbar (1993: 153) and de la Torre and Mora (2005: 158). As shown in Fig 10i (see also Table 12), there is a clear preference towards the shaping of dorsal (90.5%) over ventral (67.4%) surfaces, which is statistically significant (X^2 (2) = 15.32, $p < 0.0005$). Shaping extent (sensu McNabb et al., 2004) is overwhelmingly partial marginal (92.8%) (SE3 in Fig. 12j), with similar patterns across dorsal and ventral faces (Table 12). Shaping of the entire LCT perimeter is seen on just 34.6% of pieces (Table 12), and façonnage is concentrated primarily in the medial and distal areas (Fig. 12k). In general, the angle of removals is acute (78.4%), although steep angles are also found on dorsal face removals, and flat shaping on ventral sides (see Table 12). These differences are explained by the pre-existing plano-convex morphology of handaxe blanks, which favour flat removals on the ventral face and steeper removals on the convex dorsal face. Trimming is only observed in 5.2% of LCTs, and regularisation of edges is not evident in most handaxes (Table 12).

The shape of the tip is markedly convergent (following terminology by McNabb et al., 2004) on most LCTs (Table 13) (Fig. 12j). On 50.5%, convergence is aided by one or two removals that penetrate deeply into the LCT edge, creating notched tips (Fig. 13; SOM S8 and S9). A variety of single and double notches are documented, although the most common patterns are direct (i.e., from ventral to dorsal) or reverse (from dorsal to ventral) retouching of a single notch on the distal end of handaxes to create a tip (see Fig. 13a-b).

Most EF-HR handaxes lack all-round cutting edges, and 87.8% show an area that forms a steep, blunt angle with respect to the edge. Potentially, this could be related to the prehensile area of handaxes, and is informally considered here as the handling area; such 'handling' area is often the butt (53.1%) –which is normally rather thick on LCTs–, or steep angles on the dorsal or natural planes of blanks (17.3%), cortical surfaces (14.3%) and Siret flakes (3.1%) – these Siret, split blanks thus replicate the pattern described above for retouched tools. The handling area is located primarily at the end opposite the tip (i.e., proximal part; 41.9%) or on the right side of the handaxe (38.4%) (Table 13). The proximal end (i.e., the base) shows no clear morphological dominance, although straight (37.1%) and convex (34%) shapes are more common (see Table 13) (fig. 12o).

Production of LCT blanks

Table 11 shows that 90% of LCTs are on flake blanks. The lack of LCT cores in the EF-HR assemblage constrains reconstruction of LCT blank production to the data provided by small and intermediate flakes, and debitage patterns observed on the LCTs themselves.

As mentioned above, small flakes attributed to the LCT chaîne opératoire may derive from both shaping (Fig. 7c-d) and debitage stages. In the debitage phase, these small flakes were struck to initiate and maintain bifaciality of the core edge, prepare core edge convexities on the flaking surface, and prepare striking planes on the knapping platform for LCT blank removal (Fig. 14a). The main role of intermediate flakes was to rejuvenate core edges (Fig. 8b), and prepare the volume and shape of LCT blanks via invasive removals on the flaking surface of cores (Fig. 14b); substantial length and/or width of intermediate flakes would leave large removals on the core flaking surfaces, and their thin sections guide the amount of volume available for the subsequent production of the LCT blank.

Dorsal schemes, butts and overall techno-morphological features of LCTs also inform on the production patterns of LCT blanks. Some LCTs show that, in some instances, there was almost no preparation of cores; for example, in the case of Fig. 14c1 the LCT blank was removed from a fully cortical flaking surface, and the only preparation was on the core striking platform (as preserved in the multifaceted butt of the handaxe). Such preparation, and the location of the striking platform far from the core edge, could be aimed at concentrating the mass in the proximal area of LCT blanks (see scheme in Fig. 14c), a technique observed in similar assemblages (de la Torre et al., 2008). Fig. 14c2 is another example of LCT blanks flaked from fully cortical surfaces. In this instance, core preparation is even more expedient than in Fig. 14c1, as it is limited to cortex removal with no further faceting; yet, the obtuse angle of such removal once again enabled production of a blank with a thick proximal area.

While fully cortical LCTs are scarce, Fig. 12f shows that dorsal removals during the debitage stage are not abundant either, supporting the notion that long sequences of core preparation were an exception. The most common pattern is that of LCTs bearing a few unidirectional dorsal removals associated with the butt. The butt is often wide, covering most (if not all) of one side of the blank. In this scheme (Fig. 15), often impact points of scars are preserved on the LCT butt, indicating that core rotation prior to LCT blank removal was minimal, with most flaking aimed at preparation of core edges. This unidirectional, short flaking sequence of LCT cores was repeated systematically and shows a remarkably consistent pattern across the assemblage (see examples in Fig. 15).

Rotation of core knapping surfaces is observed on the dorsal patterns of some LCTs. Fig. 16a is an example of partial rotation, with debitage scars on the proximal and left sides of the LCT butt, but showing no preparation of the distal and right areas of the core prior to LCT blank removal. Fig. 16b shows a more systematic preparation of the core edge via proximal (with respect to the butt) removals, and some lateral rotation. Complete rotation is seen in Figs. 16c-d, where dorsal scars nearly (Fig. 16c) or fully (Fig. 16d) removed cortex from core knapping surfaces before LCT blank extraction. Interestingly, in both examples the large size of some scars could be those of LCT blanks previously removed from cores. Therefore, despite predominance of minimally prepared core flaking surfaces, LCTs from Fig. 16 are evidence of a more structured management of flaking volumes.

Organization of core volume is best observed in those LCTs where, apart from the butt –which on occasion shows preparation of striking platforms prior to LCT blank removal–, additional edges of cores are preserved. These are LCTs on *éclats débordants* or edge-core blanks, and examples such as Fig. 13a and Fig 13d (which preserve two and three core edges respectively) or Fig. 13b (which removes a bifacial edge of the core), indicate that rotation of the flaking surface was accompanied by preparation of flaking platforms, hence resulting in cores with bifacial edges around large parts of their contour. We have argued elsewhere (de la Torre et al., 2008) that configuration of core edges may operate not only to manage core volume, but also to guide the shape of *éclats débordants* used as LCT blanks (Fig. 17a). In these instances, the mass is balanced towards the core edge preserved on one or more sides of the large flake (Fig. 17a1), with blank morphology largely dictated by core edge preparation (Fig. 17a2).

Control of blank shape can also be inferred from the axis of striking points. As shown in Fig. 17b, the striking axis is consistently oblique to the maximum length of blanks, hence

producing side-struck, short, wide flakes. As with *éclats débordants*, the mass is concentrated on one edge of the blank, and is achieved by striking one end of the core platform, resulting in wide butts with a decentred point of percussion (see examples in Fig. 17b). Some LCTs show that production of flakes with an offset axis (*éclat déjeté*) can proceed without much core preparation; a least-effort option is to strike one cortical end of the cobble, and rely on the natural morphology of cores to obtain a side-struck blank with a thick, cortical base (Fig. 17c1 and Fig. 17d2). In other instances, the core knapping surface is prepared with unidirectional scars from the same striking platform as the butt (Fig. 17c2), which guide the termination of the LCT blank. Albeit technically simple, anticipation embodied in the debitage schemes of Fig. 17 is remarkable, as the rounded base and/or overall pointed shape of blanks are obtained prior to the façonnage stage.

Overall, LCTs indicate that EF-HR knappers employed a number of options in core preparation. Synthesised in the examples in Fig. 17d, such options range from fully cortical blanks (Fig. 17d2), to highly formatted flaking surfaces and platforms of bifacial cores (Fig. 17d4). This suggests considerable plasticity in the choice of LCT blank production techniques, and raises the question of the influence of cobble morphology on core preparation.

Although strictly Fig. 17d1 cannot be considered as an LCT core –removals are small and there is no evidence linking it to LCT production–, it certainly has dimensions (18 cm long and weighing over 3 kg) suitable as a source of LCT blanks. While Fig. 17d1 serves to characterise the type of cobbles available to EF-HR knappers, morphological attributes of a number of LCTs suggest that often cores were not very large; for example, the position and angulation of cortex with respect to the striking point on the butt in LCTs of Fig. 16a and Fig. 18a, indicate that cobble blanks were rather thin (approximately 4 cm in the case of Fig. 18a). Similar inferences can be drawn from Fig. 18d, and although in this case the core blank was thicker (7- 8 cm), it is apparent that a large portion of the core was removed with each LCT blank. This is particularly evident on LCT blanks that break cores nearly into two halves, and which could be considered essentially as split cobbles. Examples such as Fig. 14c1 and Fig. 18c (two knives practically a mirror image of each other), and Fig. 18b, indicate that core blanks were often no longer than, and no more than twice the thickness, of the LCTs themselves.

These features, alongside the alternating rhythm of bifacial removals observed on some handaxe butts (to prepare striking platforms on cores before LCT blank removal), do not suggest use of the stationery technique, at least during preparation of core volumes. They also indicate that often cores were exhausted after production of a single LCT blank. Some exceptions certainly exist; Fig. 16d, for example, preserves large scars that could be those of earlier LCT blank extractions and, if so, the core would have been massive. But, overall, the techno-morphological features of LCTs lead us to conclude that most EF-HR cores were relatively small, relative at least when compared to the 'giant' cores described in other Acheulean assemblages (e.g., Sharon, 2009).

The above applies to the main part of the LCT assemblage, made on lava flakes. However, as shown in Table 11, a small sample of LCTs is on metamorphic rocks and/or other blanks that are not flakes. Whilst virtually all lavas at EF-HR derive from river cobbles, hominins may have sourced metamorphic rocks directly from Naibor Soit (see discussion in McHenry and

de la Torre, submitted). Although most quartzite LCTs are on flakes (see Table 11), it was only possible to ascertain the original source of quartzite LCTs in 10 blanks; within that sample, five were from river cobbles and the remainder were flaked from Naibor Soit tabular cores.

LCTs made on flakes from quartzite cobbles show the same features as described above for lava handaxes. Likewise, quartzite flake blanks from Naibor Soit blocks suggest that knappers adapted core preparation to the tabular features of blocks in order to produce flakes of a similar shape to those made on cobbles. This technical transfer is exemplified in Fig. 19a; here, as in lava schemes using natural (Fig. 17c) or bifacial edges (Fig. 17a) to guide extraction, the blank is flaked from one end of the knapping platform, and the mass is concentrated on the base of the blank through the inclusion of areas of three planes of the core. In fact, Naibor Soit blocks required even less preparation than lava cobbles; as shown in Fig. 19b, the tabular morphology of quartzite blocks facilitated blank removal that, in this particular case, entailed dihedral preparation of the knapping platform to remove the type of *éclats déjetés* discussed above.

Shaping of LCT blanks

Although quantitative attributes of LCT shaping have been discussed above (see also Tables 12 and 13), it is relevant to consider such features in the context of LCT blank production, as façonnage patterns at EF-HR are intimately related with blank morphology. As illustrated in the examples shown in Figs. 13-20, shaping can be characterised summarily by the predominance of denticulate retouching that forms an acute angle between the striking platform and the flaking surface, and the absence of trimming. Retouch is mostly unifacial, non- invasive, often involving a single edge of the blank (and more often than not just part of that edge). It is discontinuous (scars do not align consecutively across the edge), direct (i.e., mostly from the ventral onto the dorsal face), and limited to one sequence of shaping (i.e., there is no overlapping of scars from consecutive stages of façonnage).

The predominance of denticulate retouch produces uneven planforms, and indicates a lack of concern for regularised edges. Such lack of interest in obtaining straight edges is supported further by the absence of trimming. Preference for direct retouch is probably due to the least-effort solution offered by use of the ventral sides of LCT blanks as knapping platforms (ventral faces present flat surfaces ideal for striking), and to the plano-convex morphology of LCT blanks (which by default provide no volume on ventral faces to exploit). Since retouching aims to modify just the edge of blanks –rather than penetrating their volume via invasive removals–, the shaping angle on these plano-convex blanks becomes acute. In turn, this explains the brevity of façonnage sequences; steepness of flaking angles would require that subsequent shaping strikes deep into the knapping platforms, which would reduce the outline of blanks dramatically. As a result, LCTs at EF-HR are constrained to one shaping sequence per edge. When combined, the shaping angle and plano-convex morphology of blanks are factors that may also explain the prevalence of unifacial retouch; a lack of suitable striking angles on dorsal surface scars, and of exploitable volume on the ventral face, hinders bifacial reduction and furthers the prevalence of short shaping sequences.

The brevity of the façonnage stage is evidenced also in the low number of scars per LCT (Table 11, Fig. 12h), and the fact that many preserve their percussion points –which would have been removed had subsequent shaping sequences been superimposed. Scar percussion

points and overlapping of scar ridges allow the timing of shaping removals on some LCTs to be addressed; some blanks show a series of clockwise rotation (e.g., Fig. 15b, Fig. 16d, Figs. 21a, 21b and 21d), others counter-clockwise (Fig. 13b, parts of Fig. 14c2, Fig. 16c), and some LCTs show both (e.g., Fig. 18b). Therefore, no conclusive rotation patterns can be discerned. In fact, most examples from Figs. 13-21 show changing directions of removals, and thus random rotation of blanks during shaping is the most likely scenario. In the limited number of cases where more than one edge is shaped, sets of scars on each edge show no overlapping of removals, and thus temporality cannot be ascertained. In itself, this indicates lack of continuity in the shaping of blank edges; rather than a steady rotation of blanks, shaping aims to configure one edge and, in a separate set of removals, the opposite; rhomboidal shaping (e.g., Fig. 21b) is an example of this design. Overall, on most façonnage options found at EF-HR, the morphology of the LCT blank guides the type and location of retouch, and series of façonnage barely modify the original shape.

Exceptions to these patterns actually provide additional support for the influence of blank shape on façonnage techniques. Thus, the few flat scars observed are almost invariably on ventral faces (see Table 12), which is to be expected given the plano-convex morphology of flake blanks, and rules out the possibility of such removals being aimed at volume reduction. Similarly, often reverse and/or bifacial retouch is only associated with the thinning of butts, which are the only areas of the flake, apart from the dorsal face, where pre-existing volume is available.

While, from the above, it is evident that shaping is adapted to pre-existing blank morphology, a separate question is how the final LCT shape is predetermined by the blend of retouch and debitage techniques or, in other words, to what extent debitage and façonnage templates are intentionally combined to achieve particular LCT morphologies. We argue that both are intimately related, and that there is evidence of strong predetermination of blank morphologies (see previous section) and of imposition of remarkably similar shaping schemes on such blanks.

The overarching scheme is one where façonnage is concentrated on an edge opposite the butt of short, wide, thick flake blanks. The general lack of bifaciality and restricted shaping (usually one part only) of a single edge likens these pieces to massive ‘denticulate scrapers’ (as described by de la Torre et al., 2008), where the goal is to produce cutting edges opposite a thick handling area. This handling area is usually the butt, although in some cases natural planes or Siret fractures –just as with retouched tools on intermediate flakes (see Fig. 11)– function as ‘backing’. The resulting morphotype is repeated regardless, thus reinforcing the notion that LCT blank production is predetermined to serve this specific shape template. Examples from Fig. 20 can be seen essentially as variations of the same theme; most of these ‘massive scrapers’ have a tip at the end where the butt (which often runs through an entire edge of the blank) meets the opposite edge. As mentioned above, often such a tip is obtained by notches that deeply penetrate the edge/s of the blank. Examples from Fig. 13d, Fig. 15a, and Fig. 21a are very similar to each other not only in their general shape, but they are identical in the way notching operated over the volume of the butt (i.e., thinning it at one end to create a thick notched tip), thus suggesting a highly standardised combination of debitage and façonnage actions.

Such combination led to a predominance of pointed (Fig. 20a) and 'crescent-shape' knives (Fig. 20b) with shaping of one edge opposite the butt, alongside some knives with convergent retouch on two edges, a few bifaces, and other LCTs with trihedral cross-sections (i.e., picks; Fig. 20d) or with edges transverse to the long axis (cleavers; Fig. 20c). These forms constitute the variability of debitage plus façonnage options observed at EF-HR, and are discussed as formal techno-typological classes in the next section.

Types of Large Cutting Tools

EF-HR handaxes are largely dominated by knives (n=69), picks (n=14) and cleavers (n=9), most of which are unifacial (see Table 13) (Fig. 12m). Bifaces are marginally represented (5%). Statistically significant differences are observed in LCT type per raw material (X^2 (7) = 15.22, $p<$ 0.0.332), and the adjusted residuals point to an overrepresentation of unifacial knives on lava, and a higher-than-expected proportion of metamorphic unifacial picks. Their techno-morphological features are as follows:

Knives As the most common group at EF-HR, distinctive traits of knives were mentioned earlier when discussing key technological features of the handaxe population. Fig. 21 includes some typical examples and captures their main features: knives are made either on side-struck (80.6%) or end-struck (19.4%) flakes, show denticulate retouch, often unifacial and direct, on one edge only, opposite the butt. When two edges are shaped, reverse or alternating retouch partially or totally thins the butt. Most knives show retouch –often via deeper removals ('notches')– on the end where the butt and its transverse edges meet, to create a tip. In those cases where this occurs, most of the retouch on two edges is concentrated at the tip area.

Picks These are characterised by a trihedral section at the tip area (see examples in Fig. 22). Most EF-HR picks do not show shaping from three separate platforms (but see Fig. 22a); instead, the triangular profile is determined by steep retouch at the tip from one or (more rarely) two striking platforms, and/or the natural shape of the blank (Figs. 22b, 22d). In this regard, the morphology of Naibor Soit quartzite appears to play a role, as angular planes present in this raw material are favourable to the production of trihedral sections (Fig. 19c). This would explain the comparatively large proportion of quartzite picks –as shown in Table 14, it is the only group where metamorphic almost equals lava LCTs. As with knives, picks are primarily made on side-struck (69.23%) or end-struck (15.38%) flakes although, in this group, there are also LCTs on cobbles (7.69%) (Fig. 22d) or blocks (7.69%) (Fig. 19d).

Cleavers As in the previous LCT groups, side-struck flake blanks predominate over end-struck blanks (66.7% versus 33.3%, respectively). There is no clear preference for a particular cleaver morphology –according to Clark and Kleindienst's (2001) types–, with similar frequencies of parallel (n=3), convergent (n=3) and divergent (n=2) outlines, plus one ultra-convergent cleaver. Technologically, however, patterns are clearer; following Tixier's (1956) classification, most (n=5) are 'Type 0' (i.e., cleavers with a cortical the transverse bit) (Fig 23a). There is one example of 'Type 1' (blanks preserving cortex and a debitage scar that configures the bit) (Fig. 23b). More structured debitage patterns are observed in 'Type 2' cleavers (n=3). Despite the existence of some LCTs where the bit can be attributed (relatively) confidently to predetermination via a tranchet flake removal during the debitage stage (e.g. Fig. 23c), prototypical cleavers with a straight bit are not abundant at EF-HR, where cortical and/or irregular bits predominate. Overall, cleavers are technologically

identical to the knives described above, and the distinction between the two may become semantic, thus artificially separating LCTs into distinct morphotypes which differ only slightly on the angle of the distal end (see example of Fig. 23d).

Bifaces Handaxes where shaping involves bifacial reduction of biconvex volumes exist, but are rare (n=5). They show higher numbers of removals, in some cases invasive, more extensive shaping of edges and, overall, more intense reduction, and are smaller than other LCT classes (compare Fig. 24b with Figs. 24c-d). In fact, the only two pieces considered here as LCTs despite being smaller than Kleindienst's (1962) 10 cm arbitrary threshold, are bifaces (although both are > 90 mm), and the distinction between retouched tools on medium-sized blanks (Fig. 24a) and 'proper' bifaces (Fig. 24b) is blurry. Three bifaces are on cobble rather than flake blanks (n=2), in contrast to the pattern of the other LCTs. This could explain the more intense reduction observed on bifaces; whereas edges of LCTs on flakes are produced mainly during the debitage stage, cobble blanks require a longer series of bifacial removals to obtain sharp edges (see discussion in Jones, 1994).

Morphometric features General dimensional patterns are relatively similar across the LCT population (Figs. 25a-b). The Kruskal Wallis test found no statistical differences per raw material for any of the variables in Table 14 (see results in SOM S19a), which is also supported by a principal component analysis (Fig. 25c). Comparisons of the variance in length (Bartlett's test, p=0.3202; Levene's test, p=0.3713), thickness (Bartlett's test, p=0.6063; Levene's test, p=0.7051) and weight (Bartlett's test, p=0.1426; Levene's test, p=0.0732) indicate an absence of statistically significant differences per LCT class. On the other hand, an ANOVA comparison of knives, picks, cleavers and bifaces together indicates statistically significant differences in the mean of five variables from Table 14, namely length, width, elongation, length/weight and edge length (see results in SOM S19b). Some of this variability is illustrated in SOM S20 and, in Table 14, considerably higher values of cleaver edge length are evident too. Table 14 also shows that, on average, bifaces are consistently smaller than other LCT classes: when biface dimensions are compared to the most abundant LCT type (i.e., knives), the Student's *t*-test confirms that statistically significant differences exist in mean length (t (72) =-3.174, p= 0.002), although not in the other dimensions (width: t (72) =-1.202, p= 0.233; thickness: t (72) =1.064, p= 0.291; weight: t (72) =-0.518, p= 0.606).

Discussion

Two chaînes opératoires for one technology

Because of its defining character, traditionally the handaxe has been the focus of studies on Acheulean technology. However, most East African Acheulean sites also contain other tool types, and recent years have witnessed a growing interest in the non-handaxe component of assemblages as a means to better characterise the origins and variability of this technology (e.g., Texier and Roche, 1995a; de la Torre, 2009; Gallotti, 2013). The non-handaxe component is considerable at EF-HR, and co-existence of two separate reduction sequences in the same assemblage is well attested. As illustrated in Fig. 26a –where the source of flakes in the small debitage chaîne opératoire (#2) is compared to a flake blank sourced within the LCT sequence (#1)–, such differences are substantial. The small debitage chaîne opératoire

seeks to produce small (~3 cm) flakes, which remain mostly unretouched. Debitage stages in the LCT chaîne opératoire produce a wide range of flakes, and the main objective is to obtain large (~14 cm) blanks that are subsequently shaped.

Raw material patterns and skill investment are also different in each chaîne opératoire. Raw material patterns show a clear dominance of phonolite in the small debitage (where it reaches 15.8 kg, i.e., 24.7% of this chaîne opératoire) when compared to LCT production (phonolite = 8.7 kg; 7.8%). A more nuanced dominance of quartzite in LCT production (26.3kg; 23.6%) than in small debitage reduction (8.8kg; 13.8%) is also observed, while the other main groups proportionally have a similar representation (basalt = 43.7 kg; 39.2% in LCT production versus 24.6 kg; 38.5% in small debitage. T-Ta = 32.4 kg; 29% versus 14.5 kg; 22.7%, respectively). Overrepresentation of phonolite in the small debitage chaîne opératoire is particularly evident in cores, whereas flaked artefacts (i.e., handaxes and retouched tools) are under-represented (see Table 3) in LCT production. These differences may be explained by the size of available raw material: phonolite cores have a mean length (77.5 mm) and weight (341 g) below the average (81.6 mm and 448 g; see details in Table 6), so it is likely that larger phonolite cobbles suitable for LCT production were scarce. A proportionally higher weight contribution of quartzite to LCT production than to small debitage is also observed; lava and metamorphic rocks show nearly identical proportions of LCTs (17% and 16.7%, respectively), whereas the relative frequency of metamorphic small cores (17.1%) is far lower than that for lavas (43.7%) (Table 4).

Investment of skill and complexity of the reduction sequence in the small debitage chaîne opératoire is significantly lower than in LCT production. Small cores show unstructured flaking surfaces and were abandoned after short series of removals (Table 9). Although the resulting flakes are of good quality (i.e., they have sharp edges, regular shapes, thin sections and feathered terminations) and thus can be broadly distinguished from their counterparts in earlier Oldowan sites (where flaking products are rarely complete, yield low edge productivity and have irregular shapes; e.g., de la Torre and Mora, submitted), knapping schemes are not significantly different. Since most products were not subsequently retouched, and given the brief nature of the series of removals, it can be concluded therefore that the small debitage chaîne opératoire at EF-HR was simple, opportunistic and short-lived.

In comparison, LCT production at EF-HR is much more structured. The prevalence of fine-grained, fissure-free raw materials across the LCT population (see McHenry and de la Torre, submitted) indicates selectivity of high-quality rocks, particularly T-Ta. Such high quality raw material was a necessary condition to produce the large flakes that served as LCT blanks; as reported above, even in instances where LCT cores underwent little preparation, LCT blanks were flaked following fixed procedures to obtain shapes with standardized volumes and morphologies. Once such blanks were produced, shaping patterns were imposed in a very similar manner, resulting in distinctive morphotypes. As discussed below, such morphotypes convey considerable manual, technical, and cognitive skill within a longer reduction sequence than that of small debitage, and thus clearly distinguish LCT production from its co-occurring chaîne opératoire.

Techno-economic patterns at EF-HR

Irrespective of the chaîne opératoire, the ratio of flakes to the main flaked artefacts (i.e., cores and handaxes) of the entire assemblage is 2.25 (Table 15). The total scar counts on cores

(n=384) and LCTs (debitage scars, n= 238; façonnage scars, n=634) are conservative estimates, and yet when compared to the number of flakes documented at the site, the overall ratio (0.41) becomes even smaller (Table 15). This clearly indicates that all the debitage expected from core flaking and LCT production is not preserved in the assemblage.

Fluvial disturbance is attested at EF-HR (de la Torre and Wehr, submitted), and partially explains underrepresentation of small debris when compared to expected frequencies (de la Torre et al., 2017). However, factors other than taphonomic should be considered when interpreting patterns in Fig. 25d, which shows clear ratio differences per raw material between small debitage production and LCT façonnage. Although this comparison is biased by the uncertainty of flake attribution to either of the two chaînes opératoires (see details above and in Table 15 caption), imbalance between metamorphic and lava small flakes is far more acute in the small debitage sequence than in LCT production. In fact, the sharp deficit of lava debitage is even more accentuated when the two chaînes opératoires are pooled together. Exactly as at HWK EE (de la Torre and Mora, submitted), underrepresentation of lava versus quartzite cannot be explained by water disturbance, and hence behavioural patterns should be sought.

Although part of the EF-HR assemblage is found in a conglomeratic context (de la Torre et al., submitted), natural cobbles of a size equivalent to LCT cores are absent, and thus a systematic comparison of the unmodified and archaeological components such as that conducted for HWK EE (de la Torre et al., submitted 'b'; McHenry and de la Torre, submitted) is not possible. Nevertheless, given that EF-HR was paleo-geographically positioned at the bottom of a river valley (de la Torre et al., submitted; Stanistreet et al., submitted), and that raw material features of small cores are similar to cobbles documented in other Bed II conglomerates such as at HWK EE (de la Torre et al., submitted 'b'), we assume that provenance of small debitage cores on lava and quartzite cobbles was probably local. This would explain the low reduction intensity observed in this chaîne opératoire although, admittedly, not the paucity of lava debitage (beyond an attribution to water disturbance).

The dynamics of LCT production may be different, and an assessment of the possible spatial and temporal fragmentation of this chaîne opératoire can be discussed. Two options may explain the virtual absence of cores for LCT blank production in the assemblage. One possibility is that they are now 'invisible' due to complete reduction of the original cores on-site. We know, for instance, that cobbles of a suitable size for LCT blank production are occasionally present in the assemblage (Fig. 17d1; Fig. 26c, #1). This, plus features of the LCTs themselves reported earlier, suggest that cores were not exceedingly large –at least not in the sense of the 'giant' cores reported elsewhere (e.g., Sharon, 2009)–, and therefore could have been transported to the site by hominins. We have also described above some LCT blanks that are almost split cobbles and, despite the lack of refit evidence, it is not implausible that in some cases the two halves were shaped into LCTs. In addition, intermediate flakes are well documented in the assemblage and, unless they all correspond to shaping processes, are indicative that LCT debitage also occurred at the site. Further evidence is provided by large hammerstones which, although scarce, do appear in the assemblage; probably too big for shaping or flaking of small debitage, they may have been used for LCT blank production (see Fig 26c, #3). Overall, it seems that, with the exception of cores, all elements of the LCT reduction sequence are present in the assemblage (see Fig. 26c #1-7), and therefore some LCT blank production should have occurred on-site. As a general pattern,

however, the possibility of LCT cores 'disappearing' during reduction is unlikely; small cores mostly preserve the original cobble shape and confirm they were small-sized from the start (i.e., reduced size is not due to heavy reduction). Conversely, core features preserved on many handaxes indicate that, after one LCT blank removal, cores were discarded as unsuitable for further removals due to the limited volume available. Since they were not recycled for small debitage flaking, they would be visible in the assemblage, should LCT blank removal have taken place on-site.

The second option is that most LCT blanks were obtained elsewhere, and then transported to EF-HR. This is the almost certain scenario for some LCT blanks derived from very large cobbles or boulders (e.g., Figs. 16c-d), and is a possibility for other handaxes from smaller, more easily transportable cobble cores. Given the lack of LCT cores in the assemblage, we favour this option here, which thus encompasses a fragmentation in the LCT chaîne opératoire.

Nevertheless, blank production at the site should not be completely ruled out: a fraction of the intermediate flakes documented at EF-HR was most likely produced during LCT core preparation and therefore, except if they had been transported to the site alongside LCT blanks, they should be considered as evidence of partial on-site LCT blank production. This is supported by refitting results; although conjoining pieces are rare at EF-HR (de la Torre and Wehr, submitted), they include intermediate flakes and other elements clearly linked to on-site LCT production.

An additional consideration involves whether or not the subsequent façonnage stage also occurred elsewhere. Overall, the small flake: LCT ratio is significantly higher than that of the small debitage chaîne opératoire (see Table 15), and therefore it is safe to assume that shaping took place on-site. LCT fragments are present at EF-HR (see Table 4), and include both tips and proximal/distal parts (Fig. 26b). Although tool fracturing can also be caused during use, breakage during manufacture is known to be a common technical accident (e.g., de la Torre et al., 2014), and thus fragments are considered here as additional support for façonnage activities taking place on-site, during which some LCTs broke.

Even if a spatial/temporal fragmentation of the LCT chaîne opératoire did exist –with LCT blanks sourced elsewhere and then transported to the site–, this chaîne opératoire was never very long. As discussed above, many LCT cores would have had to be discarded after a single blank removal. Furthermore, the 'use-life' (sensu Hayden, 1989; Shott, 1989) of EF-HR handaxes was rather short, with LCTs rarely bearing more than one sequence of shaping. The conception of handaxes as re-sharpened objects (McPherron, 2000) with long use-lives, as argued for other assemblages (e.g., Shipton, 2016), is absent at EF-HR, where LCTs were shaped just once (presumably) before use and discard.

In summary, and according to our interpretation, two separate procurement and manufacturing strategies co-exist at EF-HR for which, apart from LCT cores, all elements are represented in the assemblage (Fig. 26c). Small cobbles were sourced locally, and knapped on-site. Phonolites were probably abundant in the local conglomerates, and were used preferentially for the short reduction sequences of small flakes. On the other hand, LCT blanks were probably produced elsewhere. Procurement trips to Naibor Soit were likely for quartzite, as suggested by the tabular aspect of some LCT blanks, but some were also sourced from river banks (as indicated by the rounding of cortical surfaces). Although sourcing in

local conglomerates for LCT blanks cannot be excluded (see e.g., de la Torre et al., submitted, Fig.8f), the remarkably good quality of raw material of many handaxes should be highlighted: some basalts and (particularly) T-Ta are excellent but also elusive in Olduvai conglomerates. This is likely evidence of strong raw material selectivity, which is necessary given the technical requirements of handaxe production, and would support the hypothesis of a spatial-temporal fragmentation of the LCT reduction sequence. While not excluding the formatting of some LCTs before they were brought to the site (in the event that LCT blanks were indeed obtained elsewhere), it is also evident that (at least part of) façonnage processes were conducted on-site.

These technological strategies led to an accumulation of 214 kg of stone tools during the formation of Interval 1 in the paleo-landscape excavated by OGAP. With 111 kg attributed to the LCT chaîne opératoire, it is clear that handaxe manufacture was a key aspect of activities conducted at the main site. Nonetheless, small debitage flaking involved no less than 64 kg of raw materials, and thus highlights the relevance of technological processes other than handaxe production during the beginning of the Acheulean. In combination, both handaxe manufacture and small debitage flaking testify to the complementarity of different procurement and technical schemes. Overall, techno-economic aspects of the EF-HR assemblage reinforce the notion of technological adaptability across the landscape during the Acheulean in general (Goren-Inbar and Sharon, 2006; Potts et al., 1999; de la Torre, 2009; de la Torre et al., 2014; Pope and Roberts, 2005; Truffeau et al., 1997) and, in the particular case of Olduvai, the differences between the Acheulean and the Oldowan (de la Torre and Mora, 2005).

Technical skill and mental templates in the production of handaxes at EF-HR

The earliest handaxes in Kokiselei (Lepre et al., 2011) and Konso (Beyene et al., 2013) are characterised by poor planform symmetry, rare bifaciality and crude shaping of large flakes and/or cobble blanks, with most of the slightly younger assemblages sharing similar patterns (see a summary in de la Torre, 2016). Some of the typical elements of handaxe 'design form' (Gowlett, 2006) are already present in those early Acheulean assemblages, EF-HR included. The conservative butt mass is a prevalent aspect of LCTs at EF-HR which, as Gowlett (2006) indicates, balances out the forward extension of the handaxe; in EF-HR, the butt mass is located laterally to –rather than opposite– the tip on the major axis. Thus, support for the working edge (as per its relation to the butt mass) indicates prominence of the lateral part of the handaxe; this is shown not only by the mass being balanced towards the lateral area, but also by shaping consistently concentrated on the edge opposite the butt mass. Thickness adjustment as considered by Gowlett (2006) is also evident at EF-HR; control of tip thickness and (especially) working edge angle is achieved via steep-angled shaping removals. However, overall mass is not adjusted via shaping, as volume management through bifacial thinning is rare in EF-HR handaxes. Instead, overall thickness is controlled during the debitage phase, rather than during the shaping process.

The presence of these handaxe 'imperatives' (Gowlett, 2006) enable us to differentiate EF-HR from earlier –or potentially contemporaneous– Oldowan assemblages at Olduvai, but further morphometric and/or technological elements of characterization might help explore similarities and differences between early Acheulean assemblages.

Growing attention to handaxe morphometrics has included symmetry (e.g., Lycett, 2008) and refinement (McNabb and Cole, 2015) as aspects to explore using Olduvai datasets (see also McNabb, 2017). These efforts add to earlier work (e.g., Roe, 1994; Callow, 1994) on the morphometrics of Bed II-Bed IV Acheulean assemblages, and help towards a better understanding of the typological composition of Olduvai handaxes. Standard shape indices in EF-HR (Table 14) (SOM S20) show some differences between LCT groups, although they are not significant when raw materials are compared (SOM S19). Generally, however, our dimensional analysis based on bivariate ratios common in the literature (e.g., Roe, 1994; McPherron, 2000) does not yield conclusive results on aspects such as the degree of standardization of LCT production. Pending the outcome of multivariate morphometrics, this lack of resolution might be explained, at least in part, by the cursory façonnage observed in EF-HR handaxes, and suggests that shape as a product of skill and technical templates should also include an evaluation of the debitage stage.

In fact, we believe that the debitage stage is key to understanding LCT technology at EF-HR. It has been argued above that the overall morphology and mass balance of the final handaxe is already present in handaxe blanks. Specific patterns are consistently applied to LCT blank production, whereby side-struck flakes are removed from core ends via striking at an oblique angle deep into core platforms. This produces thick flakes with an offset axis, where the mass is balanced on the latero-proximal part of the blank. This blank morphology is then barely modified during the façonnage stage, in which denticulate retouch cursorily shapes the edge opposite the butt mass, and the distal end where a thick tip is created by means of a few notches. Reconsidering some of our earlier conclusions based on the Leakey collection (de la Torre and Mora, 2005), we now see evidence that this blending of debitage and façonnage techniques follows a remarkably consistent pattern, and delivers technologically, morphologically and dimensionally similar LCTs, some of which are near-mirrors of each other (e.g., Figs. 15c and 18d; Fig. 14c1 and 18c). In our opinion, there is clear evidence of a procedural template (sensu Gowlett, 1984) in LCT manufacture at EF-HR. Given the short use-life of EF-HR handaxes (which only show a single sequence of shaping), such patterns cannot be attributed to reduction intensity as proposed for younger Acheulean assemblages (e.g., McPherron, 2000), and may reflect the existence of a genuine mental template.

While use of oblique flaking to determine LCT blank morphology has been observed elsewhere (e.g., Texier and Roche, 1995b; Petraglia et al., 2005; Shipton, 2016), and the predetermination of LCT shape beginning in the debitage stage has been known for a long time (e.g., Goodwin and Van Riet Lowe, 1929), usually both have been reported in later Acheulean assemblages (Tixier, 1959; Texier and Roche, 1995b; Gowlett, 2006; Sharon, 2009). EF-HR indicates that the required mental and technical abilities were already present in the early Acheulean, and may help when reconsidering interpretations of skill level throughout the span of this techno-complex. Although early Acheulean handaxes may initially seem crude when compared to later assemblages due to lack of planform and biconvex symmetry, the case of EF-HR indicates that standardization may exist in other parameters beyond handaxe morphometry.

In fact, it could be argued that the interplay between debitage and façonnage templates seen at EF-HR is not technically any simpler than the refinement through shaping observed in later handaxes. It could be the case, then, that differences between the (typologically) crude early LCTs and the refined handaxes often found in s later Acheulean assemblages (e.g., Wynn,

1979; de la Torre et al., 2014; Stout et al., 2014) respond to cultural, aesthetic or functional factors, rather than linked (at least not exclusively) to advances in technical or cognitive abilities. In other words, EF-HR suggests a close interaction of debitage and façonnage patterns in which predetermined templates exist, and where the absence of symmetrical bifaces conveys no technical and/or cognitive implications.

In this regard, it is relevant to reiterate that EF-HR handaxes are not bifaces. Even in the few cases where bifacial shaping exists, there is no management of biconvex volumes, and façonnage is restricted to the edges of artefacts. Shaping is normally unifacial, discontinuous, with limited rotation and/or flipping of surfaces, largely unmodified ventral faces, and denticulate and irregular retouch opposite a blunt (normally the butt) side. Most EF-HR handaxes resemble massive side scrapers (de la Torre and Mora, 2005) which, for the lack of a better term, should be included within Kleindienst's (1962) category of knives. This morphological template also dominates the sample of non-LCT retouched tools where, in the absence of thick butts, Siret fractures or natural planes are used as the balance of mass opposite the shaped edge. This both reinforces the existence of an overarching morphotype sought in a variety of blanks, and also highlights fluidity in the use of different parts of the chaîne opératoire for the same purpose.

Comparing the late Oldowan and early Acheulean at Olduvai

Attempts have been made to identify differences beyond the presence/ absence of handaxes in assemblages between the late Oldowan and early Acheulean (e.g., de la Torre and Mora, 2005, 2014; de la Torre, 2009, 2011; Gallotti, 2013). Included among them are a proposal for more sophisticated methods of small debitage during the early Acheulean (Gowlett, 1986; de la Torre, 2009, 2011; Gallotti, 2013; Leader et al., in press), variability in types of small retouched tools (Gallotti and Mussi, 2015), and a more structured use of the Olduvai landscape in the Acheulean when compared to the Oldowan (de la Torre and Mora, 2005).

While the question of the so-called Developed Oldowan B and the emergence of the Acheulean at Olduvai is discussed separately (see below), differences between 'undisputable' Oldowan (i.e., assemblages without any handaxes) and Acheulean assemblages can be explored here by comparing HWK EE –a site excavated and analysed following the same methods as employed in this paper (de la Torre and Mora, submitted)– with EF-HR. They are separated by a considerable stratigraphic span (HWK EE is mostly below Tuff IIB and EF-HR is above Tuff IIC), and probably more than 200ka years (HWK EE is ~1.7 Ma and EF-HR is ~ 1.4 Ma). This temporal distance between the two sites enables comparison between late Oldowan and early Acheulean patterns free of the riddles of assemblages stratigraphically closer to the time of the transition, which often contain more ambiguous features.

In terms of comparisons of assemblage composition (apart from the obvious absence of LCTs in an Oldowan assemblage such as HWK EE), it is relevant to discuss the significance of retouched tool frequencies. Table 4 shows that small debitage (1.8%) and LCT (3.9%) chaînes opératoires at EF-HR have higher proportions of retouched tools than HWK EE (0.9%). However, when results of the small debitage reduction sequence at EF-HR are averaged with regards to all blanks within the size range of retouched tools (i.e., ≥ 17 mm), the ratio is virtually identical to that at HWK EE (0.02), and proportions are similar when other sub-samples are considered (compare Table 15 against de la Torre and Mora,

submitted: Table 10). Therefore, differences between the proportion of retouched tools at HWK EE and EF-HR are only conspicuous once the LCT reduction sequence is considered (Table 15) but, as far as the small debitage chaîne opératoire is concerned, ratios are very similar at both sites. Interestingly, ratios of pounded artefacts are also similar in both HWK EE and EF-HR.

With regards to small core flaking methods, the HWK EE and EF-HR assemblages are also remarkably alike. There is a predominance of TC, BALP and UAU1 techniques in the Oldowan assemblage (de la Torre and Mora, submitted: Table 8) while, as shown above for EF-HR (Table 9 and Fig. 10), BAP, TC and UAU1 schemes prevail in the Acheulean assemblage. The bipolar technique is present in nearly identical frequencies (8.3% in HWK EE versus 8.7% in EF-HR), as are unifacial (USP; 4.4% versus 4.8%) and bifacial (BSP; 8.8% versus 9.5%) choppers. All these flaking techniques are characterised by a short series of removals, lack of standardization and poor organization of knapping sequences, suggesting no significant differences in small debitage methods between HWK EE and EF-HR. De la Torre and Mora (2005: 223) identified an increase of more structured flaking techniques in TK and BK, both of which are positioned stratigraphically higher than EF-HR (Leakey, 1971; Hay, 1976). Recent work on these two latter sites (Santonja et al., 2014; Sanchez-Yustos et al., 2016) seems to confirm a consistent presence of bifacial centripetal techniques, and thus supports the proposal for a greater sophistication of flaking techniques in the early Acheulean (e.g., de la Torre, 2009, 2011). Given that small debitage techniques at EF-HR are no different from those at an Oldowan site such as HWK EE, whether or not there is a diachronic trend in structured flaking of small cores *within* the early Acheulean (rather than between the Oldowan and the Acheulean) is a hypothesis to test in future studies.

While in terms of small core knapping methods HWK EE and EF-HR are similar, the resulting debitage shows qualitative differences. De la Torre and Mora (submitted) highlight the generally poor manufacture of debitage at HWK EE, dominated by flake fragmentation and low edge productivity. For instance, complete flakes form 7.6% of the HWK EE assemblage, whereas small debitage flakes account for 33% at EF-HR. Furthermore, while mean dimensions are not too different between the two assemblages (compare Table 6 of this paper with de la Torre and Mora, submitted; Table 4), complete flakes at HWK EE are proportionally thicker, and significantly heavier than those of EF-HR. It has been proposed (de la Torre and Mora, submitted) that the 'bulky' aspect of HWK EE debitage seems to represent overall poor management of striking platforms and flaking volumes. In contrast, EF-HR flakes were struck off efficiently, despite the short-lived nature of reduction sequences and the unstructured organization of knapping. Such efficiency is best evidenced in the productivity of flake edge length; small debitage flakes of Interval 1 at EF-HR have an average cutting edge of 5.45 cm which, given their mean weight (12.9 g), results in 0.42 cm/g. This ratio is nearly twice as high as that of HWK EE (0.22 cm/g; de la Torre and Mora, submitted).

Edge length productivity at EF-HR is far higher once LCTs are considered (0.74 cm/g; see details in Table 15), and also when the two assemblages as a whole are compared; 64.43 meters of cutting edges were produced from 456 kg of raw material at HWK EE. In contrast, 98.7 meters were produced from 223 kg at EF-HR (including all material from both intervals). The contrast is staggering, with the productivity at the Acheulean site (0.44 meters per kg) three times higher than in the Oldowan assemblage (0.14 m/ kg). Although it is

important to recognise that the objectives of stone tool use may not always be related to the production of cutting edges (Mora and de la Torre, 2005; Arroyo and de la Torre, submitted), and that other functional and/or technological goals may also have been involved, differences in productivity between HWK EE and EF-HR are clear and should respond, at least in part, to distinct levels of technical proficiency.

Furthermore, such differences in productivity and technical skill should be considered in the context of raw material procurement and landscape use patterns. HWK EE shows selection of rocks with naturally available flaking angles to the detriment of cobbles which, although fine-grained, are of shapes that make knapping more challenging (de la Torre and Mora, submitted; McHenry and de la Torre, submitted). Selectivity of chert for retouched tools is documented but, apart from that, such tools are indistinguishable from those made on other raw materials. In contrast, EF-HR shows a bimodal pattern in raw material procurement; small debitage is on local rocks (typically available in Olduvai conglomerates), while the LCT chaîne opératoire indicates a preference towards large, fine-grained cobbles with excellent knapping properties, which may have been sourced non-locally (see discussion above). Prioritization of flaking quality at EF-HR is to be expected given the technical requirements involved in LCT production, but it may also be interpreted in the light of differences in landscape use when compared to HWK EE; de la Torre and Mora (2005: 232-237) argue for greater segmentation in use of the Olduvai landscape during the Acheulean, and higher density occupation in each locality, when compared to the local Oldowan. Temporal-spatial segregation between LCT blank production and shaping-use-discard as hypothesized for EF-HR, versus immediate manufacture-use-discard in HWK EE, would support the picture of more structured raw material procurement in the Acheulean. This involved accumulation of a significant number of stone tools at a discrete spot in the landscape accompanied by a diffuse (albeit pervasive) use of the surrounding EF-HR paleo-surface (see discussion in de la Torre et al., submitted), and could correspond to distinctive mobility patterns at the onset of the Acheulean.

EF-HR and inter-assemblage variability during the early Acheulean at Olduvai Gorge

As mentioned earlier, historically EF-HR played a pivotal role in the definition of the early Acheulean at Olduvai and elsewhere, due both to the age attributed to the assemblage –Leakey (1971) considered it the earliest handaxe-bearing site at Olduvai–, and the abundance of LCTs in the collection. With regards to age, it is now proposed that EF-HR is stratigraphically younger than other classic Olduvai sites where handaxes are documented (McHenry, submitted; Stanistreet et al., submitted). Even older, previously unknown Acheulean assemblages may exist in the sequence (Diez-Martin et al., 2015), thus confirming that EF-HR can no longer be considered the earliest Acheulean at Olduvai. This has implications for modelling the appearance of the Acheulean in the Olduvai sequence, since a younger age for EF-HR lessens the dilemma of a handaxe-rich assemblage at the onset of the Olduvai Acheulean supposedly followed by Developed Oldowan B (DOB) sites in which handaxes are rare (de la Torre and Mora, 2014).

The early Acheulean- DOB conundrum has been the subject of debate since originally formulated (Leakey, 1971) and later (Leakey, 1975; Hay, 1976; Bower, 1977; Stiles, 1980; Gowlett, 1988; de la Torre and Mora, 2005; 2014; Semaw et al., 2009). As an assessment of competing hypotheses on the interpretation of the archaeological record (see summary in de

la Torre and Mora, 2014) and the stratigraphic sequence (see summary in McHenry, submitted) is beyond the scope of this paper, here we follow the model whereby all Acheulean sites published so far are no older than the Middle Augitic Sandstones (Hay, 1976; McHenry, submitted; Stanistreet et al., submitted).

In this scenario, handaxe variability in the post-Tuff IIB record still needs to be addressed, as new fieldwork in classic sites such as TK (Santonja et al., 2014), SHK (Diez-Martin et al., 2014) and BK (Sanchez-Yustos et al., 2016) has confirmed Leakey's (1971) observations on the inter-assemblage disparity of handaxes in Middle and Upper Bed II. Systematic descriptions of LCTs across sites are now essential; the remarkable resemblance between EF-HR and Peninj LCTs have long been noted (Isaac, 1965, 1967; de la Torre et al., 2008), so it would seem surprising to find similarities to be closer between assemblages from separate sedimentary basins, than within Olduvai itself. As yet, EF-HR is the only Olduvai Bed II site with a clear predominance of lavas which, as suggested elsewhere (de la Torre and Mora, 2014), could explain some of the differences with other handaxe-bearing sites at Olduvai. Nevertheless, the scope of technological –rather than morphometric– comparisons of early Acheulean assemblages within the Olduvai Middle and Upper Bed II sequence (de la Torre and Mora, 2005, 2014) are still too limited to provide an accurate picture. In this paper, we have proposed that 'proper' bifaces are not characteristic of EF-HR, cleavers are rare (and their transversal bits might mostly be randomly obtained), and picks might be largely mediated by pre-existing morphologies of raw materials. Knives are the prevalent morphotype, and given that planform and biconvex symmetries (features that generally characterize Acheulean handaxes) are normally absent, in the future it is pertinent to investigate to what extend EF-HR's features are shared by other early Acheulean handaxes, and what temporal, technical, ecological and raw material patterns drive variability in handaxe manufacture in Bed II and beyond.

This paper has reported one hundred LCTs in stratigraphic position at EF-HR which, even if a substantial sample in itself, is still below the total number of handaxes at the site; de la Torre et al. (this volume) calculate that the extension of EF-HR is far greater than the area excavated by OGAP, and it can only be expected that many more handaxes are preserved in the remaining Interval 1 deposits. And, of course, there is also the assemblage excavated by Leakey (1971); Table 16 aggregates the OGAP and Leakey collections, which together total 284 kg of worked stone, and includes no less than 133 LCTs.

As such, EF-HR contains one of the largest clusters of handaxes at Olduvai, and highlights stark contrasts in assemblage composition across Middle and Upper Bed II. Since the role of hydraulic processes in the formation of EF-HR is well attested (de la Torre and Wehr, submitted), it might be tempting to attribute such a high density of handaxes in EF-HR to post-depositional factors. However, the fresh conditions of EF-HR handaxes indicate that water was not the prime agent of accumulation. Moreover, other handaxe-bearing Bed II deposits are also in channels – e.g., BK (Leakey, 1971; Sanchez-Yustos et al., 2016), SHK (Leakey, 1971; Diez-Martin et al., 2014); FLKW (Diez-Martin et al., 2015)–, and yet handaxe frequencies are far lower or negligible.

As evolutionary, techno-cultural and paleo-ecological dimensions of such variability have been reviewed elsewhere (de la Torre and Mora, 2014), given the revised chrono-stratigraphic position of EF-HR (McHenry, submitted), here we may briefly consider

diachronic aspects. Handaxe: retouched tool ratios have been used before to explore normative aspects of Acheulean variability (e.g., Isaac, 1977). Although core: handaxe (Bamforth and Becker, 2000) and handaxe: core (Parry and Kelly, 1987) ratios were designed to address reduction intensity and foraging mobility in very different archaeological contexts, to avoid any potential post-depositional bias at EF-HR (even when we argue that taphonomic factors are not responsible for handaxe accumulation) and other sites, comparisons can be normalised using such indices. Figure 27 makes a broad-brush comparison of Acheulean assemblages at Olduvai Gorge, and shows a strong time trend in the increase of handaxes to the detriment of cores from Bed II up to Masek, and a more nuanced pattern in LCT: retouch tool ratios. Interestingly, this pattern works not only at the level of the major time spans represented by sedimentary beds, but also (although more moderately, as would be expected) between more narrowly time-constrained intervals such as Middle and Upper Bed II.

While stressing the reductionist nature of the comparison (where site specifics thus cannot be considered), Fig. 27 provides a general picture whereby handaxe frequencies seem to show a diachronic trend. This could help better understand inter-assemblage variability at the onset of the Acheulean at Olduvai, particularly now that the chrono-stratigraphic position of EF-HR has been reconsidered. Of course, this does not preclude the contribution to such variability of other dimensions such as site function, length of occupation and assemblage formation, raw material constraints, paleo-ecological, paleo-geographical and even cultural factors. Attributing the large concentration of handaxes at EF-HR to diachronic trends only provides some clues to explain patterns that generated the concentration. Hominins accumulated over 75 kg of lava and metamorphic rocks shaped into handaxes at EF-HR, whereas at other sites only some handaxes were discarded. Future research should strive to provide a better understanding of what behaviour drives such differences in artefact discard patterns.

Conclusions

Once considered the world's earliest Acheulean site, EF-HR became one of the most emblematic assemblages at Olduvai Gorge due to the work undertaken by Mary Leakey (1971). Recent excavations by OGAP at the main locality and across the same stratigraphic interval in nearby outcrops (de la Torre et al., submitted), has provided new data on the chrono-stratigraphy (McHenry, submitted), sedimentology (Stanistreet et al., submitted) and formation processes (de la Torre and Wehr, submitted) of the site. Although now placed above Tuff IIC and therefore in Upper Bed II (McHenry, submitted; Stanistreet et al., submitted), EF-HR remains a pivotal site in understanding the origins of the Acheulean at Olduvai Gorge. It contains one of the largest stone tool assemblages for this period in East Africa which, combining the Leakey and OGAP collections, includes > 2700 artefacts (~284 kg), of which 133 are LCTs.

With over 2300 stone tools in stratigraphic position, the OGAP collection forms the greater part of the EF-HR assemblage. Our results highlight the co-occurrence of two reduction sequences in the same assemblage, one geared towards production of LCTs, and the other based on the flaking of small debitage. The small debitage chaîne opératoire is characterised by low- intensity reduction of cobbles that we presume were sourced locally. Knapping methods were expedient and, overall, small debitage flaking techniques are not dissimilar to

those documented in earlier Oldowan sites such as HWK EE (de la Torre and Mora, submitted), although the quality of resulting products (i.e., flakes) is higher at EF-HR.

Over 110 kg of worked stone are attributed to the LCT chaîne opératoire, which includes abundant debitage resulting from handaxe production and 100 LCTs collected during excavation. We hypothesize that most LCT blanks were produced off-site from high-quality large lava cobbles and boulders, although the shaping of handaxes and some LCT blank production may also have taken place on-site. Albeit generally debitage schemes were not elaborate, LCT blank production is considerably standardized, resulting in large flakes with remarkably similar morphometric characteristics. Such standardization continued during the façonnage stage which, again, is rather expedient (shaping is discontinuous and barely modifies the original morphology of blanks), but follows fixed rules that are applied systematically to every handaxe. We thus conclude that EF-HR hominins were combining debitage and façonnage patterns to produce specific LCT morphotypes. Although handaxe bifaciality, symmetry, refinement and resharpening are concepts alien to the EF-HR Acheulean, the interplay of standardized flaking and shaping schemes evidence the existence of carefully-designed mental and technical templates. Technological and cognitive requirements involved in the management of raw materials and stone tool production in EF-HR are considerably structured, and mark a genuine leap between the early Acheulean and the Oldowan, which may be linked potentially with the emergence of a new species –*Homo ergaster*/ *erectus*– and the demise of *Homo habilis*.

Acknowledgements

Fieldwork at EF-HR by OGAP was authorized by the Commission for Science and Technology (COSTECH), the Ngorongoro Conservation Area Authority, and the Department of Antiquities, Tanzania. Funding by the NSF (BCS-0852292) and the European Research Council-Starting Grants (283366) is acknowledged. Drawings by A. Theodoropoulou. We are grateful for their contributions to OGAP researchers and collaborators. Pioneering work by Mary Leakey at EF-HR inspired the study presented here.

References

Arroyo, A.,de la Torre, I., (submitted). Pounding tools in HWK EE and EF-HR (Olduvai Gorge, Tanzania): percussive activities in the Oldowan - Acheulean transition. J. Hum. Evol.

Bamforth, D.B., Becker, M.S., 2000. Core/Biface Ratios, Mobility, Refitting, and Artifact Use-Lives: A Paleoindian Example. Plains Anthropologist 45, 273-290.

Beyene, Y., Katoh, S., WoldeGabriel, G., Hart, W.K., Uto, K., Sudo, M., Kondo, M., Hyodo, M., Renne, P.R., Suwa, G., Asfaw, B., 2013. The characteristics and chronology of the earliest Acheulean at Konso, Ethiopia. Proc. Natl. Acad. Sci. 110, 1584-1591.

Bibi, F., Pante, M., Souron, A., Stewart, K., Varela, S., Werdelin, L., Boisserie, J.-R., Fortelius, M., Hlusko, L., Njau, J., de la Torre, I.(submitted). Mammals and Fish from the

Oldowan-Acheulean Transition at Olduvai Gorge, Tanzania, and the Paleoecology of the Serengeti J. Hum. Evol.

Bleed, P., Douglass, M., Sumner, A., Behrendt, M., Mackay, A., 2017. Photogrammetrical Assessment of Procedural Patterns and Sequential Structure in “Handaxe” Manufacture: A Case Study along the Doring River of South Africa. Lithic Technology, 1-10.

Bower, J.R.F., 1977. Attributes of Oldowan and Lower Acheulean tools: "tradition" and design in the Early Lower Palaeolithic. The South African Archaeological Bulletin 32, 113-126.

Callow, P., 1994. The Olduvai bifaces: technology and raw materials, in: Leakey, M.D., Roe, D.A. (Eds.), Olduvai Gorge. Volume 5. Excavations in Beds III, IV and the Masek Beds, 1968-1971. Cambridge University Press, Cambridge, pp. 235-253.

Clark, J.D., Kleindienst, M.R., 2001. The Stone Age cultural sequence: terminology, typology and raw material, in: Clark, J.D. (Ed.), Kalambo Falls Prehistoric Site, III: The Earlier Cultures: Middle and Earlier Stone Age. Cambridge University Press, Cambridge, pp. 34-65.

Dag, D., Goren-Inbar, N., 2001. An actualistic study of dorsally plain flakes: a technological note. Lithic Technology 26, 105-117.

de la Torre, I., 2009. Technological Strategies in the Lower Pleistocene at Peninj (West of Lake Natron, Tanzania), in: Schick, K., Toth, N. (Eds.), The Cutting Edge: New Approaches to the Archaeology of Human Origins. Stone Age Institute Press, Bloomington, pp. 93-113.

de la Torre, I., 2011. The Early Stone Age lithic assemblages of Gadeb (Ethiopia) and the Developed Oldowan / early Acheulean in East Africa. J. Hum. Evol. 60, 768-812.

de la Torre, I., 2016. The origins of the Acheulean: past and present perspectives on a major transition in human evolution. Philos Trans R Soc Lond B 371, 20150245.

de la Torre, I., Mora, R., 2005. Technological Strategies in the Lower Pleistocene at Olduvai Beds I & II. ERAUL 112, Liege.

de la Torre, I., Mora, R., 2014. The Transition to the Acheulean in East Africa: an Assessment of Paradigms and Evidence from Olduvai Gorge (Tanzania). Journal of Archaeological Method and Theory 21, 781–823.

de la Torre, I., Mora, R. (submitted). Oldowan technological behaviour at Olduvai Gorge, Tanzania: The HWK EE stone tool assemblage. J. Hum. Evol.

de la Torre, I., Mora, R., Arroyo, A., Benito-Calvo, A., 2014. Acheulean technological behaviour in the Middle Pleistocene landscape of Mieso (East-Central Ethiopia). J. Hum. Evol. 76, 1-25.

de la Torre, I., Mora, R., Domínguez-Rodrigo, M., Luque, L., Alcalá, L., 2003. The Oldowan industry of Peninj and its bearing on the reconstruction of the technological skills of Lower Pleistocene hominids. J. Hum. Evol. 44, 203-224.

de la Torre, I., Mora, R., Martínez-Moreno, J., 2008. The early Acheulean in Peninj (Lake Natron, Tanzania). J. Anth. Arch. 27, 244-264.

de la Torre, I., Albert, R.M., Macphail, R., McHenry, L., Pante, M., Rodríguez-Cintas, A., Stanistreet, I., Stollhofen, H. submitted. The contexts and early Acheulean archaeology of the EF-HR landscape (Olduvai Gorge, Tanzania). J. Hum. Evol.

de la Torre, I., Albert, R.M., Arroyo, A., Macphail, R., McHenry, L., Mora, R., Njau, J.K., Pante, M.C., Rivera Rondón, C., Rodríguez-Cintas, A., Stanistreet, I., Stollhofen, H., Wehr, K. submitted "b". New excavations at the HWK EE site: archaeology, palaeo-environment and site formation processes in the basal part of Middle Bed II (Olduvai Gorge, Tanzania). J. Hum. Evol.

de la Torre, I., Benito-Calvo, A., Proffitt, T., (2017). The impact of hydraulic processes in Olduvai Beds I and II, Tanzania, through a particle dimension analysis of stone tool assemblages. Geoarchaeology, XXX.

de la Torre, I., and Wehr, K. (submitted). Site formation processes of the early Acheulean assemblage at EF-HR (Olduvai Gorge, Tanzania). J. Hum. Evol.

Diez-Martín, F., Sánchez Yustos, P., Uribelarrea, D., Baquedano, E., Mark, D.F., Mabulla, A., Fraile, C., Duque, J., Díaz, I., Pérez-González, A., Yravedra, J., Egeland, C.P., Organista, E., Domínguez-Rodrigo, M., 2015. The Origin of The Acheulean: The 1.7 Million-Year-Old Site of FLK West, Olduvai Gorge (Tanzania). Scientific Reports 5, 17839.

Diez-Martín, F., Sánchez-Yustos, P., Uribelarrea, D., Domínguez-Rodrigo, M., Fraile-Márquez, C., Obregón, R.-A., Díaz-Muñoz, I., Mabulla, A., Baquedano, E., Pérez-González, A., Bunn, H.T., 2014. New archaeological and geological research at SHK main site (Bed II, Olduvai Gorge, Tanzania). Quatern. Intl. 322–323, 107-128.

Gallotti, R., 2013. An older origin for the Acheulean at Melka Kunture (Upper Awash, Ethiopia): Techno-economic behaviours at Garba IVD. J. Hum. Evol. 65, 594-620.

Gallotti, R., Mussi, M., 2015. The Unknown Oldowan: ~1.7-Million-Year-Old Standardized Obsidian Small Tools from Garba IV, Melka Kunture, Ethiopia. PLOS One 10, e0145101.

Goodwin, A.J.H., Lowe, C.V.-R., 1929. The Stone Age Cultures of South Africa. Annals of the South African Museum, nº XXVII, Edinburgh.

Goren-Inbar, N., Sharon, G., 2006. Invisible handaxes and visible Acheulian biface technology at Gesher Benot Ya'aqov, Israel, in: Goren-Inbar, N., Sharon, G. (Eds.), Axe Age. Acheulian Toolmaking from Quarry to Discard. Equinox, London, pp. 111-135.

Gowlett, J.A.J., 1979. Complexities of cultural evidence in the Lower and Middle Pleistocene. Nature 278, 14-17.

Gowlett, J.A.J., 1984. Mental Abilities of Early Man: A Look at Some Hard Evidence, in: Foley, R. (Ed.), Hominid Evolution and Community Ecology. Prehistoric Human Adaptation in Biological Perspective. Academic Press, London, pp. 167-192.

Gowlett, J.A.J., 1986. Culture and conceptualisation: the Oldowan-Acheulian gradient, in: Bailey, G.N., Callow, P. (Eds.), Stone Age Prehistory: studies in memory of Charles McBurney. Cambridge University Press, Cambridge, pp. 243-260.

Gowlett, J.A.J., 1988. A case of Developed Oldowan in the Acheulean? World Archaeology 20, 13-26.

Gowlett, J.A.J., 2006. The elements of design form in Acheulian bifaces: modes, modalities, rules and language, in: Goren-Inbar, N., Sharon, G. (Eds.), Axe Age. Acheulian Toolmaking from Quarry to Discard. Equinox, London, pp. 203-221.

Hay, R.L., 1976. Geology of the Olduvai Gorge. University of California Press, Berkeley.

Hayden, B., 1989. From chopper to celt: the evolution of resharpening techniques, in: Torrence, R. (Ed.), Time, energy and stone tools. Cambridge University Press, Cambridge, pp. 7-16.

Isaac, G.L., 1965. The Stratigraphy of the Peninj Beds and the Provenance of the Natron Australopithecine Mandible. Quaternaria 7, 101-130.

Isaac, G.L., 1967. The Stratigraphy of the Peninj Group- Early Middle Pleistocene Formations West of Lake Natron, Tanzania, in: Bishop, W.W., Clark, J.D. (Eds.), Background to Evolution in Africa. University of Chicago Press, Chicago, pp. 229-257.

Isaac, G.L., 1977. Olorgesailie. Archeological Studies of a Middle Pleistocene Lake Basin in Kenya. University of Chicago Press, Chicago.

Isaac, G.L., 1982. The earliest archaeological traces, in: Clark, J.D. (Ed.), Cambridge History of Africa. Volume 1. From the Earliest Times to c500 BC. Cambridge University Press, Cambridge, pp. 157-247.

Isaac, G.L., Harris, J.W.K., Kroll, E.M., 1997. The Stone Artefact Assemblages: A Comparative Study, in: Isaac, G.L. (Ed.), Koobi Fora Research Project. Volume 5: Plio-Pleistocene Archaeology. Oxford University Press, Oxford, pp. 262-362.

Jones, P.R., 1994. Results of experimental work in relation to the stone industries of Olduvai Gorge, in: Leakey, M.D., Roe, D.A. (Eds.), Olduvai Gorge. Volume 5. Excavations in Beds III, IV and the Masek Beds, 1968-1971. Cambridge University Press, Cambridge, pp. 254-298.

Jorayev, G., Wehr, K., Benito-Calvo, A., Njau, J., de la Torre, I. 2016. Imaging and photogrammetry models of Olduvai Gorge (Tanzania) by Unmanned Aerial Vehicles: A high-resolution digital database for research and conservation of Early Stone Age sites. J. Archaeol. Sci. 75, 40–56.

Kimura, Y., 2002. Examining time trends in the Oldowan technology at Beds I and II, Olduvai Gorge. J. Hum. Evol. 43, 291-321.

Kleindienst, M.R., 1962. Component of the East African Acheulian assemblage: an analytic approach, in: Mortelmans, G., Nenquin, J. (Eds.), Actes du IV Congrès Panafricain de Préhistoire et de l´Etude du Quaternaire, Leopoldville, 1959. Belgie Annalen, Musée Royal de l´Afrique Centrale, Tervuren, pp. 81-108.

Kuhn, S.L., 1991. "Unpacking" Reduction: Lithic Raw Material Economy in the Mousterian of West-Central Italy. Journal of Anthropological Archaeology 10, 76-106.

Laplace, G., 1972. La typologie analytique et structurale: Base rationnelle d'étude des industries lithiques et osseuses. Colloques nationaux du Centre National de la Recherche scientifique. Banques de données aechéologiques 932, 91-143.

Leader, G.M., Kuman, K., Gibbon, R.J., Granger, D.E. Early Acheulean organised core knapping strategies ca. 1.3 Ma at Rietputs 15, Northern Cape Province, South Africa. Quatern. Intl., in press

Leakey, M.D., 1971. Olduvai Gorge. Vol 3. Excavations in Beds I and II, 1960-1963. Cambridge University Press, Cambridge.

Leakey, M.D., 1975. Cultural Patterns in the Olduvai Sequence, in: Butzer, K.W., Isaac, G.L. (Eds.), After the Australopithecines. Stratigraphy, Ecology, and Cultural Change in the Middle Pleistocene. Mouton, Chicago, pp. 477-493.

Leakey, M.D., Roe, D.A., 1994. Olduvai Gorge. Volume 5. Excavations in Beds III, IV and the Masek Beds, 1968-1971. Cambridge University Press, Cambridge.

Lepre, C.J., Roche, H., Kent, D.V., Harmand, S., Quinn, R.L., Brugal, J.-P., Texier, P.-J., Lenoble, A., Feibel, C.S., 2011. An earlier origin for the Acheulian. Nature 477, 82-85.

Ludwig, B.V., 1999. A technological reassessment of East African Plio-Pleistocene lithic artifact assemblages. University of Rutgers, Unpublished Ph.D., New Brunswick.

Lycett, S.J., von Cramon-Taubadel, N., 2008. Acheulean variability and hominin dispersals: a model-bound approach. J. Archaeol. Sci. 35, 553-562.

McHenry, L., submitted. Tephrochronology of Bed II, Olduvai Gorge, Tanzania, and the chronology of the Oldowan-Acheulean transition. J. Hum. Evol.

McHenry, L., de la Torre, I. (submitted). Hominin raw material procurement in the Oldowan-Acheulean transition at Olduvai Gorge. J. Hum. Evol.

McNabb, J., 2017. Journeys in space and time. Assessing the link between Acheulean handaxes and genetic explanations. J. Archaeol. Sci.: Reports 13, 403-414.

McNabb, J., Binyon, F., Hazelwood, L., 2004. The Large Cutting Tools from the South African Acheulean and the Question of Social Traditions. Curr. Anthropol. 45, 653-677.

McNabb, J., Cole, J., 2015. The mirror cracked: Symmetry and refinement in the Acheulean handaxe. J. Archaeol. Sci.: Reports 3, 100-111.

McPherron, S.P., 2000. Handaxes as a Measure of the Mental Capabilities of Early Hominids. J. Archaeol. Sci. 27, 655-663.

Mora, R., Martínez, J., Terradas, X., 1991. Un proyeto de análisis: el Sistema Lógico Analítico (SLA), in: Mora, R., Terradas, X., Parpal, A., Plana, C. (Eds.), Tecnología y cadenas operativas líticas. Treballs d´Arqueologia, 1, Universidad Autónoma de Barcelona, Barcelona, pp. 173-199.

Mora, R., de la Torre, I., 2005. Percussion tools in Olduvai Beds I and II (Tanzania): Implications for early human activities. J. Anthropol. Archaeol. 24, 179-192.

Parry, W.J., Kelly, R.L., 1987. Expedient Core Technology and Sedentism, in: Johnson, J.K., Morrow, C.A. (Eds.), The Organization of Core Technology. Westview Press, Boulder and London, pp. 285-304.

Petraglia, M., Shipton, C., Paddayya, K., 2005. Life and mind in the Acheulean. A case study from India, in: Gamble, C., Porr, M. (Eds.), The hominid individual in context. Archaeological investigations of Lower and Middle Palaeolithic landsapes, locales and artefacts. Routledge, London, pp. 197-219.

Pope, M., Roberts, M., 2005. Observations on the relationship between Palaeolithic individuals and artefact scatters at the Middle Pleistocene site of Boxgrove, UK, in: Gamble, C., Porr, M. (Eds.), The hominid individual in context. Archaeological investigations of Lower and Middle Palaeolithic landsapes, locales and artefacts. Routledge, London, pp. 81-97.

Potts, R., Behrensmeyer, A.K., Ditchfield, P., 1999. Paleolandscape variation and Early Pleistocene hominid activities: Members 1 and 7, Olorgesailie Formation, Kenya. J. Hum. Evol. 37, 747-788.

Prassack, K., Pante, M.C., Njau, J.K., de la Torre, I. (submitted). The Paleoecology of Fossil Birds from Middle Bed II, at Olduvai Gorge, Tanzania J. Hum. Evol.

Quade, J., Levin, N.E., Simpson, S.W., Butler, R., McIntosh, W.C., Semaw, S., Kleinsasser, L., Dupont-Nivet, G., Renne, P.R., Dunbar, N., 2008. The geology of Gona, Afar, Ethiopia, in: Quade, J., Wynn, J.G. (Eds.), The Geology of Early Humans in the Horn of Africa. Geol. Soc. Am., Special Paper 446, pp. 1-31.

Roe, D.A., 1994. A metrical analysis of selected sets of handaxes and cleavers from Olduvai Gorge, in: Leakey, M.D., Roe, D.A. (Eds.), Olduvai Gorge. Volume 5. Excavations in Beds III, IV and the Masek Beds, 1968-1971. Cambridge University Press, Cambridge, pp. 146-234.

Sánchez-Yustos, P., Diez-Martín, F., Domínguez-Rodrigo, M., Fraile, C., Duque, J., Uribelarrea, D., Mabulla, A., Baquedano, E., 2016. Techno-economic human behavior in a context of recurrent megafaunal exploitation at 1.3 Ma. Evidence from BK4b (Upper Bed II, Olduvai Gorge, Tanzania). J. Archaeol. Sci.: Reports 9, 386-404.

Santonja, M., Panera, J., Rubio-Jara, S., Pérez-González, A., Uribelarrea, D., Domínguez-Rodrigo, M., Mabulla, A.Z.P., Bunn, H.T., Baquedano, E., 2014. Technological strategies and the economy of raw materials in the TK (Thiongo Korongo) lower occupation, Bed II, Olduvai Gorge, Tanzania. Quatern. Intl. 322–323, 181-208.

Semaw, S., Rogers, M.J., Stout, D., 2009. The Oldowan-Acheulian Transition: Is there a "Developed Oldowan" Artifact Tradition? in: Camps, M., Chauhan, P. (Eds.), Sourcebook of Paleolithic Transitions. Methods, Theories, and Interpretations. Springer, New York, pp. 173-193.

Sharon, G., 2009. Acheulian Giant-Core Technology. A Worldwide Perspective. Curr. Anthropol. 50, 335-367.

Shipton, C., 2016. Hierarchical Organization in the Acheulean to Middle Palaeolithic Transition at Bhimbetka, India. Cambridge Archaeological Journal 26, 601-618.

Shott, M.J., 1989. On Tool-Class Use Lives and the Formation of Archaeological Assemblages. Am. Antiq. 54, 9-30.

Stanistreet, I., Stollhofen, H., McHenry, L.J., de la Torre, I., submitted. Bed II Sequence Stratigraphic context of EF-HR and HWK EE archaeological sites, and the Oldowan/ Acheulean succession at Olduvai Gorge, Tanzania. J. Hum. Evol

Stiles, D., 1977. Acheulian and Developed Oldowan. The Meaning of Variability in the Early Stone Age. Mila 6, 1-35.

Stiles, D., 1980. Industrial Taxonomy in the Early Stone Age of Africa. Anthropologie XVIII, 189-207.

Stout, D., Apel, J., Commander, J., Roberts, M., 2014. Late Acheulean technology and cognition at Boxgrove, UK. J. Archaeol. Sc. 41, 576-590.

Texier, P.-J., Roche, H., 1995a. Polyèdre, sub-sphéroïde, sphéroïde et bola: des segments plus ou moins longs d´une même chaîne opératoire. Cahier Noir 7, 31-40.

Texier, P.-J., Roche, H., 1995b. The impact of predetermination on the development of some acheulean chaînes opératoires, in: Bermúdez de Castro, J.M., Arsuaga, J.L., Carbonell, E. (Eds.), Evolución humana en Europa y los yacimientos de la Sierra de Atapuerca, Vol 2. Junta de Castilla y León, Valladolid, pp. 403-420.

Tixier, J., 1956. Le hachereau dans l'Acheuléen Nord-Africain: notes typologiques, Congrès préhistorique de France: comptes rendus de la XVème session, Poitiers'Angoulème, July 15-22, 1956. Société Préhistorique Française, pp. 914-923.

Toth, N., 1982. The Stone Technologies of Early Hominids at Koobi Fora, Kenya; An Experimental Approach, Unpublished Ph. D., Berkeley, University of California.

Tuffreau, A., Lamotte, A., Marcy, J.-L., 1997. Land-Use and Site Function in Acheulean Complexes of the Somme Valley. World Archaeology 29, 225-241.

Wynn, T., 1979. The intelligence of later Acheulean hominids. Man 14, 371-391.

CAPTIONS

Figures

Figure 1. a) Aerial view of OGAP trenches in the main EF-HR outcrop, and their location at Olduvai Gorge. Outline of Olduvai Gorge and aerial photography after Jorayev et al. (2016). b) T2- Main Trench and T9 during the 2012 excavations. c) Handaxe in situ during the 2010 excavation of T2-Main Trench.

Figure 2. Handaxe attributes and terminology. a) Artefact with ID #249 from archaeological level 20 in Trench* 12 [T12-L20-249], as an example of conventions used in the analysis of LCTs [*Accession numbers where only level and artefact ID is noted and no trench is coded, belong to T2-Main Trench]. The morphological axis (i.e., major axis: white line in Fig. 2a) was considered as the length and used to orientate EF-HR artefacts, irrespective of the technological axis (i.e., point of percussion in flakes: green line in Fig. 2a). 'D' refers to scars from the debitage stage on the dorsal face. ('S') refers to façonnage/ shaping removals on the dorsal (direct retouch) and/or ventral (reverse retouch) sides. The shaping stage ('S') may include more than one series of scars superimposed over each other (S1, S2, S3…). Shaping is usually discontinuous along the edge, and absence of overlapping scars often prevents reconstruction of the chronological order of removals; thus, one single series of shaping (S1) may include several sets of scars (S1A, S1B, S1C…) for which the sequence is unknown. When possible, order of removals within each set on each series is shown (S1A-1, S1A-2,

S1A-3…), and blank rotation (clockwise or counter-clockwise) is noted. Colours are normally used to denote sequential order. Bars on all scales throughout the paper are 1 cm each (i.e., total scale length in Fig.2a is 5 cm). b) Tip shapes (redrawn from McNabb et al., 2004: 657). c) Handaxe shaping extent (redrawn from McNabb et al., 2004: 658). d) Base shapes of handaxes as defined in this paper. e) Symbols used in diacritic schemes: 1- Location of striking point on the flake butt. 2- Inferred location of butt. 3- Location of striking point on Siret (split) flake. 4- Flaking direction of scar with percussion point. 5- Flaking direction of scar where percussion point is absent. 6-Inferred flaking direction of scar. 7-Percussion point of scar on the adjacent flaking surface. 8- Location of scar lacking percussion point on the adjacent flaking surface.

Figure 3. The EF-HR stone tool assemblage.

Figure 4. a-b) Number of artefacts (a) and weight (b) per raw material in the whole assemblage (all artefacts from Intervals 1 and 2). Chert is not visible in Figure 4b due to its negligible representation in the assemblage. Data from Table 2. c-d) Number of artefacts (c) and weight (d) of relevant technological categories in the main EF-HR assemblage (i.e., non-rounded artefacts from Interval 1) per chaîne opératoire and raw material. Data from Tables 4 and 5. e) Factorial Correspondence Analysis of all technological categories in the main EF-HR assemblage. Data from Table 4.

Figure 5. Dimensional features of the main EF-HR assemblage. a-d) Length (a & b) and weight (c & d) of relevant categories in the chaînes opératoires of small debitage (a, c) and LCT production (b, d). e-f) Length-width scatterplots of all flakes per raw material (e) and chaîne opératoire (f). g-h) Length-width scatterplots of cores per raw material (g) and retouched tools per chaîne opératoire (h).

Figure 6. Dimensions and cortex coverage on whole flakes (a-d) and cores (f-h) of the small debitage chaîne opératoire at the main EF-HR assemblage. a & e) Mean size (mm) and weight (g) of whole flakes (a) and cores (e). b & f) Length classes of flakes (b) and cores (f). c) Flake striking platforms. d) Flake cortex coverage, following Toth's types. g) Core weight classes. h) Cortex coverage on cores.

Figure 7. Small flakes from small debitage (a) and LCT production (b-e). a) Whole flakes attributed to the small debitage reduction sequence. b) Small flakes from the LCT chaîne opératoire. c) Position of small flakes with complex dorsal patterns during LCT shaping. d) Position of Kombewa flakes in LCT shaping. e) Striking platform's view of small flakes during LCT shaping. [d & e: these are not refits but inferred origin of small flakes during handaxe shaping].

Figure 8. a) Intermediate flakes [see 3D models in SOM S3]. b) Core-edge intermediate flake alongside an LCT with similar dorsal patterning. c-d) Large unretouched flakes [3D models in SOM S4].

Figure 9. Bifacial lava cores [see 3D models in SOM S5]. a-d) Bifacial abrupt partial flaking scheme. e) Bifacial abrupt total. f) Bifacial simple partial.

Figure 10. Flaking schemes of small debitage cores. Abbreviations: TC: Test core. USP: Unifacial simple partial exploitation. USP2: Unifacial simple partial exploitation on two independent knapping surfaces. BSP: Bifacial simple partial. UAU1: Unidirectional abrupt unifacial exploitation on one knapping surface. UAU2: Unidirectional abrupt unifacial exploitation on two independent knapping surfaces. UAUT: Unifacial abrupt unidirectional total exploitation. UABI: Unifacial abrupt bidirectional. BAP: Bifacial abrupt partial. BALP: Bifacial alternating partial. BALT: Bifacial alternating total. UP: Unifacial peripheral. BP: Bifacial peripheral. UC: Unifacial centripetal. BHC: Bifacial hierarchical centripetal. [See de la Torre (2011), and de la Torre and Mora (submitted) for a detailed description of flaking scheme types].

Figure 11. Retouched tools from the small debitage (a-c) and LCT (d-i) chaînes opératoires. (a, d-f): sidescrapers. (b-c, g-i): denticulates. All are on flake/ flake fragments except Fig. 11h, on a quartzite block.

Figure 12. Dimensional and techno-typological features of Large Cutting Tools. Data from Tables 11-13.

Figure 13. Knives (a-d) and pick (e) with notched tips. a-b): single notch. c-e): double notch. a) [L2-1001] Debitage stage: the blank is an *éclat débordant* that removes two sides of the core. Façonnage stage: unifacial direct retouch, mostly on the edge opposite the butt, with one series of removals (S1) that does not follow a particular rotation order. b) [L2-2105] Debitage stage: edge-core, end-struck flake showing bifacial preparation of core edges. Façonnage stage: a single, unifacial sequence of shaping on the ventral side (S1). The entire series is counter clockwise, starting with small removals and ending with a large notch (S1-5) closer to the tip. c) [L2-355] Debitage stage: several scars show core rotation. The central scar is over 10 cm long and potentially corresponds to an earlier LCT blank. Façonnage stage: rhomboidal shaping, with denticulate direct retouch on the edge opposite the butt, and reverse retouch on the proximal edge that thins the butt. Two opposite, reverse removals create a double notch on the tip. d) [L2-549] Debitage stage: *éclat débordant* that removes part of the knapping platform on three sides of the core. Façonnage stage: rhomboidal shaping almost identical to Fig. 13c, with direct, denticulate retouch (S1A) opposite the butt, and thinning of the butt with reverse retouch (S1B) that also creates a notch next to the tip. e) [T13-L20-15]: Debitage stage: side-struck flake with remnants of unidirectional scars from

the core striking platform. Façonnage stage: bifacial retouch that thins the butt and shapes the base. Unifacial direct retouch to create a double notch at the tip. [yellow D: direct. R: reverse]. [See SOM S8 and S9 for 3D videos].

Figure 14. LCT production models. a) Role of small flakes in the preparation of convexities on flaking surfaces (#1) and flaking platforms (#2). b) Role of intermediate flakes in rejuvenating core edges (#3), and preparing convexities for LCT blank removal in both the flaking surface (#4) and flaking platform (#5). c) Removal of LCT blanks with thick butts that balance the mass towards the proximal section of flakes. c1-c2) T-Ta knives on side-struck flakes. c1) [L2-784] Debitage stage: dorsal face is fully cortical, and the only preparation is on the facetted butt. The striking platform is close to the proximal area (morphological orientation)/ left-hand corner of the LCT (technological orientation), and almost splits the cobble in two halves. Façonnage stage: mainly unifacial denticulate retouch opposite the butt on each edge of the LCT (S1A and S1B). c2) [L2-554] Debitage stage: the dorsal face was fully cortical when the blank was removed. The only removal attributed to the debitage stage is that producing a unifaceted butt. Façonnage stage: denticulate unifacial direct retouch mostly on the edge opposite the butt (series S1A), with few removals on the right edge (series S1B). No obvious directional shaping rotation with the exception of sequence S1A-1b, flaked counter- clockwise. [See 3D models in SOM S10].

Fig. 15. Unidirectional scheme of LCT blank production*. a-d) Trachyte-trachyandesite knives. a) [L2-48] Debitage stage: unidirectional removals from the core striking platform preserved on the multifaceted LCT butt. Façonnage stage: a series of removals (S1C), mostly unifacial, runs across the edge opposite the butt (i.e. typological right edge), whereas two isolated removals (S1A-1 and S1B-1) are on the edge associated with the butt (typological left edge), one of them (S1B-1) interpreted as a notch to shape the LCT tip (see other examples of notched LCTs in Fig. 13). b) [L2-1673] Debitage stage: same pattern as Fig 15a. Façonnage stage: denticulate removals on the edge opposite the butt (S1A), all unifacial except S1A-6, and in a clockwise direction. Sequential order of S1A with respect to the inverse notch on the opposite edge (S1B-1) is unknown. c) [L2-36] Debitage stage: same dorsal pattern as Figs. 15a-b, but in this case the butt was thinned. Façonnage stage: unifacial, direct retouch over most of the edge opposite the thinned butt (S1A). The other edge shows reverse retouch to thin the butt (S1B), and direct removals to create a notch (S1C). d) [L2-1326] Debitage stage: same dorsal pattern as Figs. 15a-b. Façonnage stage: denticulate bifacial retouch on the edge opposite the butt, and reverse notches at the tip. *Drawings and diacritics oriented according to the typological axis, sketches oriented on the technological axis. [See 3D models in SOM S11].

Figure 16. LCTs with evidence of core rotation. a) Phonolite knife [L2-2107]. Debitage stage: proximal and left lateral removals with respect to the LCT butt. Façonnage stage: retouch opposite the LCT striking platform (S1B), mostly direct with the exception of S1B-2 and S1B-4, which serve to thin the area of the butt. S1A-1 is an isolated direct notch associated with the tip. b) Possible cleaver of trachyte-trachyandesite [L2-866]. Debitage stage:

abundant proximal removals from the LCT butt, which runs through the entire edge of the piece, and is unifaceted. One scar has potentially been removed from the left lateral, indicating core rotation and preparation of the cleaver bit prior to LCT blank removal. Façonnage stage: a single shaping series (S1) of unifacial, direct retouch opposite the butt, and roughly following a counter clockwise sequence. c-d) Trachyte-trachyandesite knives. c) [L2-1077] Debitage stage: three removals (two of them of large and potentially from earlier LCT blanks) from different directions, indicating core rotation. Façonnage stage: the pointed tip is natural and shaping involved one single removal (S1-1). d) [L2-817] Debitage stage: size and shape of scars indicate the core was significantly large, rotated centripetally, and earlier LCT blanks potentially removed. Façonnage stage: unifacial reverse retouch to thin the butt (S1-1 to S1-6) and shape the tip (S1-7) made in a clockwise direction. Direct retouch was applied to shape the base (S2), also clockwise. [See 3D models in SOM S12].

Figure 17. a) Production of LCT blanks on *éclats débordants*. Fig. 17a1: Model of *éclat débordant* edge with mass concentrated on the side preserving part of the core edge (adapted from de la Torre et al., 2008). Fig. 17a2: Knife showing three planes of the core knapping platform (KP 1-3) that guide the shape of the LCT blank (diacritic drawing not to scale). b) Striking axis and shape of LCT blanks. c) Position of offset-axis flakes (*éclats déjetés*) on cores. d) Sequence of preparation at one end of cobbles, with core (Fig. 17d1) and LCTs with cortical (Fig. 17d2), partially flaked (Fig. 17d3) and bifacial (Fig. 17d4) ends. In these examples, the lateral part of cobbles forms the morphological base of handaxes and are all associated with one end of the butt.

Figure 18. Morphology of cores as deduced from LCT features. a-d) Trachyte-trachyandesite knives. a) [L2-665] Debitage stage: some scars could correspond either to debitage or shaping (hence 'D-S' on the photograph). If debitage, core rotation is evidenced by preparation removals which are proximally and distally (left) located with respect to the butt. Cortex covers part of the dorsal and lateral (right) side of the LCT. Façonnage stage: shaping starts on the ventral face, which shows thinning of the butt (S1). The subsequent series (S2) includes shaping of the tip on the ventral side, and denticulate retouch on the dorsal face on the edge opposite to the butt. b) [L2-835] Debitage stage: The angle of cortex on both ends of the knife and the morphology of the ventral face suggest that this blank nearly split the core in two halves. Façonnage stage: two unconnected shaping series. S1A is counter clockwise, commencing with alternating retouch at the base (S1A-1 to 3) followed by direct removals up to the tip (S1-8). Series S1B seems to run clockwise, and shows alternating thinning of the butt followed by a larger removal (S1B-7) around the tip. c) [L2-785] Debitage stage: a fully cortical flake was removed, nearly splitting the cobble in two halves. Façonnage stage: bifacial thinning of the striking platform (S1B), and unifacial reverse denticulate retouch on the edge opposite the butt (S1A). d) [L2-1079] Debitage stage: angle of the striking axis in sagittal view shows that the blank went through the entire thickness of the core, removing two of its ends (part of the knapping platform preserved on the butt, and the core base). Façonnage stage: direct retouch on the edge opposite the butt and on the proximal edge near the tip. [See 3D models in SOM S13].

Figure 19. Quartzite LCTs. a) Knife on flake [L2-1461], presumably from a Naibor Soit tabular core. Debitage stage: natural surfaces are preserved on three planes of the blank. Unidirectional scars from the core knapping platform run across the left edge (typological) of the LCT, which is entirely taken up by the butt. Façonnage stage: alternating retouch on the edge opposed the butt, including a large notch by the tip. It is unclear whether all removals on the typological left edge belong to the debitage stage, or if some correspond to shaping. b) Cleaver [T12-L20-261] Debitage stage: one single scar on a predominantly cortical dorsal face. Butt is dihedral and located on a corner of the blank (see striking axis in Fig. 17b). Façonnage stage: bifacial retouch of the base and part of the edge opposite the butt. c) Pick on side-struck flake [L2-634]. Debitage stage: the butt runs across the entire right (typological) edge of the LCT, with no visible debitage scars. Façonnage stage: alternating bifacial retouch in the edge opposite the butt, and reverse retouch on the opposite edge to thin the butt. d) Pick on tabular block [L2-941]. Shaping stage: the flat surface of a cleavage plane is used as a knapping platform for unifacial, non-invasive shaping around the entire circumference excepting the base, which remains cortical. [See 3D models in SOM S14].

Figure 20. a) Trachyte-trachyandesite pointed knives on side-struck flakes. b) Examples of "crescent-shape" knives on quartzite (left) and trachyte-trachyandesite (right), both on Siret flakes. c) Trachyte-trachyandesite cleavers. d) Trachyte-trachyandesite (top) and quartzite (bottom) picks.

Figure 21. A-d) Trachyte-trachyandesite knives. a) [L2-790] Debitage stage: side-struck flake with unidirectional scars from the striking platform. Façonnage stage: One series of direct removals (S1C) on the edge opposite the butt, and two clockwise series (S1A and S1B) on the butt edge. S1A thins part of the butt and creates a notch, and S1B is a short series of alternating removals on the other side of the butt. b) [L2-2106] Debitage stage: end-struck, mostly cortical flake with a wide-angled butt and a single unidirectional scar. Façonnage stage: rhomboidal shaping, with clockwise rotation on both edges. S1A is direct retouch on the right edge, and S1B reverse on the left edge. c) [L2-109] Debitage stage: several scars evidence a relatively structured knapping surface on the core. Façonnage stage: edge opposite the butt is shaped with direct, unifacial retouch (S1A). The striking platform edge shows bifacial alternating retouch (S1B), including a notch to create a tip. d) [L2-401] Debitage stage: very wide, short side-struck flake with one single scar. Façonnage stage: Series S1A shows clockwise, mostly unifacial, flaking of edge opposite the butt, and a reverse removal to create a notched tip (S1B-1). [See 3D models in SOM S15].

Figure 22. Picks. a-b) Trachyte-trachyandesite picks. a) [L2-572] Debitage stage: side-struck flake with only one clear scar, although the removal on the central ridge could also be part of the debitage phase. Façonnage stage: alternating retouch to thin the butt, and mostly unifacial direct retouch on the opposite edge. b) [L2-829] Debitage stage: side-struck flake, nearly a split cobble, with unidirectional scars from the butt that produced part of the triangular profile. Façonnage stage: shaping is unifacial, direct, generally clockwise, and restricted to the edge opposite the butt. c) Pick made on a phonolite cobble [L2-1800]. Façonnage stage:

the flat face of a plano-convex cobble is used as the striking platform for steep-angled scars that create a triangular section with removals on both edges. Retouching only runs through the medial and distal part of the cobble, where the trihedral tip is shaped. d) Pick on basalt flake [L1-142] Debitage stage: the butt runs across the entire edge (right side on the dorsal view), from which unidirectional flakes were struck prior to removal of the LCT blank. Façonnage stage: edge opposite the butt is shaped unifacially in the medial part, and bifacially in the tip area. [See 3D models in SOM S16].

Figure 23. A-c) Trachyte-trachyandesite cleavers. a) 'Type 0' cleaver [L2-5] Debitage stage: unidirectional scars from the butt edge in an otherwise cortical blank with an offset flaking axis. Flaking angle and cortex morphology suggest that the blank removed a significant part of the end opposite the core knapping platform. Façonnage stage: unifacial direct retouch on the edge opposite the butt, and reverse retouch on the butt side which shapes the edge adjacent to the butt. b) 'Type 1' cleaver [L2-949] Debitage stage: end-struck flake with two scars from opposite platforms (the distal scar producing the tranchet edge present on the subsequent LCT blank). Façonnage stage: one single direct removal on the right lateral edge. c) 'Type 2' cleaver [L2- 1667] Debitage stage: radial scars suggest preparation of the core knapping surface, including removal of a relatively large tranchet flake. Façonnage stage: alternating retouch to thin the butt, with a 'notch'-like removal close to the cleaver bit. d) Basalt knife with an unmodified, oblique end [T12-L20-185]. Debitage stage: side-struck flake removed from the lateral edge of a cobble core. Debitage is mostly unidirectional from the butt edge, except for a removal from an opposite knapping platform that forms an oblique 'tranchet'. Façonnage stage: the overall pointed shape of the LCT results from the debitage stage alone, and shaping removals only include a series on the dorsal edge on the edge opposite the butt (S2), plus reverse thinning of the butt at the base of the LCT. [See 3D models in SOM S17].

Figure 24. Bifacial retouched tools (a), biface (b) and typical knives (c-d) at EF-HR. a) Ultimately classified as retouched tools rather than LCTs due to their length <100 mm and relatively thin sections, these artefacts are morpho-technically and dimensionally similar to each other and to the biface in (b), but differ from the most common morphotype at EF-HR, i.e., knives (c-d). b) Trachyte-trachyandesite biface on flake [L1-125] c) Quartzite knife [L2-1328]. D) Basalt knife [T15-L22-9]. [See 3D models in SOM S18].

Figure 25. a-b) Length-width scatterplot of LCTs per class (a) and raw material (b). c) Principal component analysis of length and width of LCT classes per raw material. d) Detached: flaked ratios.

Figure 26. a) Typical small debitage core (2) compared to the average LCT on flake (1) at EF-HR. b) Broken tip and proximal/ medial part of a handaxe [these LCT fragments do not refit, but they are assembled together to illustrate their respective positions in the outline of the handaxe]. C) Main categories of LCT (#1-7) and small debitage (#8-10) chaînes

opératoires. #1: potential core* for LCT blank production. #2: LCTs. #3: large hammerstone. #4: unmodified LCT blanks. #5: intermediate flakes. #6: retouched tools on intermediate blanks. #7: small flakes attributed to LCT production. #8: small debitage cores. #9: small debitage flakes. #10: knapping hammerstone. [*Core #1 does not preserve evidence of LCT production, but its dimensions make it suitable for flaking of LCT blanks].

Figure 27. Ratios of LCTs, cores and retouched tools in selected Acheulean assemblages at Olduvai Gorge, and aggregated by main stratigraphic interval and Bed. Chrono-stratigraphic position of each assemblage is based on McHenry (submitted), Leakey (1971), Leakey and Roe (1994), and Hay (1976). Sources: FLKW (Diez-Martin et al., 2014); FCW-OF, SHK-Annexe, EF-HR, TKLF and TKUF (de la Torre and Mora, 2014); BK4b (Sanchez-Yustos et al., 2016); All Beds III to Masek sites (Leakey and Roe, 1994).

Tables

Table 1. The EF-HR lithic assemblage, including all artefacts from Intervals 1 and 2 in all trenches (see breakdowns by archaeological unit/ trench in de la Torre et al., submitted, Tables 7 and 8). Weight in grams (g).

Table 2. Absolute and relative frequencies of artefacts in the EF-HR lithic assemblage (including all trenches and intervals) per raw material, according to petrological identifications by McHenry and de la Torre (submitted).

Table 3. Total weight per category and raw material in the entire EF-HR lithic assemblage.

Table 4. Technological categories per general raw material and chaîne opératoire in the main EF-HR assemblage (i.e., Interval 1 only, and severely rounded lithics excluded).

Table 5. Total weight per category, chaîne opératoire and general raw material in the main EF-HR lithic assemblage.

Table 6. Dimensions of relevant technological categories in the small debitage chaîne opératoire.

Table 7. Dimensions of technological categories attributed to LCT production.

Table 8. Technological features of whole flakes in the reduction sequences of small debitage and LCT production (small and intermediate flakes, and LCT blanks), and those that cannot be determined (i.e., can be attributed to either chaîne opératoire).

Table 9. Technological attributes and flaking schemes of small debitage cores. * See Figure 10 for definition of abbreviations.

Table 10. Retouched tool types in the reduction sequences of small debitage and LCT production.

Table 11. Dimensional and technological attributes of LCTs.

Table 12. Shaping features of LCTs.

Table 13. Techno-morphological attributes of Large Cutting Tools. *Location of handling area is oriented with regards to the dorsal view of the handaxe with the tip on top. ** Base (proximal part) of the LCT is considered as the opposite end to the tip (distal part of the LCT).

Table 14. Dimensional features of LCTs per class and raw material.

Table 15. Ratios of debitage, cores, LCTs and retouched tools in the EF-HR assemblage (Interval 2, rounded and chert artefacts excluded). A.1. Number of flakes per core in the small debitage chaîne opératoire. A.2. Number of small flakes attributed to the LCT reduction sequence per handaxe. A.3. Total number of flakes irrespective of chaîne opératoire, per flaked artefact (both cores and LCTs). B.1. Number of small debitage flakes divided by number of scars counted on cores. B.2.1. Small flakes attributed to LCT production divided by shaping scar count on LCTs. B.2.2. Intermediate flakes divided by scars from the debitage stage on LCTs. B.3. Total number of flakes (irrespective of chaîne opératoire and size) divided by all scars (debitage and façonnage) on cores and LCTs. C.1.1. Number of small

debitage retouched tools per all potential blanks suitable for retouch (flakes, flake fragments and shatter) with dimensions equal to or above 17 mm, which is the length of the smallest retouched tool attributed to the small debitage chaîne opératoire. C.1.2. Number of retouched tools per flake and flake fragment in the small debitage reduction sequence, equal to or above 20 mm. C.1.3. Number of retouched tools per flake with length equal to or above 20 mm (as proposed by Kuhn, 1991), in the small debitage chaîne opératoire. C.2.1. Number of retouched tools on intermediate flake blanks, divided by the sum of intermediate complete flakes and fragments. C.2.2. Number of retouched tools on intermediate flake blanks, divided by number of intermediate flakes. D.1. Proportion of cores per LCT (Bamforth and Becker, 2000). D.2. Proportion of LCTs per core (Parry and Kelly, 1987) D.3. Proportion of LCTs per retouched tool (Isaac, 1977). E. Total length of cutting edge preserved on all artefacts, per core and LCT mass. [*count includes half the flakes not attributed to either reduction sequence] [**count includes all indeterminate flakes] [[***count includes all retouched tools irrespective of their chaîne opératoire].

Table 16. The EF-HR lithic assemblage from Leakey (1971) and OGAP (de la Torre et al., submitted) excavations. The OGAP assemblage includes the two intervals from all trenches, and follows results presented in this paper. The Leakey collection is presented according to analysis by de la Torre and Mora (2005, 2014).

Table_1

		Interval 1				Interval 2					
		Frequency		Weight		Frequency		Weight		Frequency	
		n	%	Sum	%	*n*	%	Sum	%	*n*	%
Detached	Flake	528	24.5	26420	12.2	48	29.3	1656	28.0	576	24.9
	Flake Frag	915	42.5	25829	11.9	79	48.2	1063	17.9	994	42.9
	Shatter <20 mm	242	11.2	218	0.1	17	10.4	11	0.2	259	11.2
	Shatter >20 mm	98	4.6	2065	1.0	7	4.3	220	3.7	105	4.5
	Total Detached	1783	82.8	54532	25.1	151	92.1	2949	49.8	1934	83.5
Flaked	Core	139	6.5	60002	27.7	5	3.0	1759	29.7	144	6.2
	Core Frag	12	0.6	2107	1.0	2	1.2	447	7.5	14	0.6
	Retouched Tool	49	2.3	4818	2.2	5	3.0	607	10.2	54	2.3
	Ret. Tool Frag	3	0.1	30	0.0		0.0		0.0	3	0.1
	LCT	100	4.6	56156	25.9		0.0		0.0	100	4.3
	LCT Frag	16	0.7	5305	2.4	1	0.6	163	2.8	17	0.7
	Split Cobble	1	0.0	434	0.2		0.0		0.0	1	0.0
	Total Flaked	320	14.9	128852	59.4	13	7.9	2976	50.2	333	14.4
Pounded	Pitted stone	2	0.1	2303	1.1		0.0		0.0	2	0.1
	Knap. Hammerst.	28	1.3	20429	9.4		0.0		0.0	28	1.2
	Knap. Ham. Frag	10	0.5	3099	1.4		0.0		0.0	10	0.4
	Other pounded	10	0.5	7764	3.6		0.0		0.0	10	0.4
	Total Pounded	50	2.3	33594	15.5		0.0		0.0	50	2.2
	Grand Total	**2153**	**92.9**	**216978**	**97.3**	**164**	**7.1**	**5925**	**2.7**	**2317**	**100.0**

Table_2

	Lava					Metamorphic								
	Phonolite	T-Ta	Basalt	Lava indet	Total lava	Quartzite	Quartz	Feldspar	Feldspatic rock	Pegmatite	Gneiss	Total metamorphic	Chert	Grand Total
Flake	91	60	245	1	397	170	2		2			174	5	576
Flake Frag	113	76	300	1	490	486	11	1	1	1		500	4	994
Shatter <20 mm	12	8	28		48	195	2	2				199	12	259
Shatter >20 mm	10	3	21		34	67		2				69	2	105
Detached	226	147	594	2	969	918	15	5	3	1		942	23	1934
Core	48	22	40		110	32			1			33	1	144
Core Frag	3	3	2		8	6						6		14
Retouched Tool	4	8	8		20	32	1					33	1	54
Ret. Tool Frag			2		2	1						1		3
LCT	7	31	40		78	22						22		100
LCT Frag	2	6	7		15	2						2		17
Split Cobble	1				1							0		1
Flaked	65	70	99		234	95	1		1			97	2	333
Pitted stone			2		2							0		2
Knapping hamm.	5	9	11		25	2					1	3		28
Knap. Ham. Frag	3	2	2		7	3						3		10
Other pounded	3	1	4		8	2						2		10
Pounded	11	12	19		42	7					1	8		50
Total (*n*)	**302**	**229**	**712**	**2**	**1245**	**1020**	**16**	**5**	**4**	**1**	**1**	**1047**	**25**	**2317**

	Phonolite	T-Ta	Basalt	Lava indet	Total lava	Quartzite	Quartz	Feldspar	Feldspatic rock	Pegmatite	Gneiss	Total metamorphic	Chert	Grand Total
Flake	30.1	26.2	34.4	50.0	31.9	16.7	12.5	0.0	50.0	0.0	0.0	16.6	20.0	24.9
Flake Frag	37.4	33.2	42.1	50.0	39.4	47.6	68.8	20.0	25.0	100.0	0.0	47.8	16.0	42.9
Shatter <20 mm	4.0	3.5	3.9	0.0	3.9	19.1	12.5	40.0	0.0	0.0	0.0	19.0	48.0	11.2
Shatter >20 mm	3.3	1.3	2.9	0.0	2.7	6.6	0.0	40.0	0.0	0.0	0.0	6.6	8.0	4.5
Detached	74.8	64.2	83.4	100.0	77.8	90.0	93.8	100.0	75.0	100.0	0.0	90.0	92.0	83.5
Core	15.9	9.6	5.6	0.0	8.8	3.1	0.0	0.0	25.0	0.0	0.0	3.2	4.0	6.2
Core Frag	1.0	1.3	0.3	0.0	0.6	0.6	0.0	0.0	0.0	0.0	0.0	0.6	0.0	0.6
Retouched Tool	1.3	3.5	1.1	0.0	1.6	3.1	6.3	0.0	0.0	0.0	0.0	3.2	4.0	2.3
Ret. Tool Frag	0.0	0.0	0.3	0.0	0.2	0.1	0.0	0.0	0.0	0.0	0.0	0.1	0.0	0.1
LCT	2.3	13.5	5.6	0.0	6.3	2.2	0.0	0.0	0.0	0.0	0.0	2.1	0.0	4.3
LCT Frag	0.7	2.6	1.0	0.0	1.2	0.2	0.0	0.0	0.0	0.0	0.0	0.2	0.0	0.7
Split Cobble	0.3	0.0	0.0	0.0	0.1	0.0	0.0	0.0	0.0	0.0	0.0	0.0	0.0	0.0
Flaked	21.5	30.6	13.9	0.0	18.8	9.3	6.3	0.0	25.0	0.0	0.0	9.3	8.0	14.4
Pitted stone	0.0	0.0	0.3	0.0	0.2	0.0	0.0	0.0	0.0	0.0	0.0	0.0	0.0	0.1
Knapping hamm.	1.7	3.9	1.5	0.0	2.0	0.2	0.0	0.0	0.0	0.0	100.0	0.3	0.0	1.2
Knap. Ham. Frag	1.0	0.9	0.3	0.0	0.6	0.3	0.0	0.0	0.0	0.0	0.0	0.3	0.0	0.4
Other pounded	1.0	0.4	0.6	0.0	0.6	0.2	0.0	0.0	0.0	0.0	0.0	0.2	0.0	0.4
Pounded	3.6	5.2	2.7	0.0	3.4	0.7	0.0	0.0	0.0	0.0	100.0	0.8	0.0	2.2
Total (%)	**13.0**	**9.9**	**30.7**	**0.1**	**53.7**	**44.0**	**0.7**	**0.2**	**0.2**	**0.0**	**0.0**	**45.2**	**1.1**	**100.0**

Table_3

	Lava					Metamorphic								
	Phonolite	T-Ta	Basalt	Lava indet	Total lava	Quartzite	Quartz	Feldspar	Feldspatic rock	Pegmatite	Gneiss	Total metamorphic	Chert	Grand Total
Flake	3573	6164	10791	9	20537	7450	10		69			7529	10	28076
Flake Frag	3072	3053	11227	90	17442	9341	32	1	60	3		9436	14	26892
Shatter <20 mm	6	3	19		29	185	2	3				189	10	228
Shatter >20 mm	212	653	561		1426	822		6				827	31	2284
Detached	6863	9873	22599	98	39434	17797	43	9	129	3		17982	66	57481
Core	15278	14182	23717		53177	8425			145			8569	15	61761
Core Frag	635	1324	257		2216	338						338		2554
Small Retouched	268	1310	1272		2850	2570	3					2573	1	5424
Small Ret. Frag			21		21	9						9		30
LCT	3980	18837	21206		44022	12134						12134		56156
LCT Frag	474	1699	2437		4610	858						858		5468
Split Cobble	434				434							0		434
Flaked	21069	37351	48910		107330	24333	3		145			24481	16	131828
Pitted stone			2303		2303							0		2303
Knapping hamm.	3828	7119	7665		18611	699					1119	1818		20429
Knap. Ham. Frag	752	688	1245		2685	414						414		3099
Other pounded	1536	991	3139		5666	2098						2098		7764
Pounded	6116	8797	14352		29265	3210					1119	4329		33594
Total (g)	**34048**	**56021**	**85861**	**98**	**176029**	**45341**	**46**	**9**	**274**	**3**	**1119**	**46792**	**82**	**222903**

	Phonolite	T-Ta	Basalt	Lava indet	Total lava	Quartzite	Quartz	Feldspar	Feldspatic rock	Pegmatite	Gneiss	Total metamorphic	Chert	Grand Total
Flake	10.5	11.0	12.6	8.6	11.7	16.4	21.0	0.0	25.2	0.0	0.0	16.1	12.3	12.6
Flake Frag	9.0	5.4	13.1	91.4	9.9	20.6	68.6	11.8	22.0	100.0	0.0	20.2	17.3	12.1
Shatter <20 mm	0.0	0.0	0.0	0.0	0.0	0.4	3.5	26.9	0.0	0.0	0.0	0.4	12.7	0.1
Shatter >20 mm	0.6	1.2	0.7	0.0	0.8	1.8	0.0	61.3	0.0	0.0	0.0	1.8	37.9	1.0
Detached	20.2	17.6	26.3	100.0	22.4	39.3	93.1	100.0	47.2	100.0	0.0	38.4	80.1	25.8
Core	44.9	25.3	27.6	0.0	30.2	18.6	0.0	0.0	52.8	0.0	0.0	18.3	18.6	27.7
Core Frag	1.9	2.4	0.3	0.0	1.3	0.7	0.0	0.0	0.0	0.0	0.0	0.7	0.0	1.1
Small Retouched	0.8	2.3	1.5	0.0	1.6	5.7	6.9	0.0	0.0	0.0	0.0	5.5	1.2	2.4
Small Ret. Frag	0.0	0.0	0.0	0.0	0.0	0.0	0.0	0.0	0.0	0.0	0.0	0.0	0.0	0.0
LCT	11.7	33.6	24.7	0.0	25.0	26.8	0.0	0.0	0.0	0.0	0.0	25.9	0.0	25.2
LCT Frag	1.4	3.0	2.8	0.0	2.6	1.9	0.0	0.0	0.0	0.0	0.0	1.8	0.0	2.5
Split Cobble	1.3	0.0	0.0	0.0	0.2	0.0	0.0	0.0	0.0	0.0	0.0	0.0	0.0	0.2
Flaked	61.9	66.7	57.0	0.0	61.0	53.7	6.9	0.0	52.8	0.0	0.0	52.3	19.9	59.1
Pitted stone	0.0	0.0	2.7	0.0	1.3	0.0	0.0	0.0	0.0	0.0	0.0	0.0	0.0	1.0
Knapping hamm.	11.2	12.7	8.9	0.0	10.6	1.5	0.0	0.0	0.0	0.0	100.0	3.9	0.0	9.2
Knap. Ham. Frag	2.2	1.2	1.4	0.0	1.5	0.9	0.0	0.0	0.0	0.0	0.0	0.9	0.0	1.4
Other pounded	4.5	1.8	3.7	0.0	3.2	4.6	0.0	0.0	0.0	0.0	0.0	4.5	0.0	3.5
Pounded	18.0	15.7	16.7	0.0	16.6	7.1	0.0	0.0	0.0	0.0	100.0	9.3	0.0	15.1
Total (%)	**15.3**	**25.1**	**38.5**	**0.0**	**79.0**	**20.3**	**0.0**	**0.0**	**0.1**	**0.0**	**0.5**	**21.0**	**0.0**	**100.0**

Table_4

	Small debitage								LCT production						Indet						Grand total	
	Lava		Metamorphic		Chert		Total		Lava		Metamorphic		Total		Lava		Metamorphic		Total			
	n	%	*n*	%	*n*	%	*n*	%	*n*	%	*n*	%	*n*	%	*n*	%	*n*	%	*n*	%	*n*	%
Flake	83	35.9	49	29.9	5	25.0	137	33.0	168	36.7	42	31.8	210	35.6	112	25.1	61	9.4	173	15.8	520	24.8
Flake Frag	34	14.7	62	37.8	4	20.0	100	24.1	179	39.1	54	40.9	233	39.5	229	51.2	337	52.0	566	51.7	899	42.8
Shatter <20 mm		0.0		0.0	8	40.0	8	1.9		0.0	1	0.8	1	0.2	40	8.9	187	28.9	227	20.7	236	11.2
Shatter >20 mm		0.0		0.0	1	5.0	1	0.2	3	0.7		0.0	3	0.5	25	5.6	55	8.5	80	7.3	84	4.0
Detached Total	117	50.6	111	67.7	18	90.0	246	59.3	350	76.4	97	73.5	447	75.8	406	90.8	640	98.8	1046	95.5	1739	82.8
Core	101	43.7	28	17.1	1	5.0	130	31.3		0.0		0.0		0.0		0.0		0.0		0.0	130	6.2
Core Frag	6	2.6	6	3.7		0.0	12	2.9		0.0		0.0		0.0		0.0		0.0		0.0	12	0.6
Retouched Tool	5	2.2	18	11.0	1	5.0	24	5.8	14	3.1	11	8.3	25	4.2		0.0		0.0		0.0	49	2.3
Ret. Tool Frag	1	0.4	1	0.6		0.0	2	0.5		0.0		0.0		0.0	1	0.2		0.0	1	0.1	3	0.1
LCT		0.0		0.0		0.0		0.0	78	17.0	22	16.7	100	16.9		0.0		0.0		0.0	100	4.8
LCT Frag		0.0		0.0		0.0		0.0	14	3.1	2	1.5	16	2.7		0.0		0.0		0.0	16	0.8
Split Cobble	1	0.4		0.0		0.0	1	0.2		0.0		0.0		0.0		0.0		0.0		0.0	1	0.0
Flaked Total	114	49.4	53	32.3	2	10.0	169	40.7	106	23.1	35	26.5	141	23.9	1	0.2		0.0	1	0.1	311	14.8
Pitted stone		0.0		0.0		0.0		0.0		0.0		0.0		0.0	2	0.4		0.0	2	0.2	2	0.1
Knapping hamm.		0.0		0.0		0.0		0.0	2	0.4		0.0	2	0.3	23	5.1	3	0.5	26	2.4	28	1.3
Knap. Ham. Frag		0.0		0.0		0.0		0.0		0.0		0.0		0.0	7	1.6	3	0.5	10	0.9	10	0.5
Other pounded		0.0		0.0		0.0		0.0		0.0		0.0		0.0	8	1.8	2	0.3	10	0.9	10	0.5
Pounded Total		0.0		0.0		0.0		0.0	2	0.4		0.0	2	0.3	40	8.9	8	1.2	48	4.4	50	2.4
Total	**231**	**11.0**	**164**	**7.8**	**20**	**1.0**	**415**	**19.8**	**458**	**21.8**	**132**	**6.3**	**590**	**28.1**	**447**	**21.3**	**648**	**30.9**	**1095**	**52.1**	**2100**	**100.0**

Table_5

	Small debitage								LCT production						Indet						Grand total	
	Lava		Metamorphic		Chert		Total		Lava		Metamorphic		Total		Lava		Metamorphic		Total			
	g	%	g	%	g	%	g	%	g	%	g	%	g	%	g	%	g	%	g	%	g	%
Flake	1378	2.5	476	5.3	10	18.2	1863	2.9	15864	18.7	5432	20.5	21295	19.1	2194	7.1	847	10.3	3041	7.8	26199	12.2
Flake Frag	387	0.7	401	4.5	14	25.5	802	1.3	14625	17.2	6047	22.8	20672	18.5	1871	6.0	2310	28.0	4181	10.7	25655	11.9
Shatter <20 mm		0.0		0.0	5	8.8	5	0.0		0.0	1	0.0	1	0.0	25	0.1	174	2.1	199	0.5	205	0.1
Shatter >20 mm		0.0		0.0	10	18.2	10	0.0	672	0.8		0.0	672	0.6	680	2.2	579	7.0	1259	3.2	1941	0.9
Detached Total	1765	3.2	876	9.8	39	70.7	2680	4.2	31161	36.7	11479	43.3	42640	38.2	4769	15.4	3911	47.5	8680	22.1	54000	25.1
Core	50728	92.3	7575	84.3	15	27.5	58318	91.1		0.0		0.0		0.0		0.0		0.0		0.0	58318	27.2
Core Frag	1769	3.2	338	3.8		0.0	2107	3.3		0.0		0.0		0.0		0.0		0.0		0.0	2107	1.0
Retouched Tool	276	0.5	187	2.1	1	1.8	464	0.7	2297	2.7	2056	7.8	4353	3.9		0.0		0.0		0.0	4818	2.2
Ret. Tool Frag	3	0.0	9	0.1		0.0	11	0.0		0.0		0.0		0.0	18	0.1		0.0	18	0.0	30	0.0
LCT		0.0		0.0		0.0		0.0	44022	51.8	12134	45.7	56156	50.4		0.0		0.0		0.0	56156	26.1
LCT Frag		0.0		0.0		0.0		0.0	4447	5.2	858	3.2	5305	4.8		0.0		0.0		0.0	5305	2.5
Split Cobble	434	0.8		0.0		0.0	434	0.7		0.0		0.0		0.0		0.0		0.0		0.0	434	0.2
Flaked Total	53211	96.8	8109	90.2	16	29.3	61335	95.8	50767	59.7	15048	56.7	65815	59.0	18	0.1		0.0	18	0.0	127168	59.2
Pitted stone		0.0		0.0		0.0		0.0		0.0		0.0		0.0	2303	7.4		0.0	2303	5.9	2303	1.1
Knapping hamm.		0.0		0.0		0.0		0.0	3075	3.6		0.0	3075	2.8	15536	50.2	1818	22.1	17354	44.3	20429	9.5
Knap. Ham. Frag		0.0		0.0		0.0		0.0		0.0		0.0		0.0	2685	8.7	414	5.0	3099	7.9	3099	1.4
Other pounded		0.0		0.0		0.0		0.0		0.0		0.0		0.0	5666	18.3	2098	25.5	7764	19.8	7764	3.6
Pounded Total		0.0		0.0		0.0		0.0	3075	3.6		0.0	3075	2.8	26191	84.5	4329	52.5	30520	77.8	33594	15.6
Total	**54975**	**25.6**	**8985**	**4.2**	**56**	**0.0**	**64015**	**29.8**	**85002**	**39.6**	**26528**	**12.4**	**111529**	**51.9**	**30978**	**14.4**	**8240**	**3.8**	**39218**	**18.3**	**214762**	**100.0**

Table_6

			Minimum	Maximum	Mean	Std. Deviation
Small flake	Total (*n* =134)	Length	16.0	68.0	34.4	11.2
		Width	8.0	62.0	25.2	9.1
		Thickness	2.0	29.0	11.0	4.7
		Weight	0.5	95.2	12.9	14.0
	Lava (*n* =80)	Length	21.0	68.0	37.1	11.4
		Width	11.0	62.0	27.3	9.4
		Thickness	4.0	29.0	11.2	4.6
		Weight	1.6	95.2	15.5	16.3
	Metamorphic (*n* =49)	Length	16.0	55.0	31.3	9.7
		Width	10.0	43.0	22.9	7.6
		Thickness	4.0	25.0	11.2	4.6
		Weight	1.7	33.2	9.7	8.3
	Chert (*n* =5)	Length	18.0	29.0	22.0	4.2
		Width	8.0	21.0	13.8	4.8
		Thickness	2.0	8.0	5.4	2.3
		Weight	0.5	3.4	2.0	1.2
Core	Total (*n* =130)	Length	35.0	181.0	81.6	23.7
		Width	21.0	137.0	66.6	19.5
		Thickness	19.0	120.0	52.1	18.1
		Weight	15.3	3165.4	448.6	470.5
	Lava (*n* =101)	Length	35.0	181.0	85.9	21.9
		Width	31.0	137.0	69.5	18.1
		Thickness	26.0	120.0	54.7	17.5
		Weight	33.5	3165.4	502.3	505.1
	Metamorphic (*n* =28)	Length	35.0	124.0	67.4	23.5
		Width	32.0	115.0	57.7	20.3
		Thickness	20.0	90.0	43.8	17.3
		Weight	20.9	960.7	270.5	248.7
	Chert (*n* =1)	Length	37.0	37.0	37.0	.
		Width	21.0	21.0	21.0	.
		Thickness	19.0	19.0	19.0	.
		Weight	15.3	15.3	15.3	.
Retouched tool	Total (*n* =24)	Length	17.0	72.0	37.3	13.9
		Width	8.0	44.0	26.2	10.3
		Thickness	4.0	25.0	12.6	5.8
		Weight	1.0	78.1	19.4	21.3
	Lava (*n* =5)	Length	48.0	72.0	58.0	10.0
		Width	35.0	44.0	40.6	3.5
		Thickness	17.0	25.0	21.0	2.9
		Weight	38.9	78.1	55.3	14.5
	Metamorphic (*n* =18)	Length	23.0	51.0	32.7	8.0
		Width	13.0	40.0	23.2	7.1
		Thickness	4.0	17.0	10.8	3.8
		Weight	1.6	39.2	10.4	9.0
	Chert (*n* =1)	Length	1.0	17.0	17.0	17.0
		Width	1.0	8.0	8.0	8.0
		Thickness	1.0	4.0	4.0	4.0
		Weight	1.0	1.0	1.0	1.0

Table_7

			Minimum	Maximum	Mean	Std. Deviation
Small flake	Total (*n* =131)	Length	22.0	97.0	57.8	14.8
		Width	9.0	68.0	37.9	10.8
		Thickness	4.0	38.0	16.0	6.4
		Weight	2.3	146.2	37.6	26.0
	Lava (*n* =110)	Length	22.0	97.0	58.0	15.1
		Width	9.0	68.0	38.5	11.2
		Thickness	4.0	38.0	16.1	6.7
		Weight	2.3	146.2	38.7	27.2
	Metamorphic (*n* =21)	Length	32.0	79.0	57.0	13.4
		Width	16.0	48.0	35.2	8.0
		Thickness	6.0	28.0	15.7	5.2
		Weight	5.9	71.1	31.7	17.7
Intermediate flake	Total (*n* =67)	Length	43.0	134.0	95.3	17.3
		Width	27.0	101.0	64.2	16.1
		Thickness	7.0	49.0	27.5	8.2
		Weight	10.7	389.6	173.1	87.7
	Lava (*n* =50)	Length	43.0	134.0	95.6	17.9
		Width	27.0	101.0	64.7	17.3
		Thickness	7.0	49.0	26.9	8.7
		Weight	10.7	384.6	170.5	89.7
	Metamorphic (*n* =17)	Length	70.0	134.0	94.4	15.9
		Width	36.0	80.0	62.6	11.9
		Thickness	21.0	42.0	29.2	6.4
		Weight	100.4	389.6	180.8	83.7
LCT blank	Total (*n* =12)	Length	92.0	152.0	122.4	17.6
		Width	43.0	104.0	76.7	17.5
		Thickness	29.0	62.0	43.3	11.9
		Weight	269.9	562.0	398.0	89.3
	Lava (*n* =8)	Length	92.0	152.0	122.8	21.1
		Width	56.0	104.0	80.9	17.2
		Thickness	29.0	60.0	40.4	10.7
		Weight	269.9	562.0	385.4	98.1
	Metamorphic (*n* =4)	Length	110.0	134.0	121.8	10.0
		Width	43.0	81.0	68.3	17.1
		Thickness	30.0	62.0	49.3	13.6
		Weight	344.8	508.0	423.2	74.4
Retouched tool	Total (*n* =25)	Length	38.0	138.0	92.9	21.4
		Width	23.0	95.0	58.5	17.6
		Thickness	9.0	45.0	29.0	8.2
		Weight	20.9	347.8	174.1	84.3
	Lava (*n* =14)	Length	73.0	109.0	90.2	11.5
		Width	23.0	77.0	56.4	13.7
		Thickness	21.0	45.0	30.2	7.6
		Weight	51.1	275.8	164.1	63.6
	Metamorphic (*n* =11)	Length	38.0	138.0	96.3	30.1
		Width	37.0	95.0	61.3	22.0
		Thickness	9.0	41.0	27.4	8.9
		Weight	20.9	347.8	186.9	107.1
LCT	Total (*n* =100)	Length	94.0	198.0	142.6	21.7
		Width	62.0	110.0	84.2	10.6
		Thickness	21.0	68.0	45.4	9.3
		Weight	267.4	1128.3	561.6	173.9
	Lava (*n* =78)	Length	94.0	198.0	144.0	22.0
		Width	62.0	110.0	84.4	11.0
		Thickness	25.0	68.0	45.7	9.6
		Weight	267.4	1128.3	564.4	176.9
	Metamorphic (*n* =22)	Length	96.0	186.0	137.6	20.5
		Width	67.0	106.0	83.4	8.8
		Thickness	21.0	61.0	44.2	8.6
		Weight	320.1	1005.6	551.5	166.4

Table_8

		Small debitage								LCT production						Indet				Total	
		Lava		Metamorphic		Chert		Total		Lava		Metamorphic		Total		Lava		Metamorphic			
		n	%	*n*	%	*n*	%	*n*	%	*n*	%	*n*	%	*n*	%	*n*	%	*n*	%	*n*	%
Length classes	<20 mm		0.0	3	6.1	1	20.0	4	2.9		0.0		0.0	0	0.0	6	5.4	9	14.8	19	3.7
	20-39 mm	50	60.2	37	75.5	4	80.0	91	66.4	14	8.3	1	2.4	15	7.1	50	44.6	26	42.6	182	35.0
	40-59 mm	26	31.3	9	18.4		0.0	35	25.5	41	24.4	9	21.4	50	23.8	37	33.0	26	42.6	148	28.5
	60-79 mm	6	7.2		0.0		0.0	6	4.4	53	31.5	14	33.3	67	31.9	19	17.0		0.0	92	17.7
	80-99 mm	1	1.2		0.0		0.0	1	0.7	36	21.4	8	19.0	44	21.0		0.0		0.0	45	8.7
	100-119 mm		0.0		0.0		0.0	0	0.0	17	10.1	7	16.7	24	11.4		0.0		0.0	24	4.6
	120-139 mm		0.0		0.0		0.0	0	0.0	5	3.0	3	7.1	8	3.8		0.0		0.0	8	1.5
	140-159 mm		0.0		0.0		0.0	0	0.0	2	1.2		0.0	2	1.0		0.0		0.0	2	0.4
	Total	83	16.0	49	9.4	5	1.0	137	100.0	168	32.3	42	8.1	210	100.0	112	21.5	61	11.7	520	100.0
Striking platform preparation	Non-faceted	15	20.5	4	8.5	2	40.0	21	16.8	13	8.2	7	16.7	20	10.0	18	18.2	6	12.8	65	13.8
	Unifaceted	54	74.0	40	85.1	3	60.0	97	77.6	117	74.1	32	76.2	149	74.5	74	74.7	36	76.6	356	75.6
	Bifaceted	2	2.7	3	6.4		0.0	5	4.0	19	12.0		0.0	19	9.5	7	7.1	3	6.4	34	7.2
	Multifaceted	2	2.7		0.0		0.0	2	1.6	9	5.7	3	7.1	12	6.0		0.0	2	4.3	16	3.4
	Total	73	15.5	47	10.0	5	1.1	125	100.0	158	33.5	42	8.9	200	100.0	99	21.0	47	10.0	471	100.0
Dorsal side cortex	Cortical	8	10.7		0.0	1	20.0	9	7.0	4	2.4	2	4.9	6	2.9	9	8.7	1	1.8	25	5.1
	Cortex >50%	10	13.3	3	6.1		0.0	13	10.1	14	8.5	10	24.4	24	11.7	10	9.7	1	1.8	48	9.7
	Cortex <50%	23	30.7	13	26.5	2	40.0	38	29.5	35	21.3	8	19.5	43	21.0	12	11.7	12	21.4	105	21.3
	Non-cortical	34	45.3	33	67.3	2	40.0	69	53.5	111	67.7	21	51.2	132	64.4	72	69.9	42	75.0	315	63.9
	Total	75	15.2	49	9.9	5	1.0	129	100.0	164	33.3	41	8.3	205	100.0	103	20.9	56	11.4	493	100.0
Toth's flakes	I	2	2.9		0.0	1	20.0	3	2.5		0.0	1	2.4	1	0.5	4	4.2		0.0	8	1.7
	II	7	10.0	4	8.5	1	20.0	12	9.8	5	3.2	3	7.3	8	4.1	6	6.3		0.0	26	5.6
	III	5	7.1		0.0		0.0	5	4.1	8	5.1	3	7.3	11	5.6	7	7.4	6	12.8	29	6.3
	IV	5	7.1		0.0		0.0	5	4.1	3	1.9	1	2.4	4	2.0	4	4.2	1	2.1	14	3.0
	V	25	35.7	12	25.5	1	20.0	38	31.1	42	26.9	15	36.6	57	28.9	14	14.7	11	23.4	120	26.0
	VI	26	37.1	31	66.0	2	40.0	59	48.4	98	62.8	18	43.9	116	58.9	60	63.2	29	61.7	264	57.3
	Total	70	15.2	47	10.2	5	1.1	122	100.0	156	33.8	41	8.9	197	100.0	95	20.6	47	10.2	461	100.0
Flake types	Regular flake	71	85.5	41	83.7	4	80.0	116	84.7	159	94.6	41	97.6	200	95.2	111	99.1	61	100.0	488	93.8
	Core/ LCT edge flake	12	14.5	1	2.0	1	20.0	14	10.2	9	5.4	1	2.4	10	4.8	1	0.9		0.0	25	4.8
	Bipolar flake		0.0	7	14.3		0.0	7	5.1		0.0		0.0	0	0.0		0.0		0.0	7	1.3
	Total	83	16.0	49	9.4	5	1.0	137	100.0	168	32.3	42	8.1	210	100.0	112	21.5	61	11.7	520	100.0

Table_9

		Lava		Metamorphic		Chert		Total	
		n	%	*n*	%	*n*	%	*n*	%
Length class	20-39 mm	1	1.0	4	14.3	1	100.0	6	4.6
	40-59 mm	5	5.0	6	21.4		0.0	11	8.5
	60-79 mm	35	34.7	11	39.3		0.0	46	35.4
	80-99 mm	40	39.6	4	14.3		0.0	44	33.8
	100-119 mm	13	12.9	2	7.1		0.0	15	11.5
	120-139 mm	4	4.0	1	3.6		0.0	5	3.8
	>140 mm	3	3.0		0.0		0.0	3	2.3
	Total	101	77.7	28	21.5	1	0.8	130	100.0
Weight class	<50 g	1	1.0	6	21.4	1	100.0	8	6.2
	50-100 g	4	4.0	4	14.3		0.0	8	6.2
	101-200 g	11	10.9	4	14.3		0.0	15	11.5
	201-400 g	39	38.6	6	21.4		0.0	45	34.6
	401-800 g	34	33.7	6	21.4		0.0	40	30.8
	801-1600 g	8	7.9	2	7.1		0.0	10	7.7
	> 1600 g	4	4.0		0.0		0.0	4	3.1
	Total	101	77.7	28	21.5	1	0.8	130	100.0
Cortex	Cortex >50%	67	69.8	7	25.9		0.0	74	59.7
	Cortex <50%	20	20.8	11	40.7	1	100.0	32	25.8
	Non-cortical	9	9.4	9	33.3		0.0	18	14.5
	Total	96	100.0	27	100.0	1	100.0	124	100.0
Blank	Cobble	75	90.4	6	33.3		0.0	81	79.4
	Block	2	2.4	4	22.2		0.0	6	5.9
	Fragment	6	7.2	5	27.8	1	100.0	12	11.8
	Flake		0.0	3	16.7		0.0	3	2.9
	Total	83	81.4	18	17.6	1	1.0	102	100.0
Battering	Esquillées	3	3.6	4	14.8		0.0	7	6.3
	Impacts	24	28.6	14	51.9		0.0	38	33.9
	Absent	57	67.9	9	33.3	1	100.0	67	59.8
	Total	84	75.0	27	24.1	1	0.9	112	100.0
Number of scars	1-3 scars	25	30.1	6	25.0		0.0	31	29.0
	4-6 scars	42	50.6	12	50.0		0.0	54	50.5
	7-9 scars	11	13.3	1	4.2		0.0	12	11.2
	> 9 scars	5	6.0	5	20.8		0.0	10	9.3
	Total	83	77.6	24	22.4		0.0	107	100.0
Flaking method*	TC	12	12.2	2	7.4		0.0	14	11.1
	USP	5	5.1	1	3.7		0.0	6	4.8
	BSP	10	10.2	2	7.4		0.0	12	9.5
	UAU1	12	12.2	1	3.7		0.0	13	10.3
	UAU2	9	9.2	1	3.7	1	100.0	11	8.7
	UAUT		0.0	2	7.4		0.0	2	1.6
	UABI	1	1.0		0.0		0.0	1	0.8
	BAP	24	24.5		0.0		0.0	24	19.0
	BALP	8	8.2	1	3.7		0.0	9	7.1
	UP	4	4.1		0.0		0.0	4	3.2
	BP	4	4.1		0.0		0.0	4	3.2
	DISC		0.0	2	7.4		0.0	2	1.6
	POL		0.0	1	3.7		0.0	1	0.8
	MLT	6	6.1	5	18.5		0.0	11	8.7
	BIPO	2	2.0	9	33.3		0.0	11	8.7
	BIPCO	1	1.0					1	0.8
	Total	98	77.8	27	21.6	1	0.8	126	100.0

Table_10

	Small debitage				LCT production			Total
	Lava	Metamorphic	Chert	Total	Lava	Metamorphic	Total	
Pointed tool					1		1	1
Denticulate	3	7		10	4	5	9	19
Notch		2		2		1	1	3
Sidescraper		7	1	8	4	5	9	17
Total (*n*)	3	16	1	20	9	11	20	40
Pointed tool	0.0	0.0	0.0	0.0	11.1	0.0	5.0	2.5
Denticulate	100.0	43.8	0.0	50.0	44.4	45.5	45.0	47.5
Notch	0.0	12.5	0.0	10.0	0.0	9.1	5.0	7.5
Sidescraper	0.0	43.8	100.0	40.0	44.4	45.5	45.0	42.5
Total (%)	7.5	40.0	2.5	50.0	22.5	27.5	50.0	100.0

Table_11

			Lava		Metamorphic		Total	
			n	%	*n*	%	*n*	%
Dimensions	Length interval	94-119 mm	7	9.0	4	18.2	11	11.0
		120-139 mm	29	37.2	8	36.4	37	37.0
		140-159 mm	20	25.6	8	36.4	28	28.0
		160-179 mm	18	23.1	1	4.5	19	19.0
		180-199 mm	4	5.1	1	4.5	5	5.0
		Total	78	100.0	22	100.0	100	100.0
	Weight interval	201-400 g	17	21.8	5	22.7	22	22.0
		401-600 g	30	38.5	9	40.9	39	39.0
		601-800 g	24	30.8	7	31.8	31	31.0
		801-1000 g	6	7.7		0.0	6	6.0
		1001-1200 g	1	1.3	1	4.5	2	2.0
		Total	78	100.0	22	100.0	100	100.0
Blank configuration	Cortex	Cortical	1	1.3	1	4.5	2	2.0
		Cortex >50%	18	23.1	5	22.7	23	23.2
		Cortex <50%	33	42.3	9	40.9	42	42.4
		Non-cortical	25	32.1	7	31.8	32	32.3
		Total	78	100.0	22	100.0	99	100.0
	Type of blank	Side-struck flake	57	73.1	13	59.1	70	70.0
		End-struck flake	15	19.2	5	22.7	20	20.0
		Cobble	3	3.8	1	4.5	4	4.0
		Block		0.0	2	9.1	2	2.0
		Indet	3	3.8	1	4.5	4	4.0
		Total	78	100.0	22	100.0	100	100.0
	Butt	Cortical	4	5.9	5	31.3	9	10.7
		Unifaceted	25	36.8	6	37.5	31	36.9
		Bifaceted	8	11.8	2	12.5	10	11.9
		Multifaceted	11	16.2	3	18.8	14	16.7
		Thinned	20	29.4		0.0	20	23.8
		Total	68	100.0	16	100.0	84	100.0
	Dorsal removals	1-3 scars	36	56.3	14	93.3	50	63.3
		4-6 scars	25	39.1	1	6.7	26	32.9
		>6 scars	3	4.7		0.0	3	3.8
		Total	64	100.0	15	100.0	79	100.0
Faconnage stage	Shaping	No shaping	2	2.6		0.0	2	2.0
		Unifacial	54	70.1	16	72.7	70	70.7
		Bifacial	21	27.3	6	27.3	27	27.3
		Total	77	100.0	22	100.0	99	100.0
	Shaping removals	1-3 scars	16	22.2	4	18.2	20	21.3
		4-6 scars	20	27.8	7	31.8	27	28.7
		7-9 scars	21	29.2	7	31.8	28	29.8
		>9 scars	15	20.8	4	18.2	19	20.2
		Total	72	100.0	22	100.0	94	100.0

Table_12

		Dorsal		Ventral		Dorsal+ventral	
		n	%	*n*	%	*n*	%
Shaping	Present	86	90.5	64	67.4	150	78.9
n =95	Absent	9	9.5	31	32.6	40	21.1
Shaping removals	Nil	5	5.3	28	29.8	33	17.6
	1-3 scars	39	41.5	33	35.1	72	38.3
	4-6 scars	33	35.1	26	27.7	59	31.4
	7-9 scars	16	17.0	5	5.3	21	11.2
	> 9 scars	1	1.1	2	2.1	3	1.6
Shaping extent	SE 1		0.0		0.0	0	0.0
n =88	SE 2	5	5.7	3	4.6	8	5.2
	SE 3	83	94.3	59	90.8	142	92.8
	SE 4		0.0	2	3.1	2	1.3
	SE 5		0.0	1	1.5	1	0.7
Location of shaping	Whole perimeter	33	37.5	20	30.8	53	34.6
n =88	Distal & Medial	20	22.7	9	13.8	29	19.0
	Distal & Proximal	2	2.3	1	1.5	3	2.0
	Distal	5	5.7	4	6.2	9	5.9
	Medial & Proximal	5	5.7	10	15.4	15	9.8
	Medial	21	23.9	15	23.1	36	23.5
	Proximal	2	2.3	6	9.2	8	5.2
Shaping angle	Flat	2	2.3	17	26.2	19	12.4
n =88	Simple	74	84.1	46	70.8	120	78.4
	Abrupt	12	13.6	2	3.1	14	9.2
Trimming	Present	4	4.6	5	5.7	9	5.2
n =87	Absent	83	95.4	82	94.3	165	94.8

Table_13

			Lava		Metamorphic		Total	
			n	%	*n*	%	*n*	%
LCT type	Knife	Unifacial	45	57.7	6	27.3	51	51.0
		Bifacial	14	17.9	4	18.2	18	18.0
		Total Knife	59	75.6	10	45.5	69	69.0
	Pick	Unifacial	4	5.1	6	27.3	10	10.0
		Bifacial	4	5.1		0.0	4	4.0
		Total Pick	8	10.3	6	27.3	14	14.0
	Cleaver	No shaping	1	1.3		0.0	1	1.0
		Unifacial	5	6.4	3	13.6	8	8.0
		Total Cleaver	6	7.7	3	13.6	9	9.0
	Biface		3	3.8	2	9.1	5	5.0
	Other		2	2.6	1	4.5	3	3.0
		Total	78	78.0	22	22.0	100	100.0
Tip notch	Single notch	Direct	14	19.4	6	28.6	20	21.5
		Reverse	10	13.9		0.0	10	10.8
	Double notch	Direct-Direct	6	8.3	1	4.8	7	7.5
		Direct-Reverse	7	9.7		0.0	7	7.5
		Reverse-Reverse	3	4.2		0.0	3	3.2
	Notch absent		32	44.4	14	66.7	46	49.5
		Total	72	100.0	21	100.0	93	100.0
Tip shape	TS-1		51	69.9	16	76.2	67	71.3
	TS-2		10	13.7		0.0	10	10.6
	TS-3		4	5.5	1	4.8	5	5.3
	TS-4		2	2.7	1	4.8	3	3.2
	TS-5		4	5.5	2	9.5	6	6.4
	TS-6		1	1.4	1	4.8	2	2.1
	TS-7		1	1.4		0.0	1	1.1
		Total	73	100.0	21	100.0	94	100.0
Handling area	Present	Cortical	12	15.8	2	9.1	14	14.3
		Steep plane	13	17.1	4	18.2	17	17.3
		Butt	37	48.7	15	68.2	52	53.1
		Siret	2	2.6	1	4.5	3	3.1
	Absent		12	15.8		0.0	12	12.2
		Total	76	100.0	22	100.0	98	100.0
Location handling area*	Left		13	20.3	4	18.2	17	19.8
	Proximal		27	42.2	9	40.9	36	41.9
	Right		24	37.5	9	40.9	33	38.4
		Total	64	100.0	22	100.0	86	100.0
Base shape**	Concave		1	1.3		0.0	1	1.0
	Convex		27	35.5	6	28.6	33	34.0
	Dihedral		15	19.7	3	14.3	18	18.6
	Pointed		7	9.2	2	9.5	9	9.3
	Straight		26	34.2	10	47.6	36	37.1
		Total	76	100.0	21	100.0	97	100.0

Table_14

All LCTs	Knife	*n*= 69	Pick	*n*= 14	Cleaver	*n*= 9	Biface	*n*= 5	Other LCT	*n*= 3	Total	*n*= 100
	Mean	Std. D.	Mean	Std. D.	Mean	Std. D.	Mean	Std. D.	Mean	Std. D.	Mean	Std. D.
Length	144.28	18.68	146.64	26.29	144.67	24.80	116.60	21.16	122.67	34.20	142.61	21.74
Breadth	85.43	10.34	78.86	11.99	89.44	6.43	79.80	5.26	71.67	7.64	84.18	10.55
Thickness	44.90	8.98	46.79	11.59	45.22	9.37	49.40	11.50	43.33	5.03	45.37	9.35
Weight grams	552.63	157.54	586.49	204.61	677.21	195.00	513.98	212.01	383.03	138.02	561.56	173.95
Elongation (L/B)	1.70	0.23	1.87	0.31	1.62	0.29	1.46	0.22	1.73	0.52	1.71	0.26
Refinement (T/B)	0.53	0.12	0.60	0.16	0.50	0.08	0.62	0.15	0.61	0.12	0.55	0.13
Breadth/ Thickness	1.98	0.46	1.82	0.67	2.06	0.46	1.67	0.32	1.68	0.37	1.94	0.49
Thickness/ Breadth	0.53	0.12	0.60	0.16	0.50	0.08	0.62	0.15	0.61	0.12	0.55	0.13
Length/ Weight	0.28	0.06	0.27	0.06	0.22	0.03	0.24	0.06	0.33	0.02	0.27	0.06
Edge length	172.42	74.89	121.83	58.45	209.38	93.94	192.00	46.67	113.00	.	162.55	81.11
Lava	Knife	*n*= 59	Pick	*n*= 8	Cleaver	*n*= 6	Biface	*n*= 3	Other LCT	*n*= 2	Total	*n*= 78
	Mean	Std. D.	Mean	Std. D.	Mean	Std. D.	Mean	Std. D.	Mean	Std. D.	Mean	Std. D.
Length	144.80	18.54	147.50	32.75	146.67	30.95	122.67	25.01	131.00	43.84	144.01	22.01
Breadth	85.41	10.27	78.38	15.42	90.17	7.99	80.67	7.23	67.50	3.54	84.41	11.03
Thickness	44.51	9.08	51.50	9.81	45.00	11.54	55.00	12.12	46.00	2.83	45.71	9.56
Weight grams	546.02	154.60	638.56	244.00	670.42	241.49	615.73	223.44	414.50	179.32	564.39	176.95
Elongation (L/B)	1.71	0.23	1.89	0.34	1.64	0.37	1.52	0.26	1.93	0.55	1.72	0.26
Refinement (T/B)	0.53	0.13	0.67	0.14	0.49	0.10	0.69	0.17	0.68	0.01	0.55	0.14
Breadth/ Thickness	2.00	0.47	1.58	0.51	2.12	0.56	1.51	0.33	1.47	0.01	1.93	0.50
Thickness/ Breadth	0.53	0.13	0.67	0.14	0.49	0.10	0.69	0.17	0.68	0.01	0.55	0.14
Length/ Weight	0.28	0.06	0.25	0.06	0.23	0.04	0.21	0.04	0.32	0.03	0.27	0.06
Edge length	168.42	64.47	123.33	61.62	252.00	96.56	.	.	.	.	163.00	78.30
Metamorphic	Knife	*n*= 10	Pick	*n*= 6	Cleaver	*n*= 3	Biface	*n*= 2	Other LCT	*n*= 1	Total	*n*= 22
	Mean	Std. D.	Mean	Std. D.	Mean	Std. D.	Mean	Std. D.	Mean	Std. D.	Mean	Std. D.
Length	141.20	20.24	145.50	17.09	140.67	5.51	107.50	16.26	106.00	.	137.64	20.49
Breadth	85.60	11.35	79.50	6.35	88.00	1.00	78.50	0.71	80.00	.	83.36	8.80
Thickness	47.20	8.42	40.50	11.47	45.67	4.16	41.00	0.00	38.00	.	44.18	8.64
Weight grams	591.62	177.50	517.05	123.98	690.80	76.76	361.35	47.87	320.10	.	551.53	166.45
Elongation (L/B)	1.66	0.24	1.84	0.29	1.60	0.06	1.37	0.19	1.33	.	1.66	0.27
Refinement (T/B)	0.56	0.10	0.51	0.15	0.52	0.05	0.52	0.00	0.48	.	0.53	0.10
Breadth/ Thickness	1.86	0.36	2.14	0.76	1.94	0.19	1.91	0.02	2.11	.	1.96	0.46
Thickness/ Breadth	0.56	0.10	0.51	0.15	0.52	0.05	0.52	0.00	0.48	.	0.53	0.10
Length/ Weight	0.25	0.04	0.29	0.07	0.21	0.03	0.30	0.01	0.33	.	0.26	0.06
Edge length	198.38	126.91	120.33	60.95	138.33	11.15	192.00	46.67	113.00	.	161.05	91.94

Table_15

	Chaîne opératoire		Index	Lava	Metamorphic	Total
Detached: flaked	Small debitage	A.1	Flake*: core	1.38	2.84	1.69
	LCT production	A.2	Small flake*: LCT	2.13	2.34	2.18
	Total**	A.3	All flakes: core & LCT	2.03	3.04	2.25
Detached: scars on flaked	Small debitage	B.1	Flake*: core scars	0.57	0.58	0.57
	LCT production	B.2.1	Small flake*: faconnage scars on LCT	0.34	0.35	0.34
		B.2.2	Intermediate flake: debitage scars on LCT	0.24	0.61	0.28
	Total**	B.3	All flakes: all scars on core & LCT	0.39	0.48	0.41
Retouched: debitage	Small debitage	C.1.1	Ret. tool: debitage ≥17 mm	0.01	0.02	0.02
		C.1.2	Ret. tool: flake & flake frag ≥20 mm	0.01	0.04	0.02
		C.1.3	Ret. tool: flake≥20 mm	0.03	0.16	0.08
	LCT production	C.2.1	Ret. tool: intermediate flakes and fragments	0.12	0.26	0.16
		C.2.2	Ret. tool: intermediate flakes	0.28	0.65	0.37
Flaked: flaked		D.1	Core: LCT	1.29	1.27	1.29
		D.2	LCT: Core	0.77	0.79	0.78
		D.3	LCT: Retouched tool***	4.11	0.76	2.04
Cutting edge (cm): flaked mass (g)	Total**	E	Cutting edge: core & LCT mass	0.60	1.38	0.74

Table_16

	Lava (*n*)		Metamorphic (*n*)		Chert (*n*)		Total	
	OGAP	Leakey	OGAP	Leakey	OGAP	Leakey	n	%
Flake	397	71	174	11	5		658	23.7
Flake Frag	490	142	500	79	4		1215	43.7
Shatter <20 mm	48	19	199	4	12		282	10.1
Shatter >20 mm	34	16	69	38	2		159	5.7
Core	110	30	33	5	1		179	6.4
Core Frag	8	3	6				17	0.6
Retouched Tool	20	4	33	1	1		59	2.1
Ret. Tool Frag	2		1				3	0.1
LCT	78	24	22	9			133	4.8
LCT Frag	15		2				17	0.6
Split Cobble	1						1	0.0
Pitted stone	2						2	0.1
Knapping hamm.	25	1	3	3			32	1.2
Knap. Ham. Frag	7	1	3	3			14	0.5
Other pounded	8		2				10	0.4
Total (*n*)	**1245**	**311**	**1047**	**153**	**25**		**2781**	**100.0**

	Lava (g)		Metamorphic (g)		Chert (g)		Total	
	OGAP	Leakey	OGAP	Leakey	OGAP	Leakey	g	%
Flake	20537	6166	7529	2200	10		36442	12.8
Flake Frag	17442	11003	9436	1674	14		39569	13.9
Shatter <20 mm	29	51	189	8	10		287	0.1
Shatter >20 mm	1426	1341	827	2891	31		6516	2.3
Core	53177	11983	8569	2409	15		76152	26.8
Core Frag	2216	350	338				2904	1.0
Retouched Tool	2850	1203	2573	132	1		6759	2.4
Ret. Tool Frag	21		9				30	0.0
LCT	44022	15057	12134	4238			75451	26.5
LCT Frag	4610		858				5468	1.9
Split Cobble	434						434	0.2
Pitted stone	2303						2303	0.8
Knapping hamm.	18611	298	1818	221			20948	7.4
Knap. Ham. Frag	2685	56	414	350			3505	1.2
Other pounded	5666		2098				7764	2.7
Total (g)	**176029**	**47507**	**46792**	**14123**	**82**		**284533**	**100.0**

Figure_1

Click here to download high resolution image

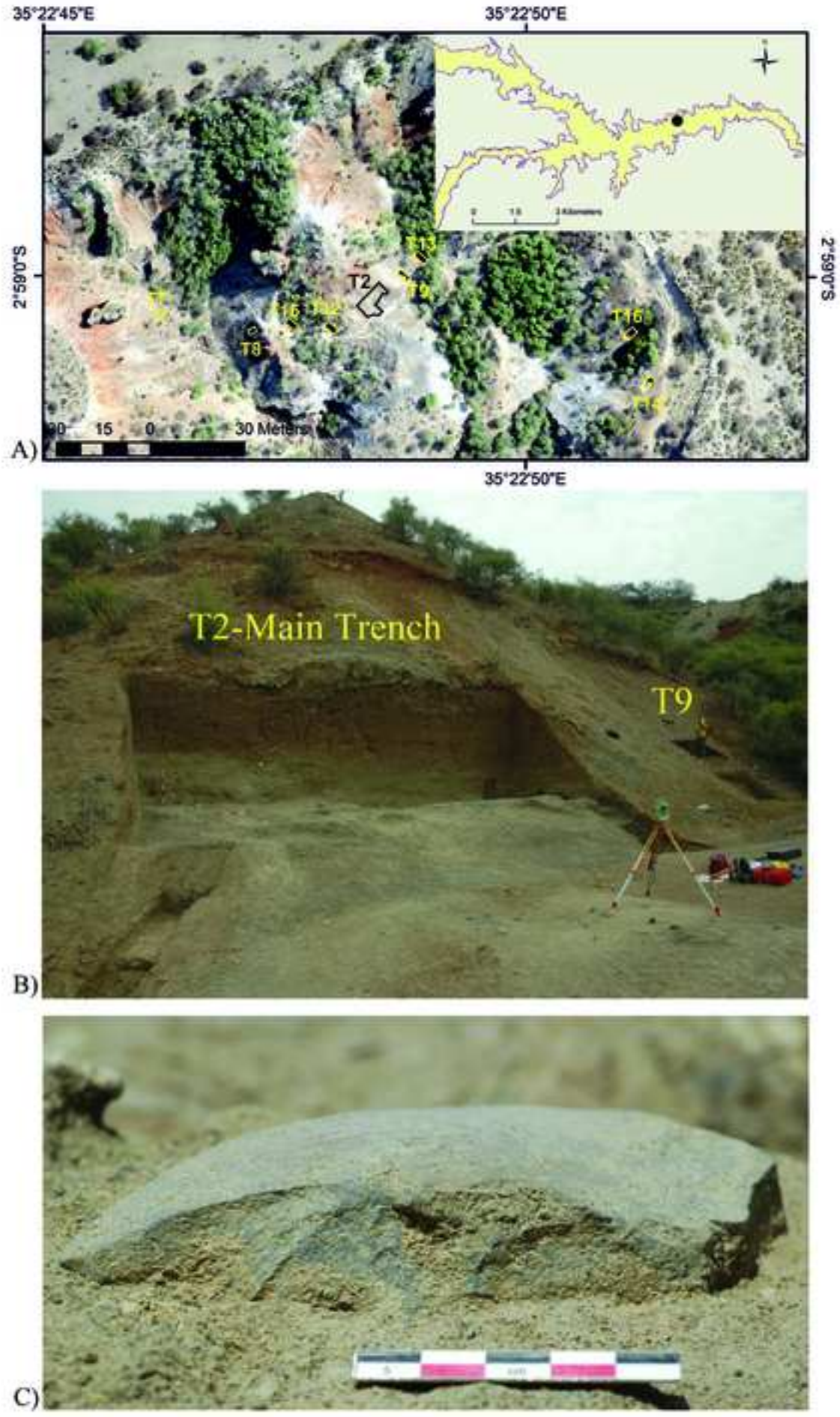

Figure_2
Click here to download high resolution image

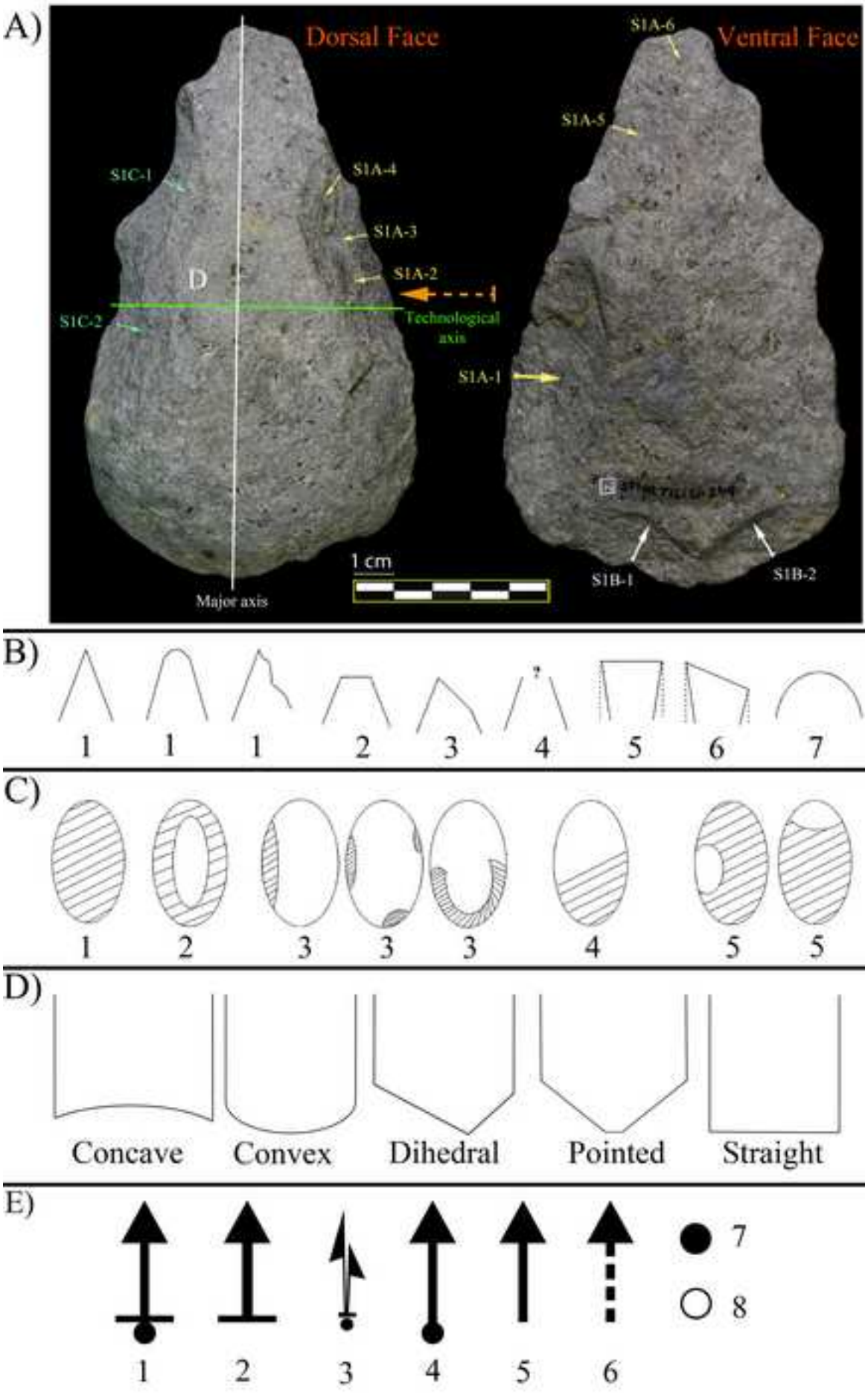

Figure_3
Click here to download high resolution image

Figure_4
Click here to download high resolution image

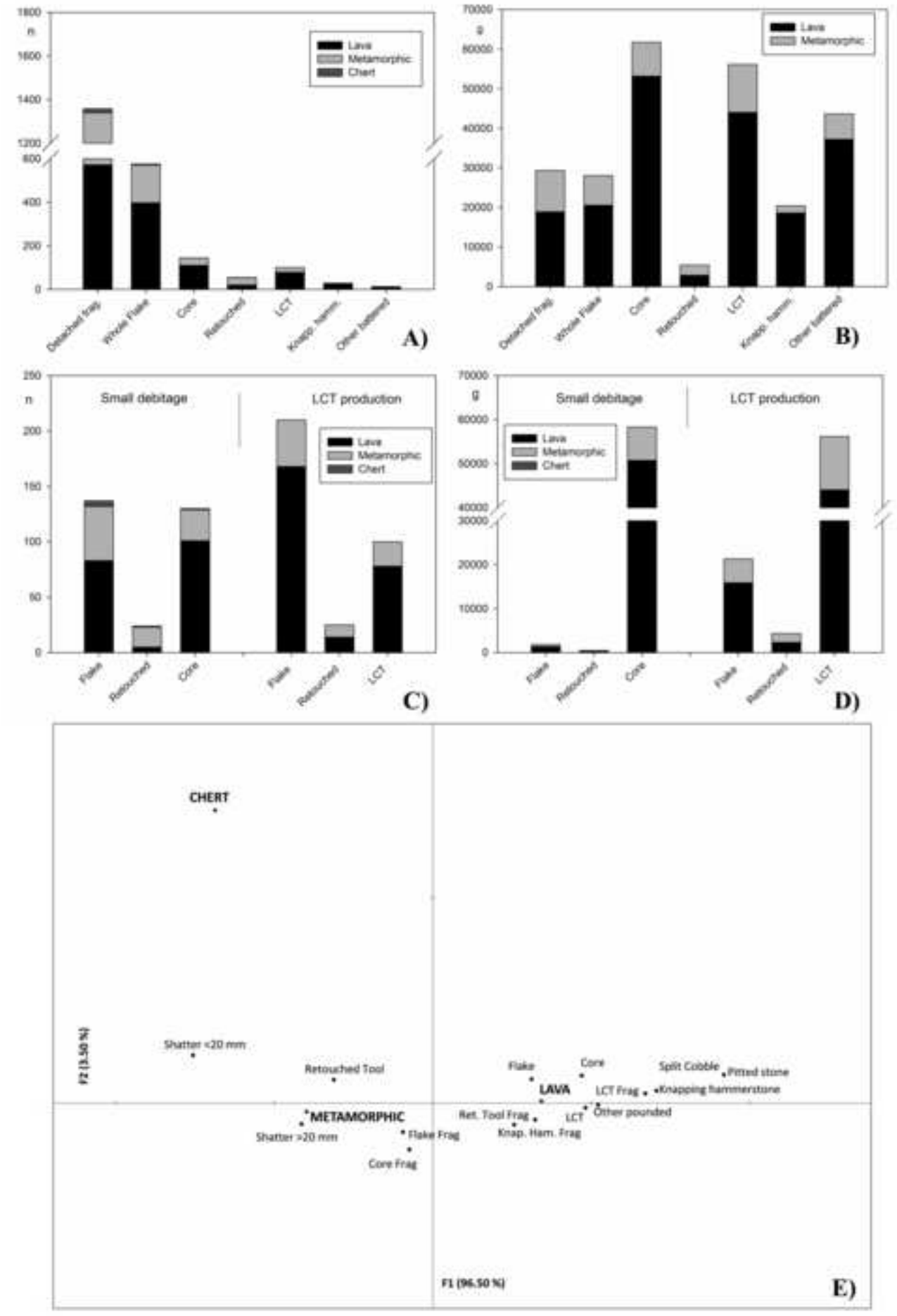

Figure_5

Click here to download high resolution image

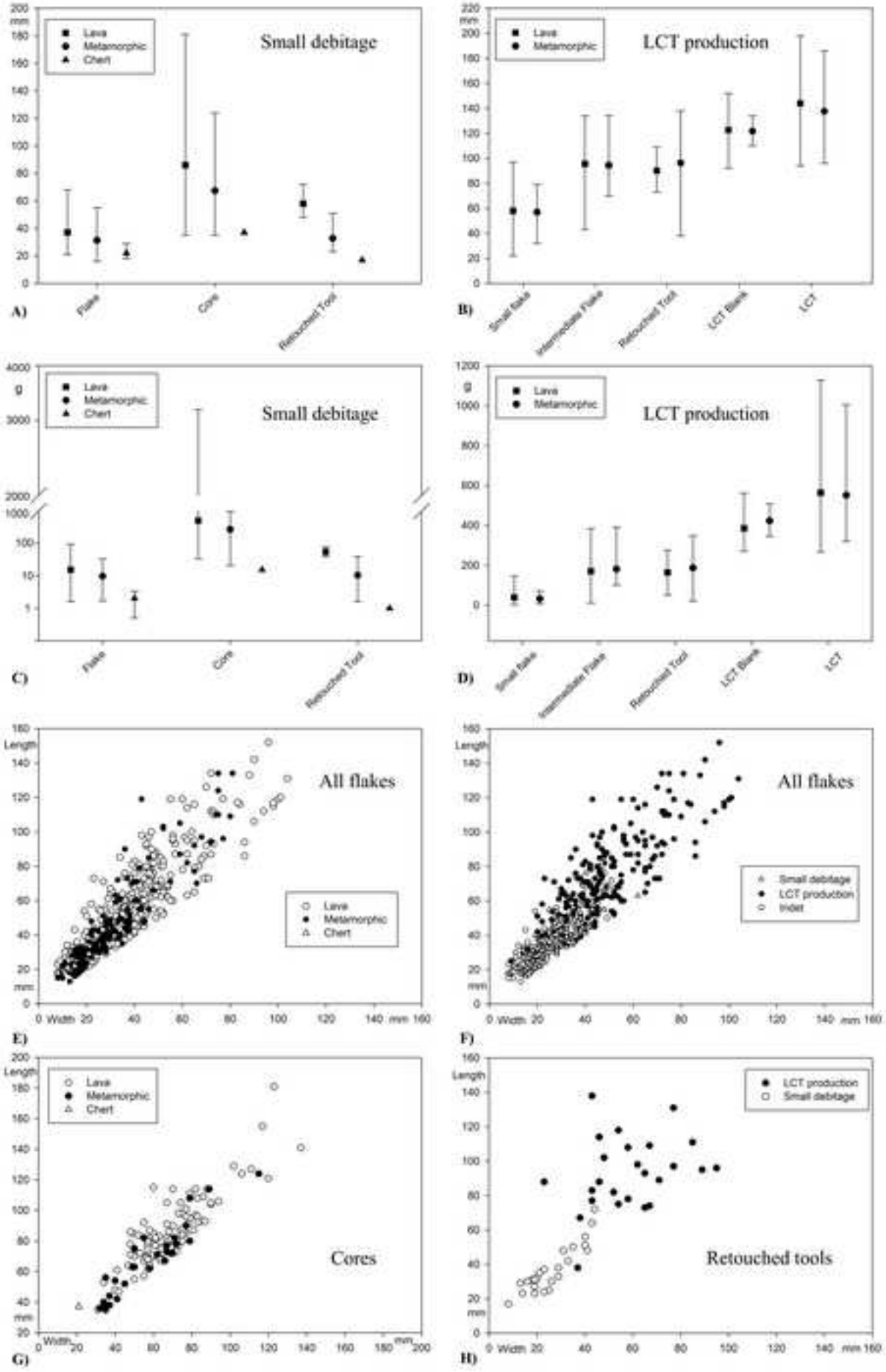

Figure_6

Click here to download high resolution image

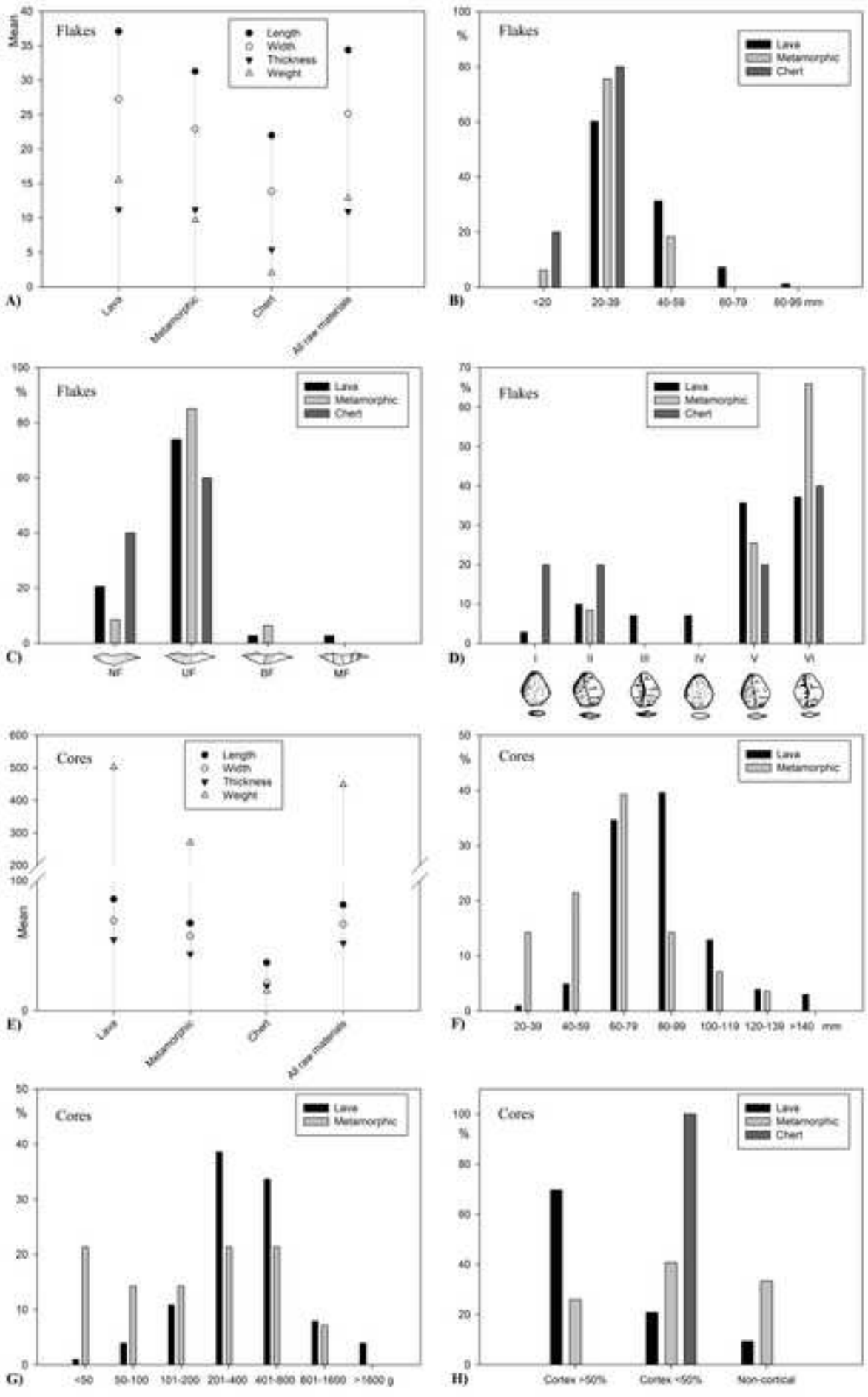

Figure_7
Click here to download high resolution image

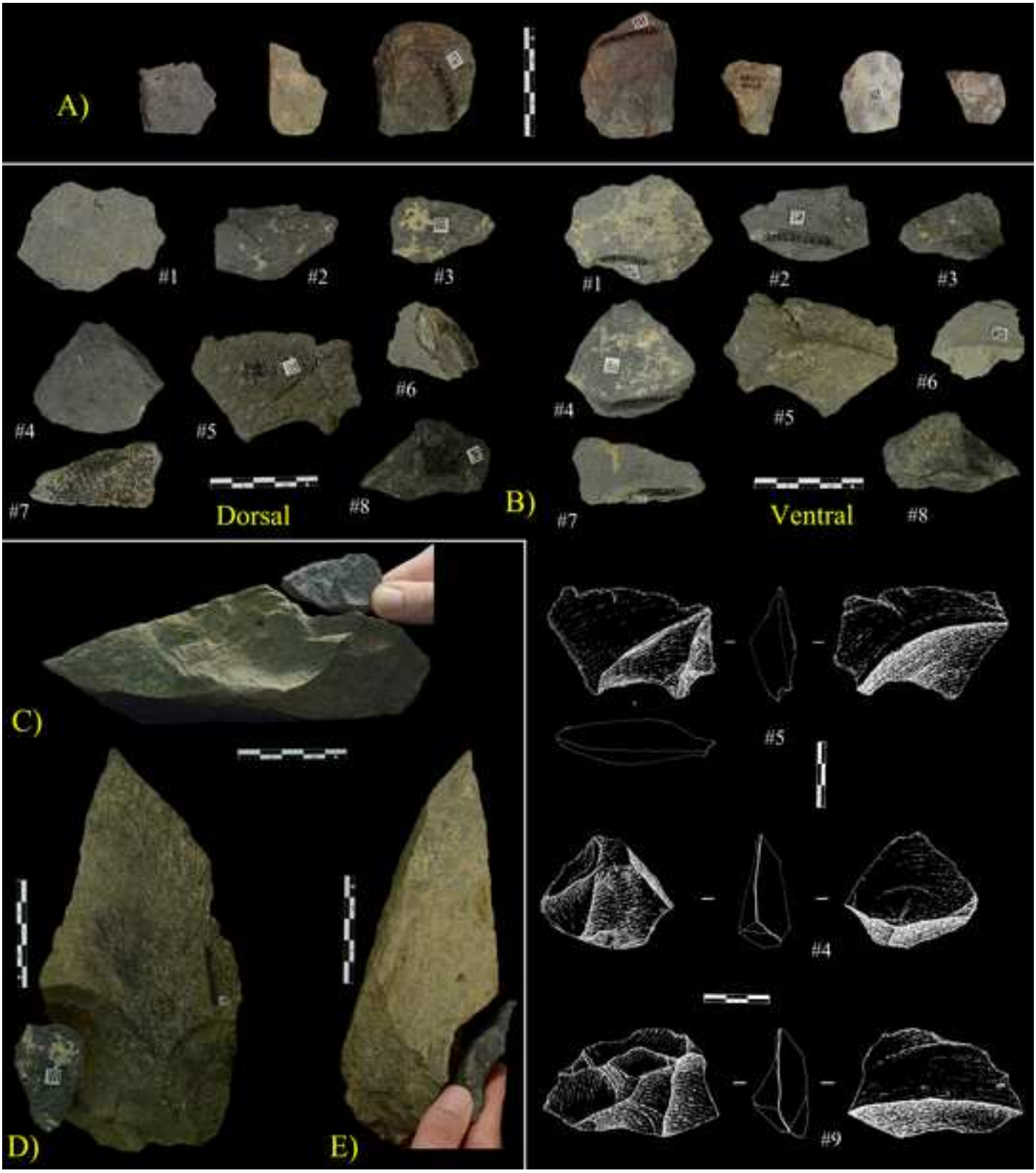

Figure_8
Click here to download high resolution image

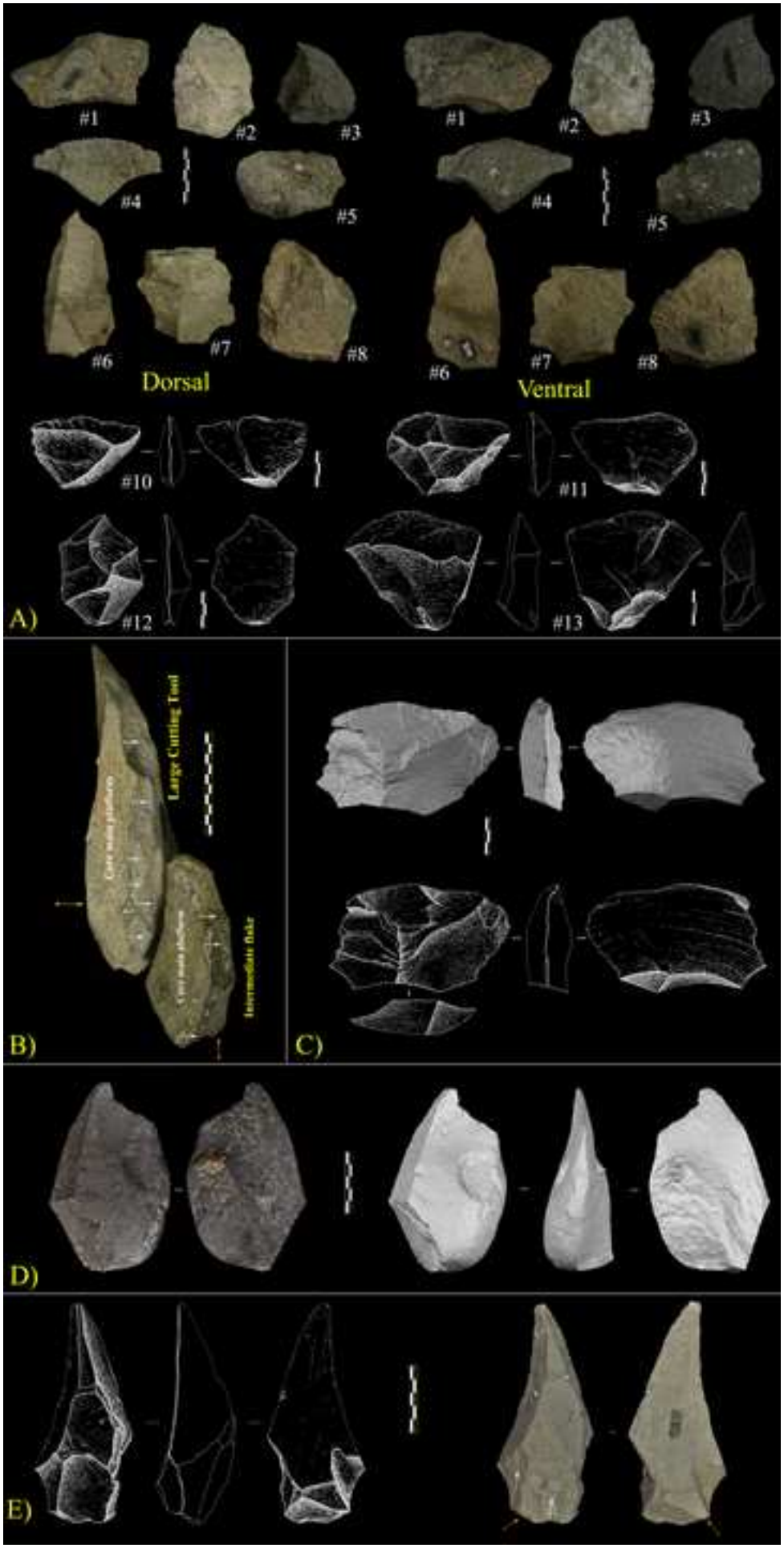

Figure_9
Click here to download high resolution image

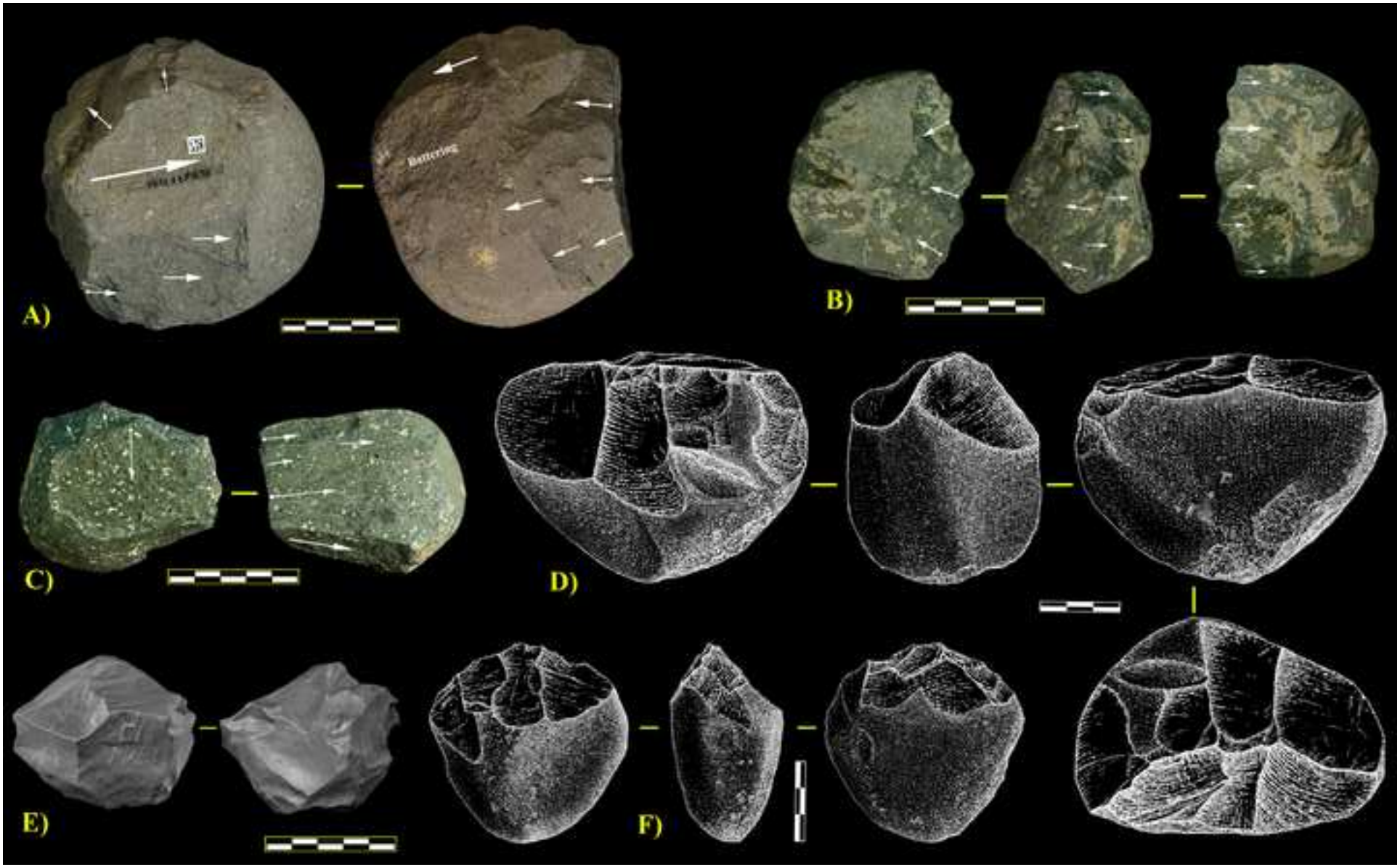

Figure_10
Click here to download high resolution image

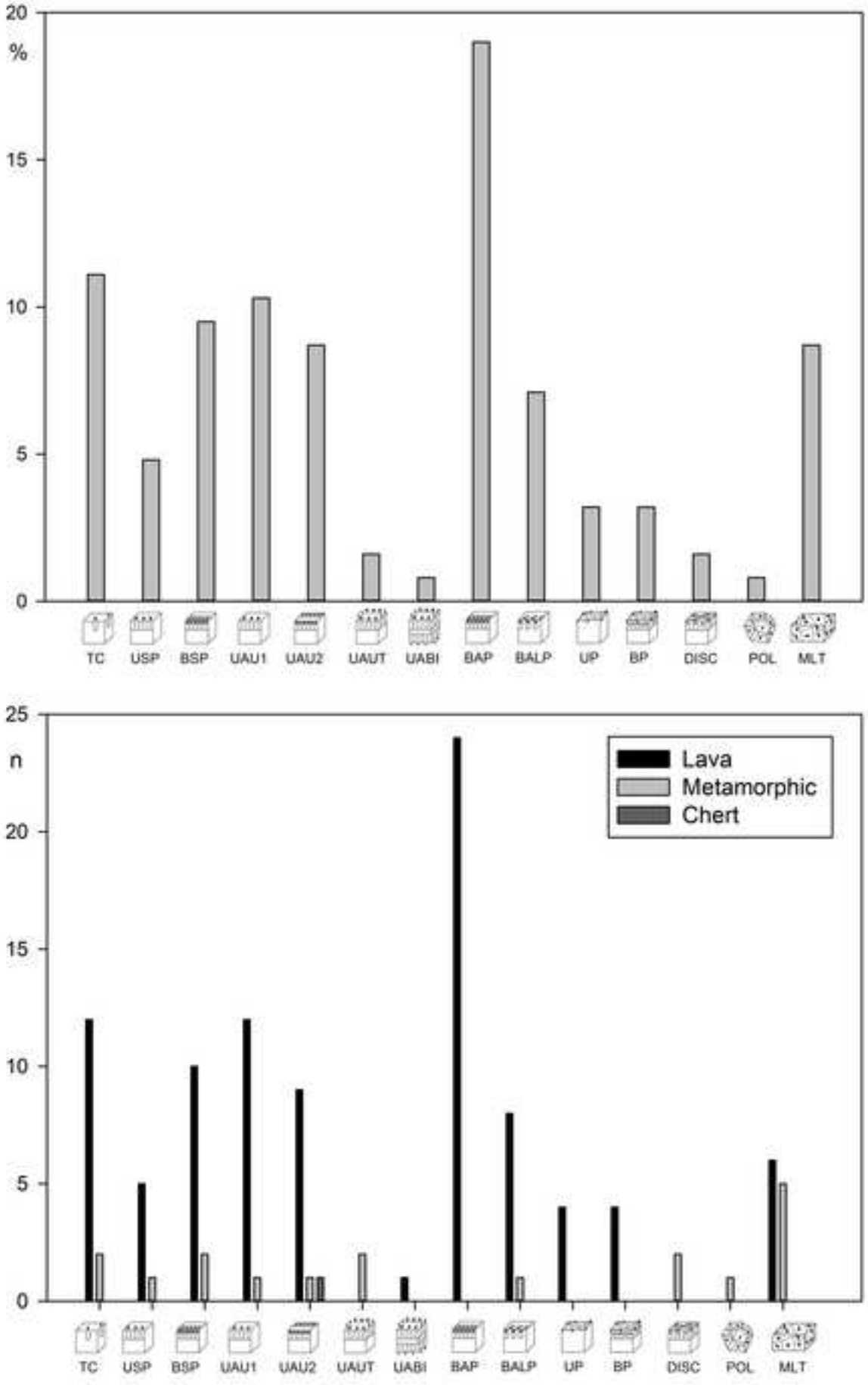

Figure_11

Click here to download high resolution image

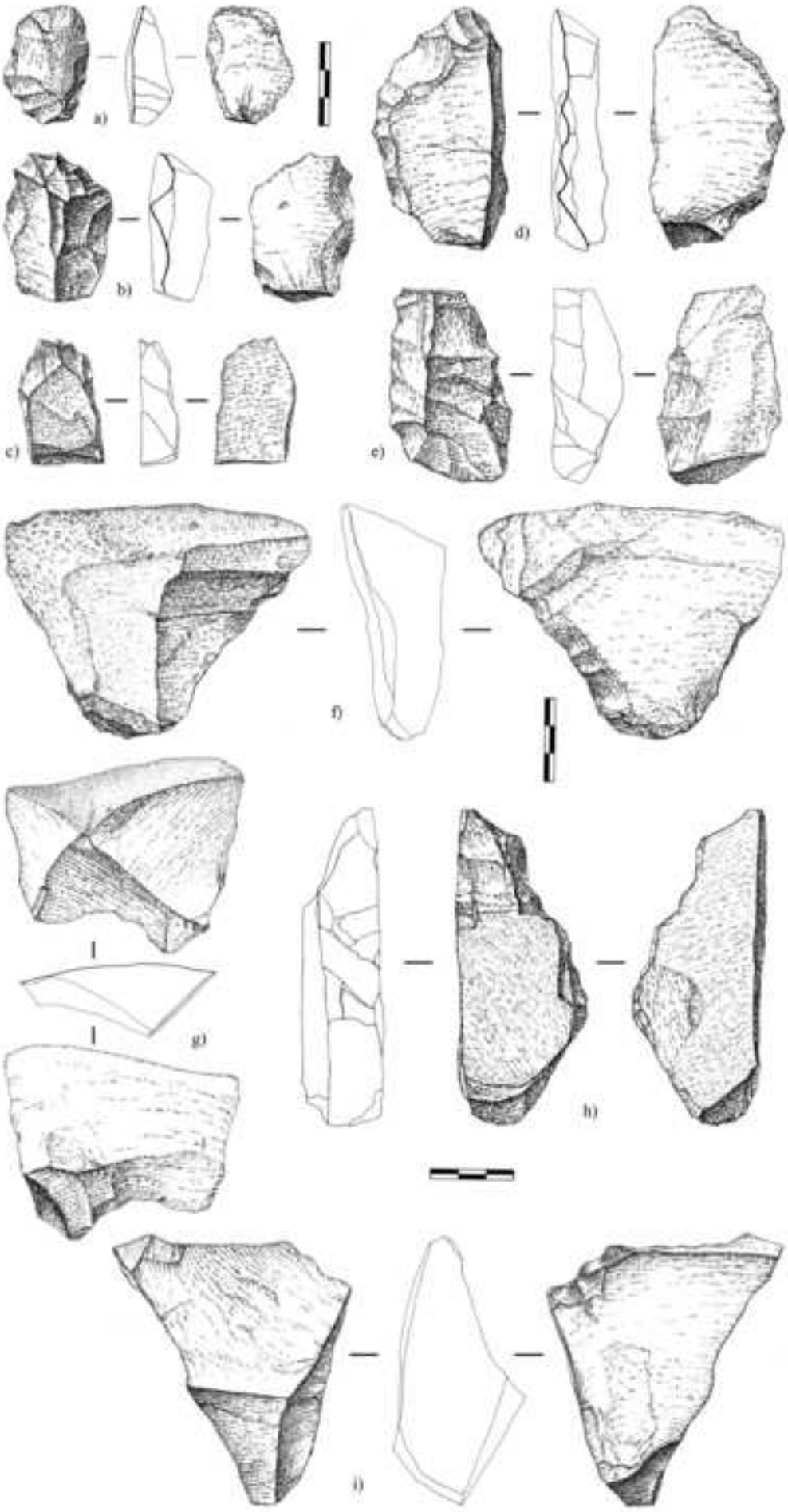

Figure_12

Click here to download high resolution image

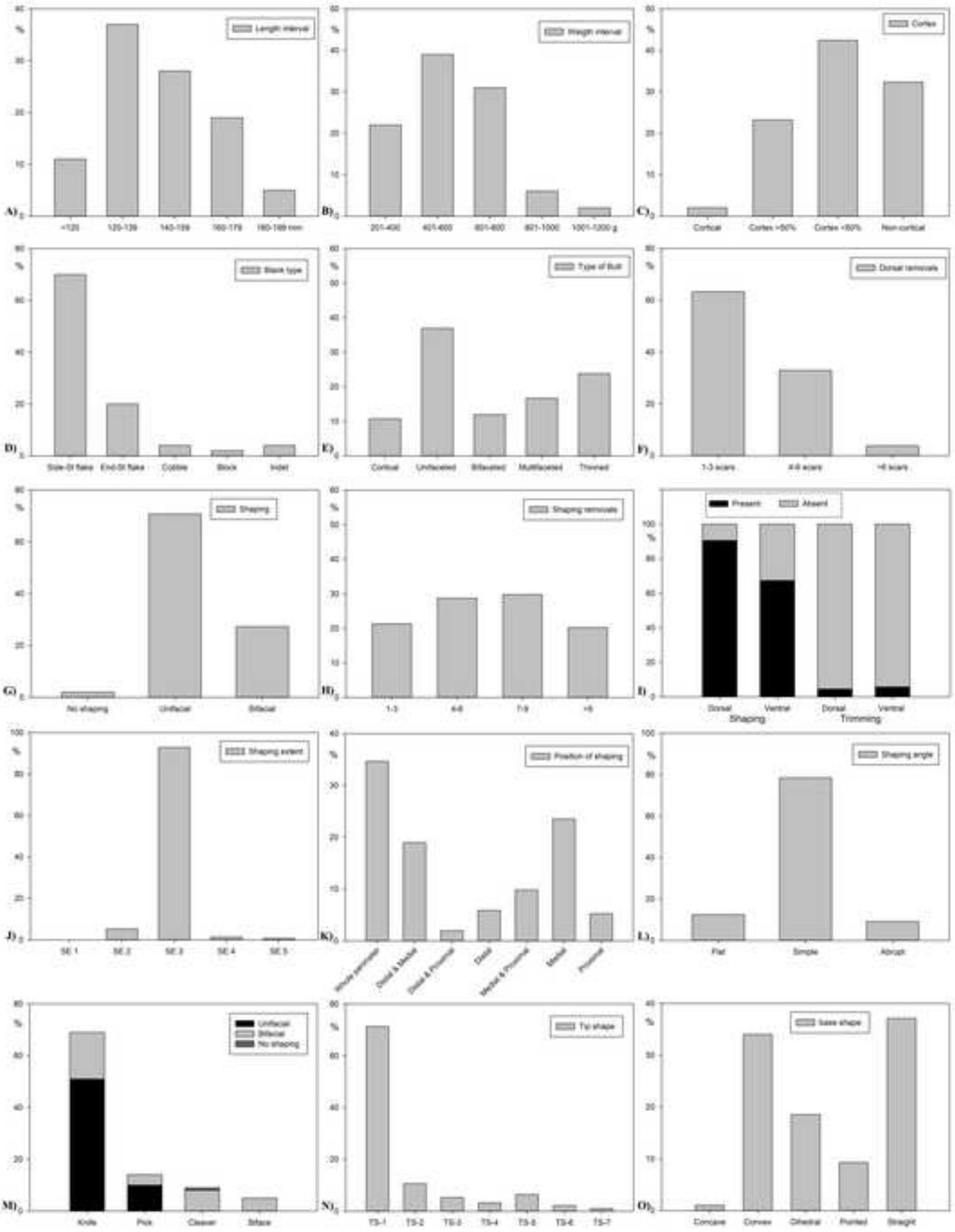

Figure_13
Click here to download high resolution image

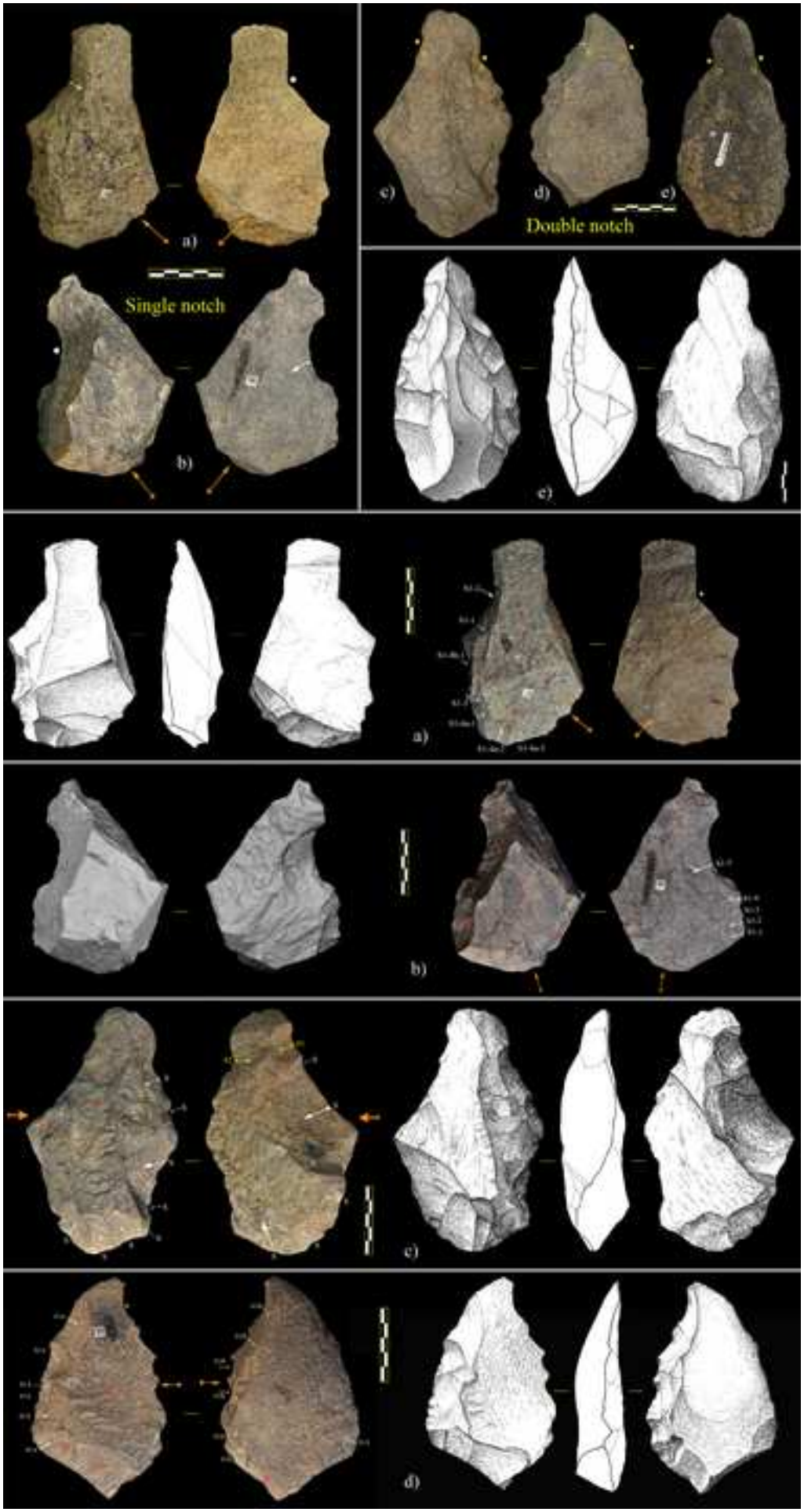

Figure_14

Click here to download high resolution image

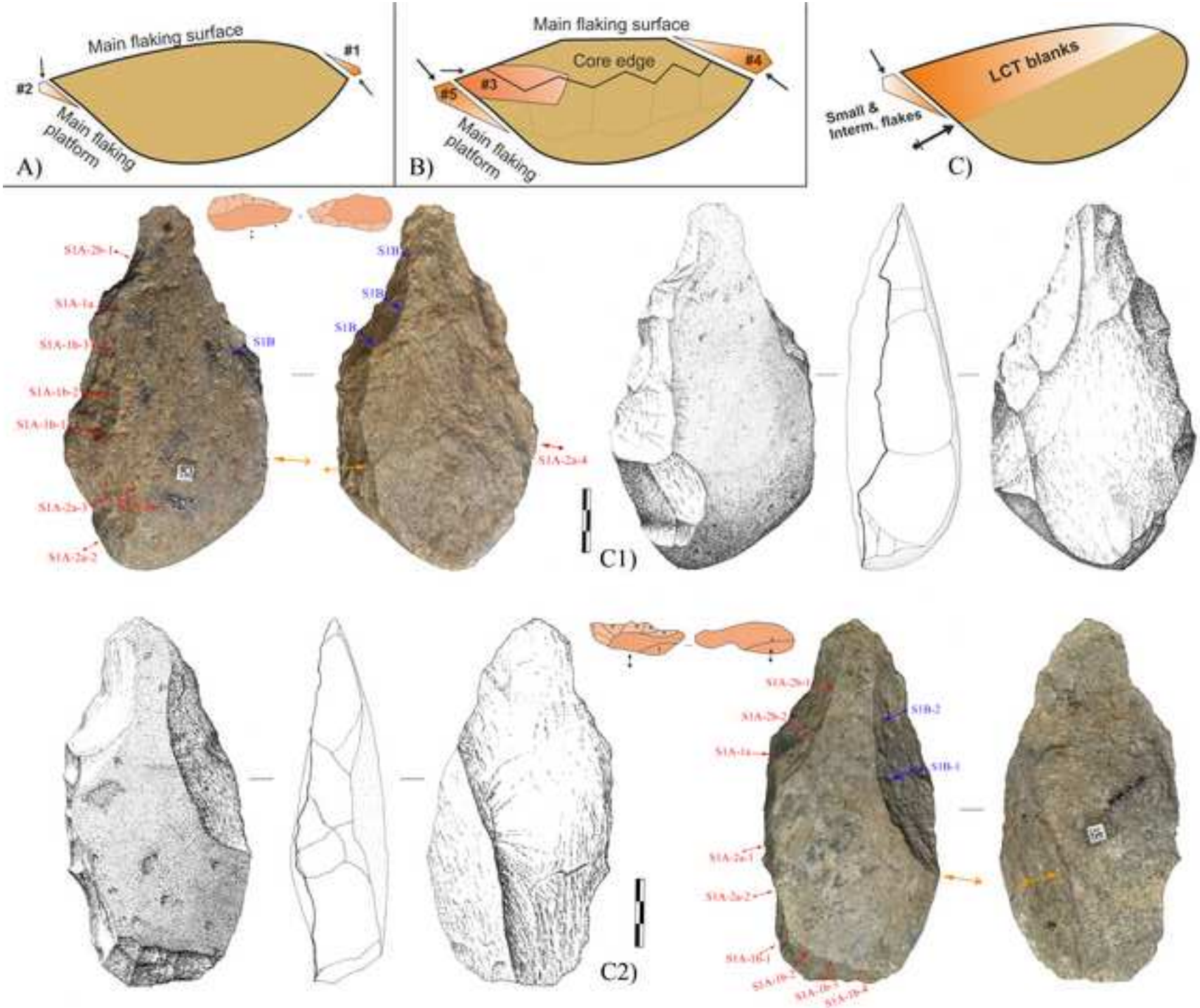

Figure_15

Click here to download high resolution image

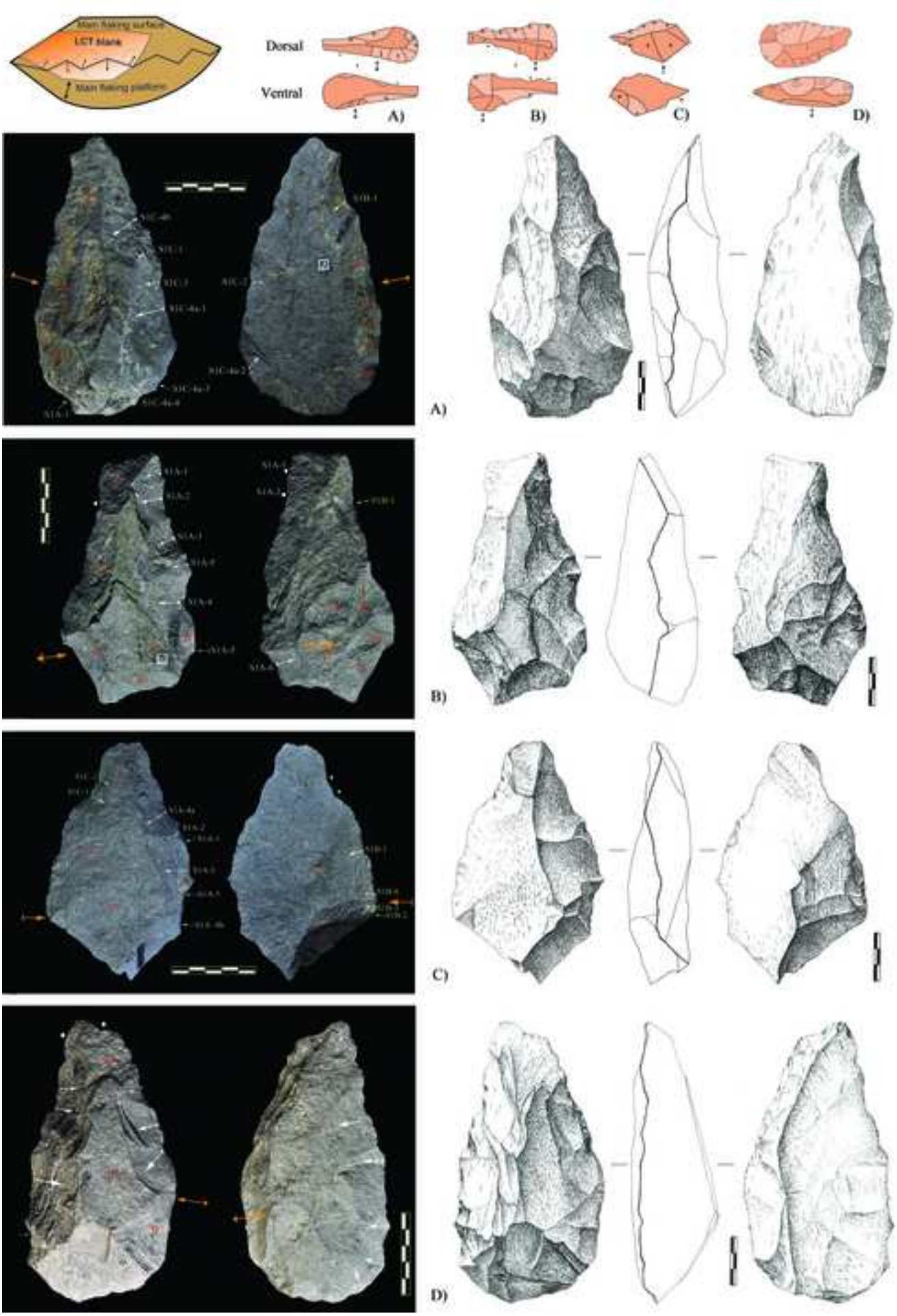

Figure_16
Click here to download high resolution image

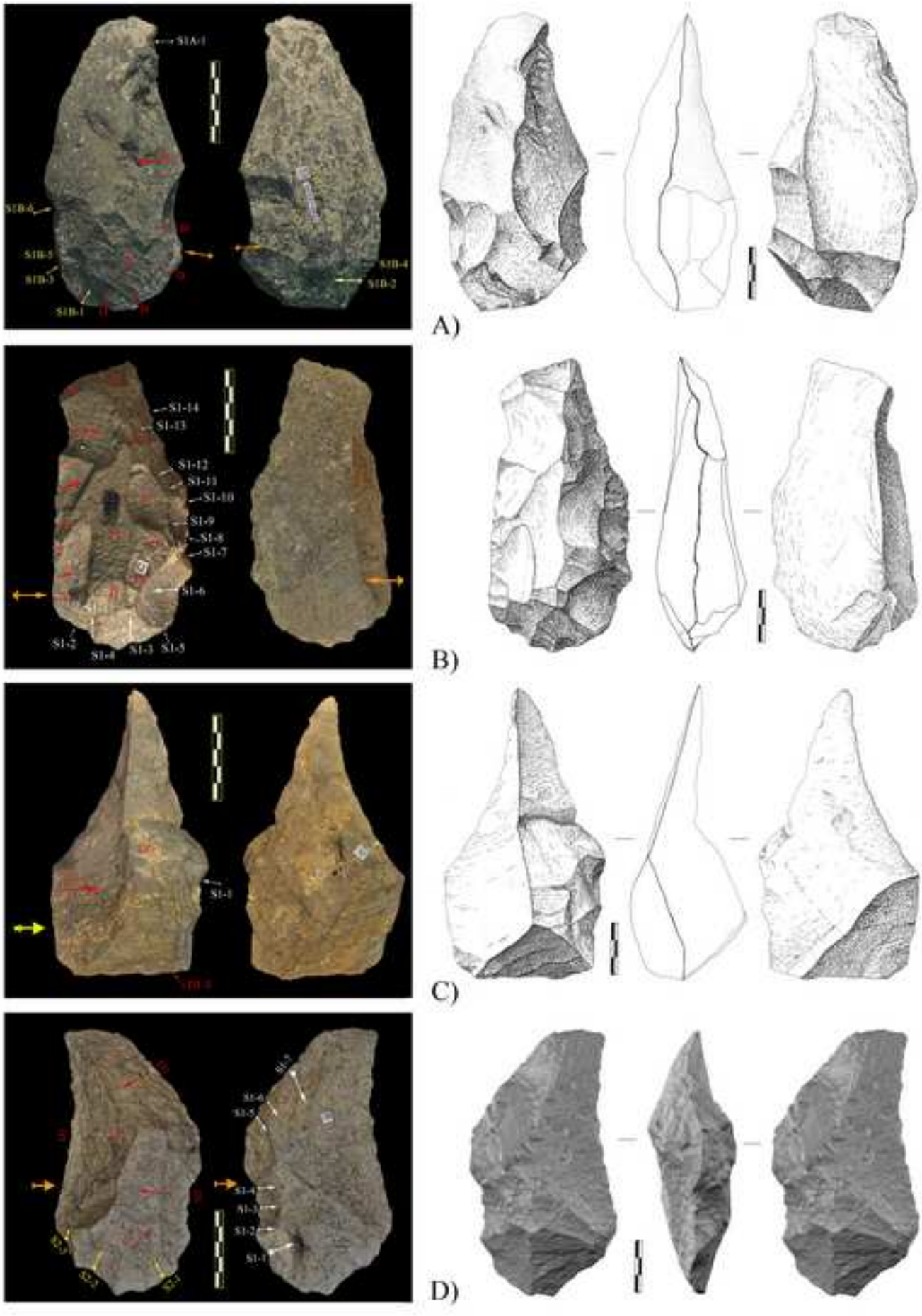

Figure_17
Click here to download high resolution image

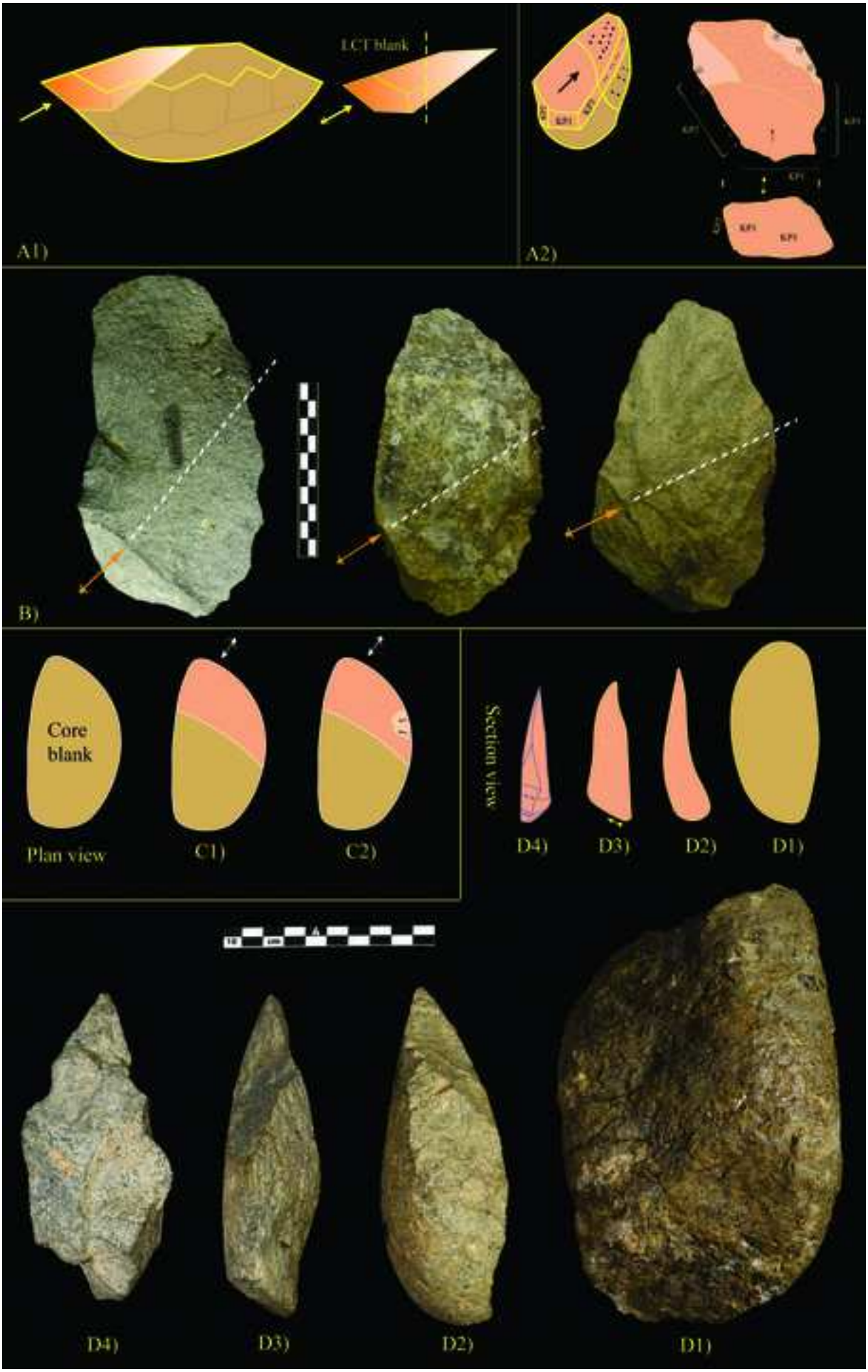

Figure_18
Click here to download high resolution image

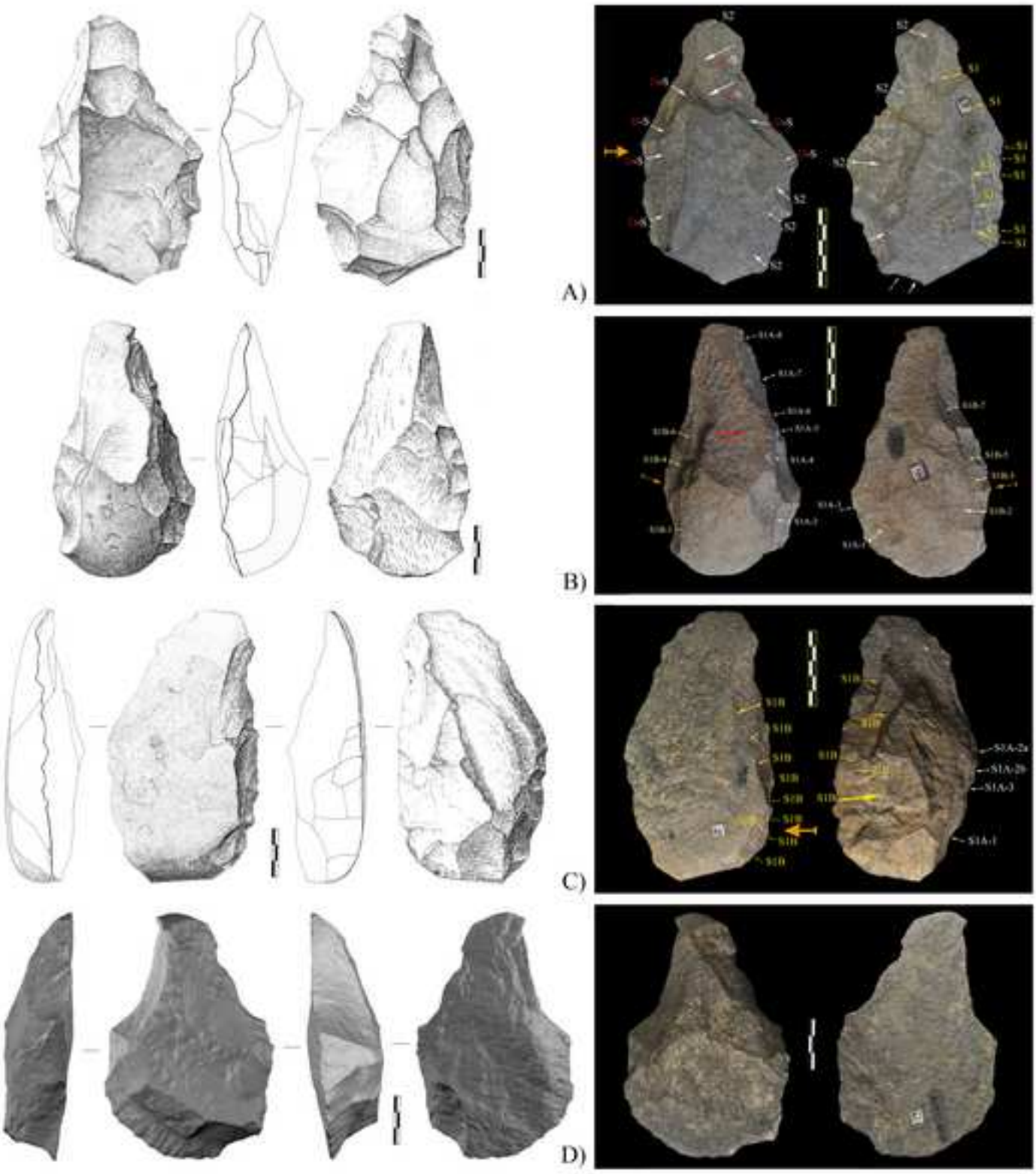

Figure_19
Click here to download high resolution image

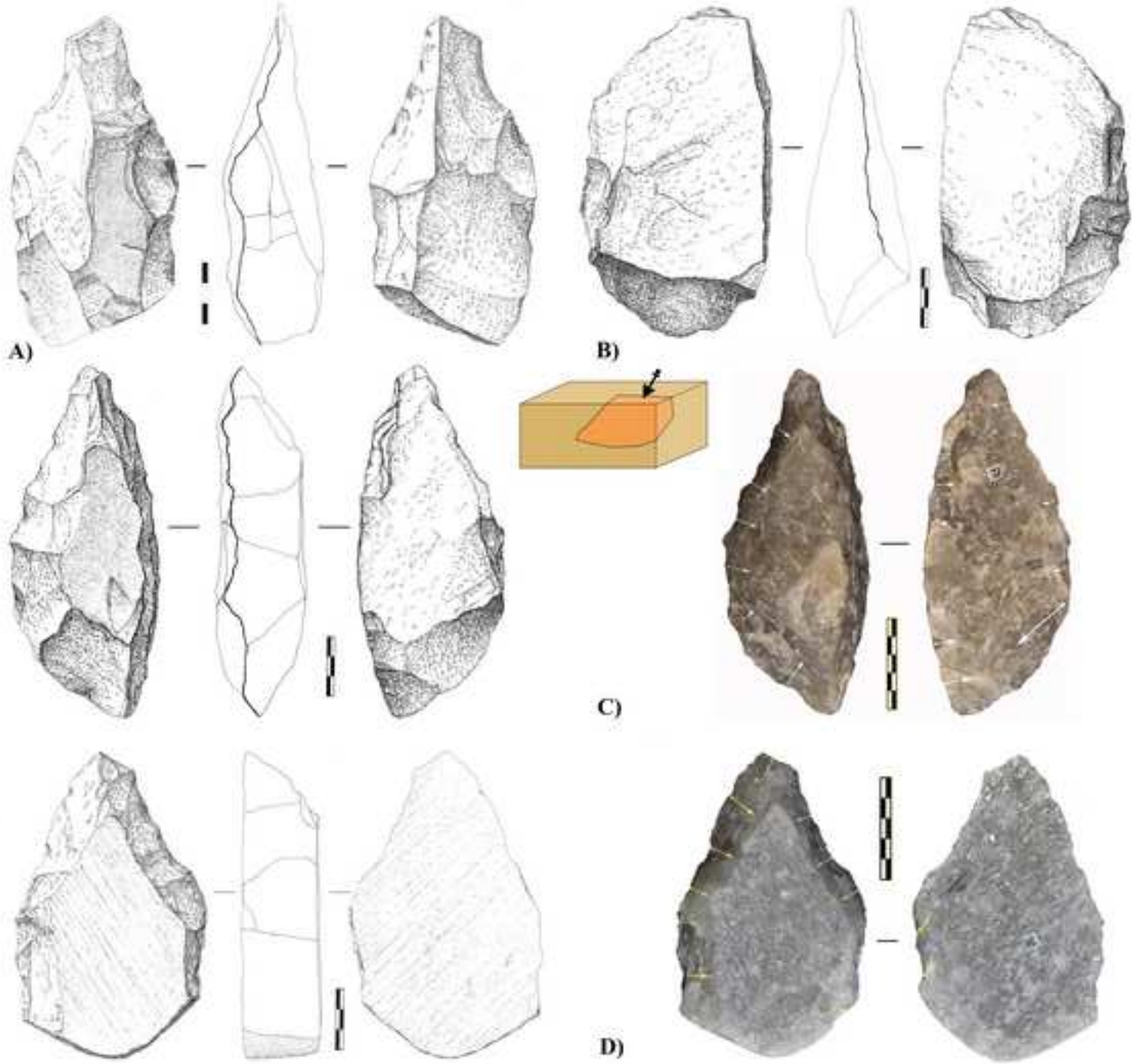

Figure_20
Click here to download high resolution image

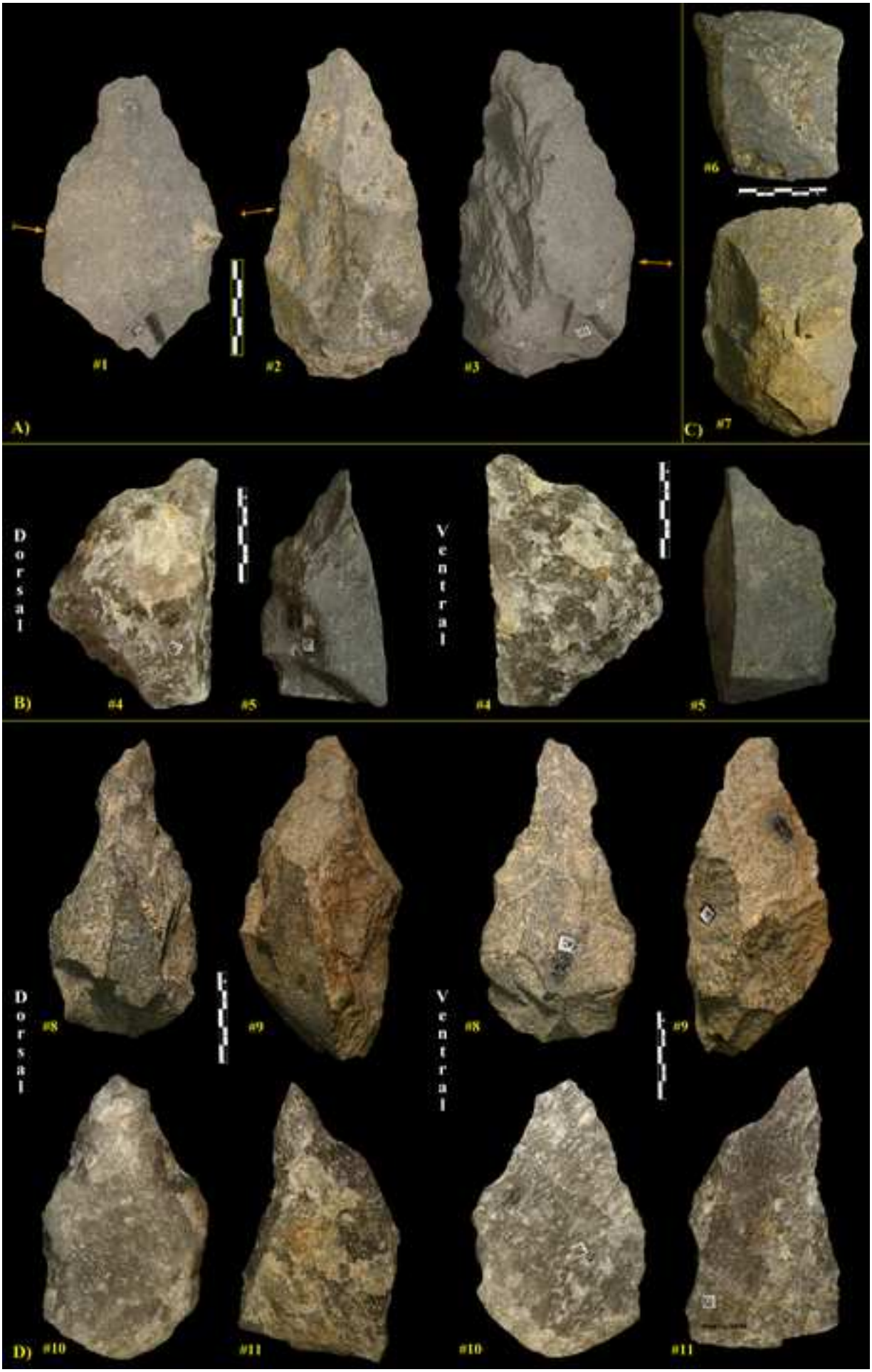

Figure_21
Click here to download high resolution image

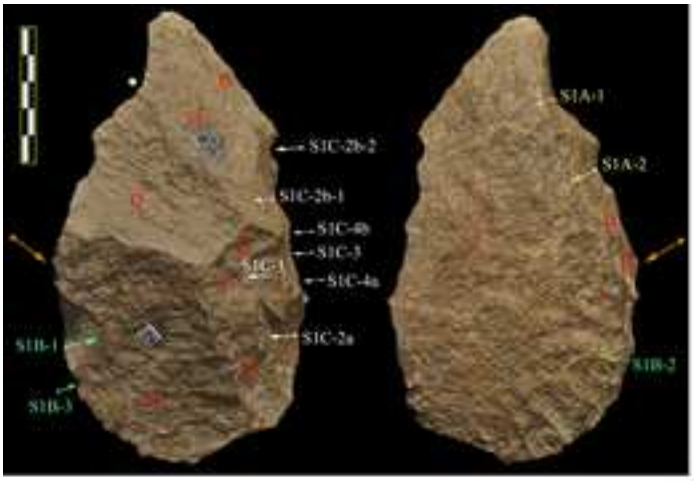

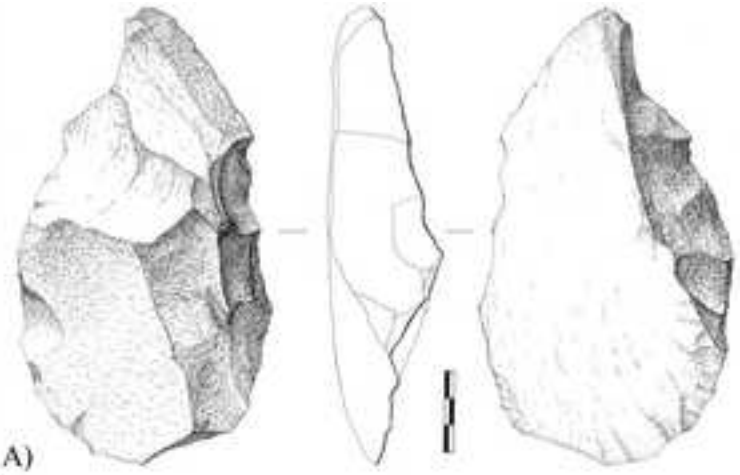

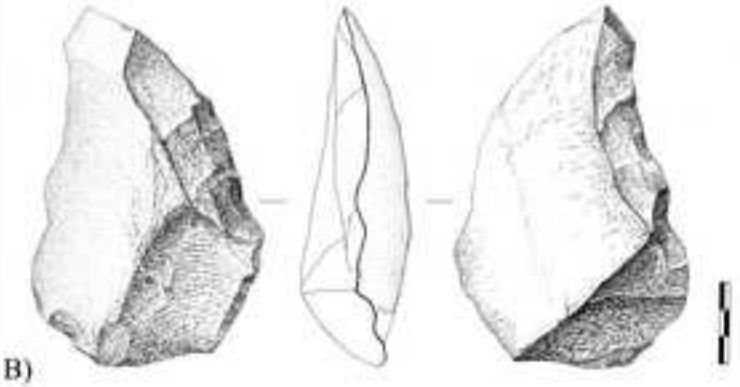

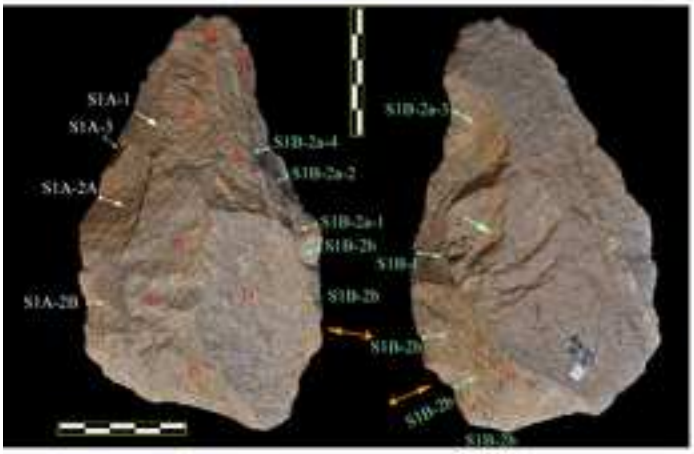

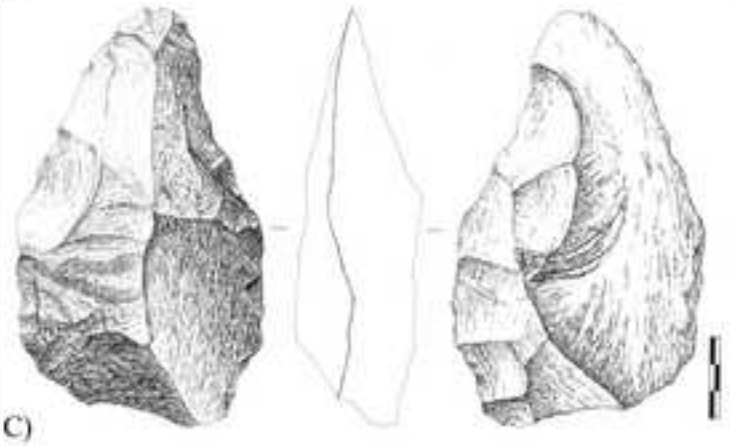

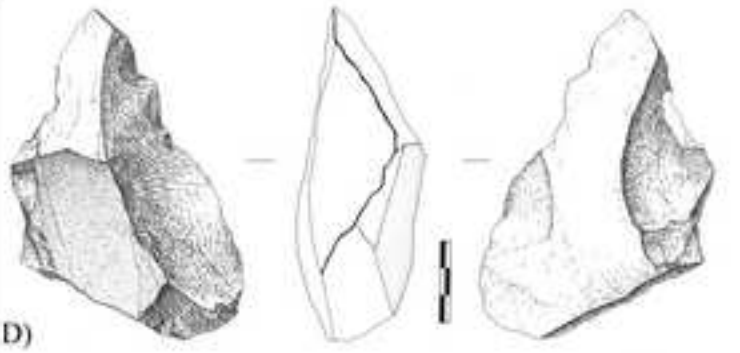

Figure_22
Click here to download high resolution image

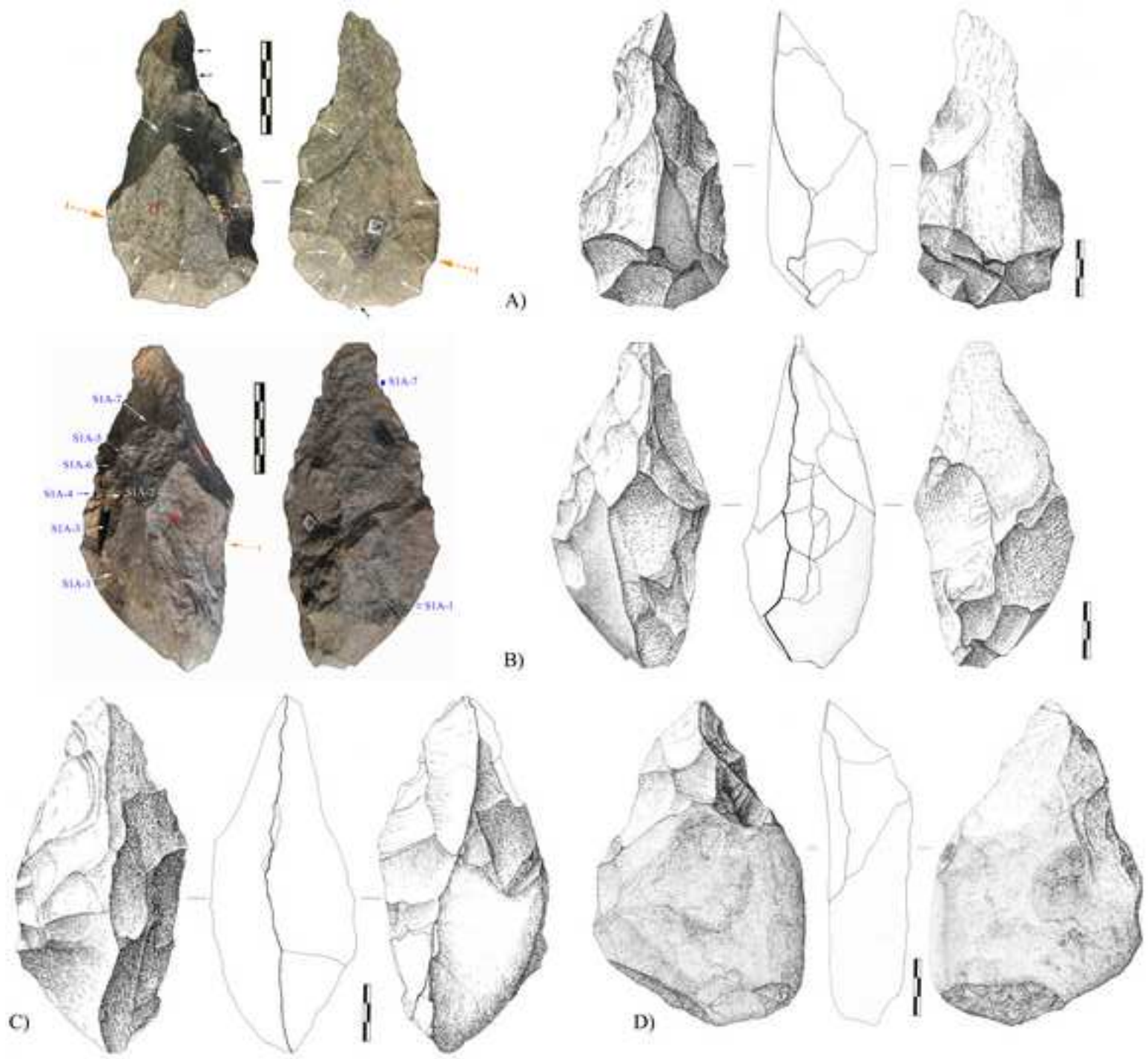

Figure_23
Click here to download high resolution image

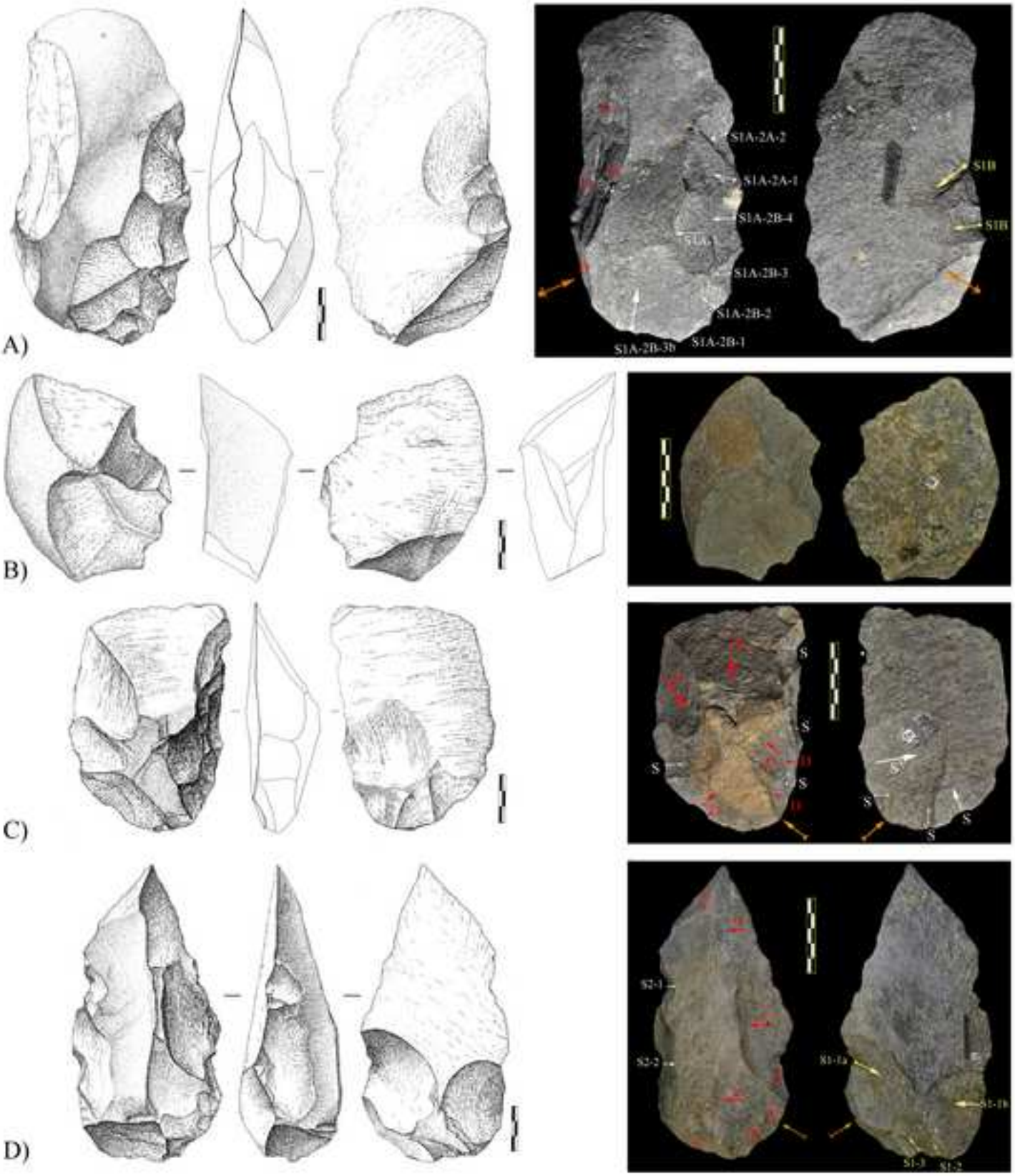

Figure_24
Click here to download high resolution image

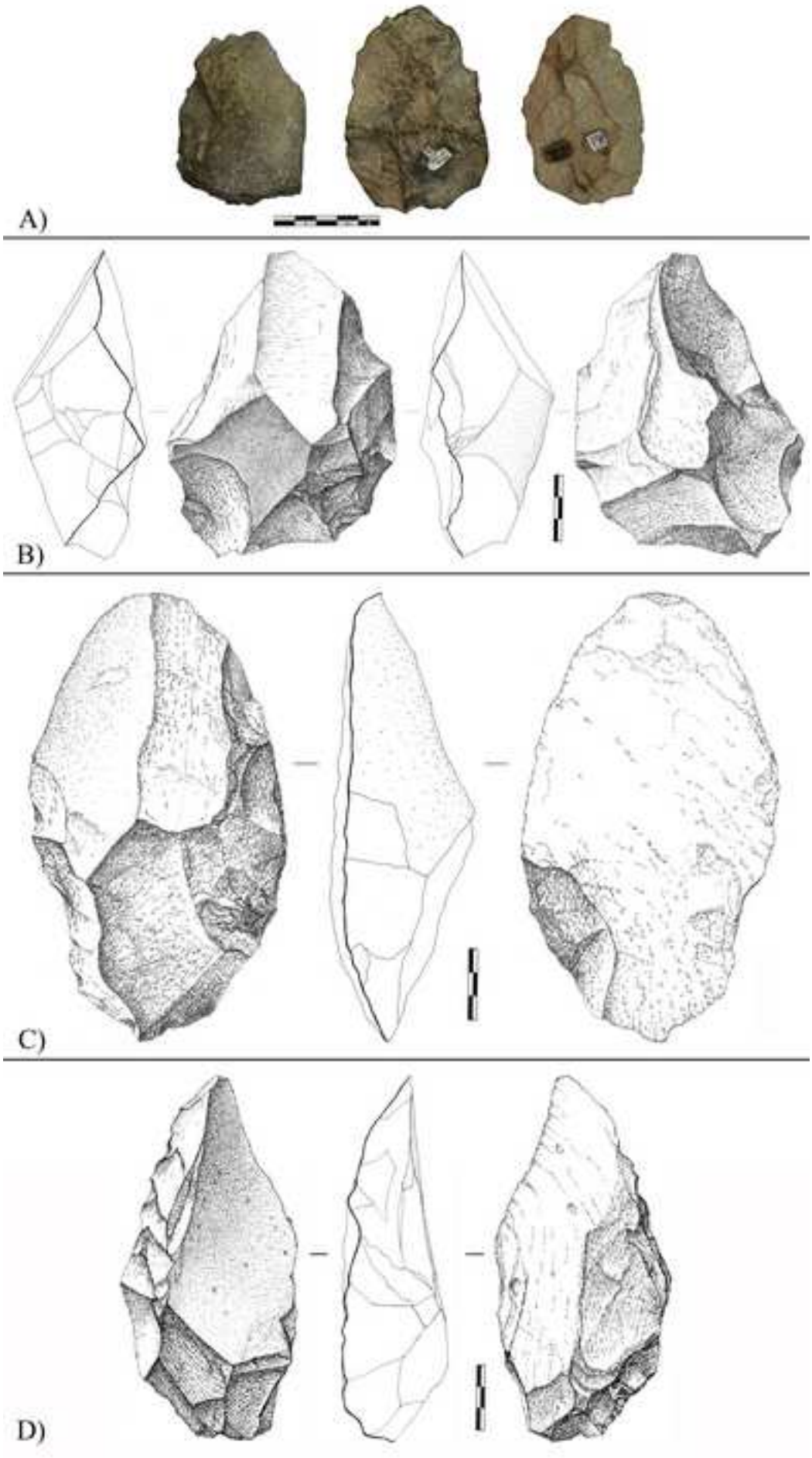

Figure_25

Click here to download high resolution image

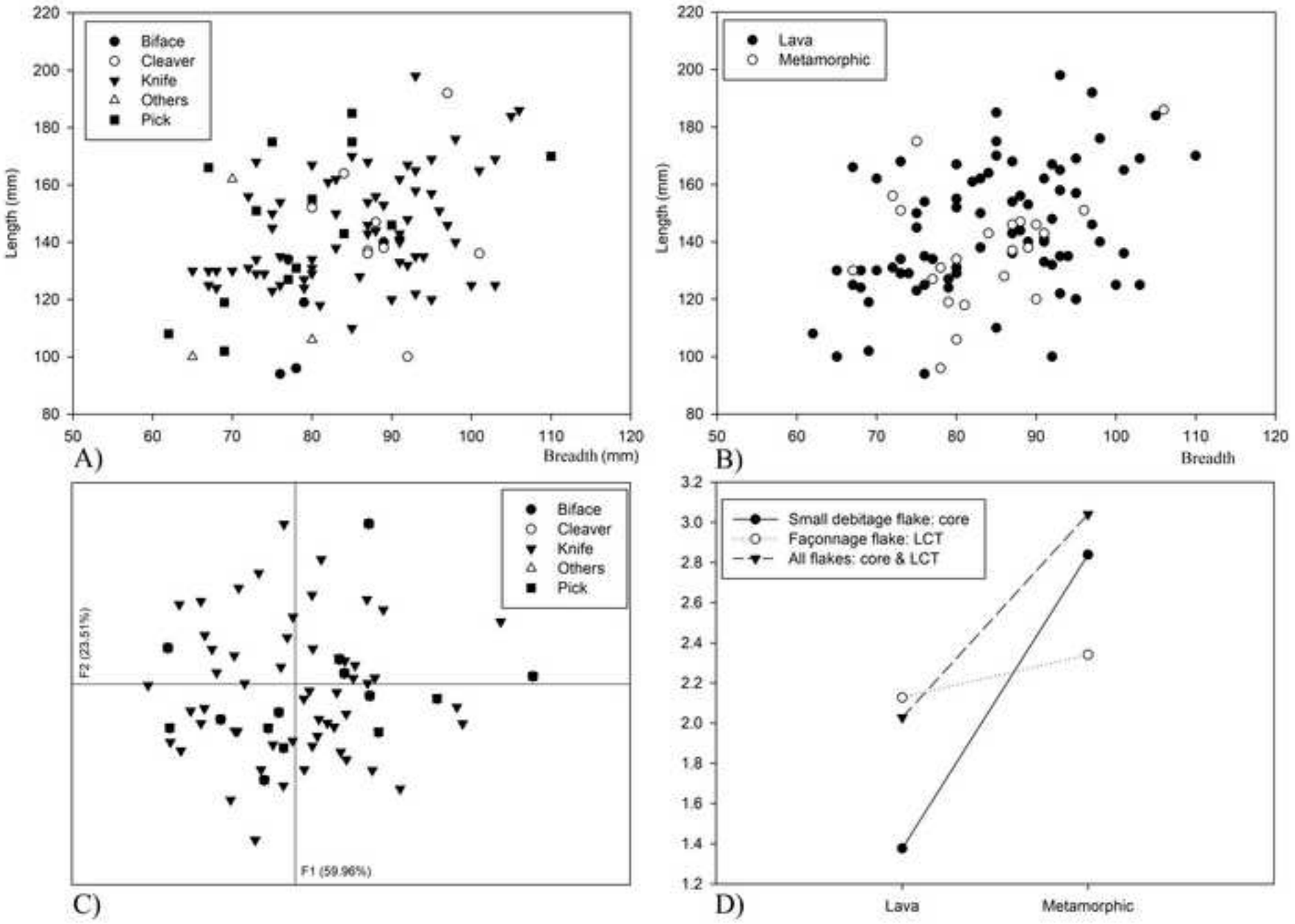

Figure_26
Click here to download high resolution image

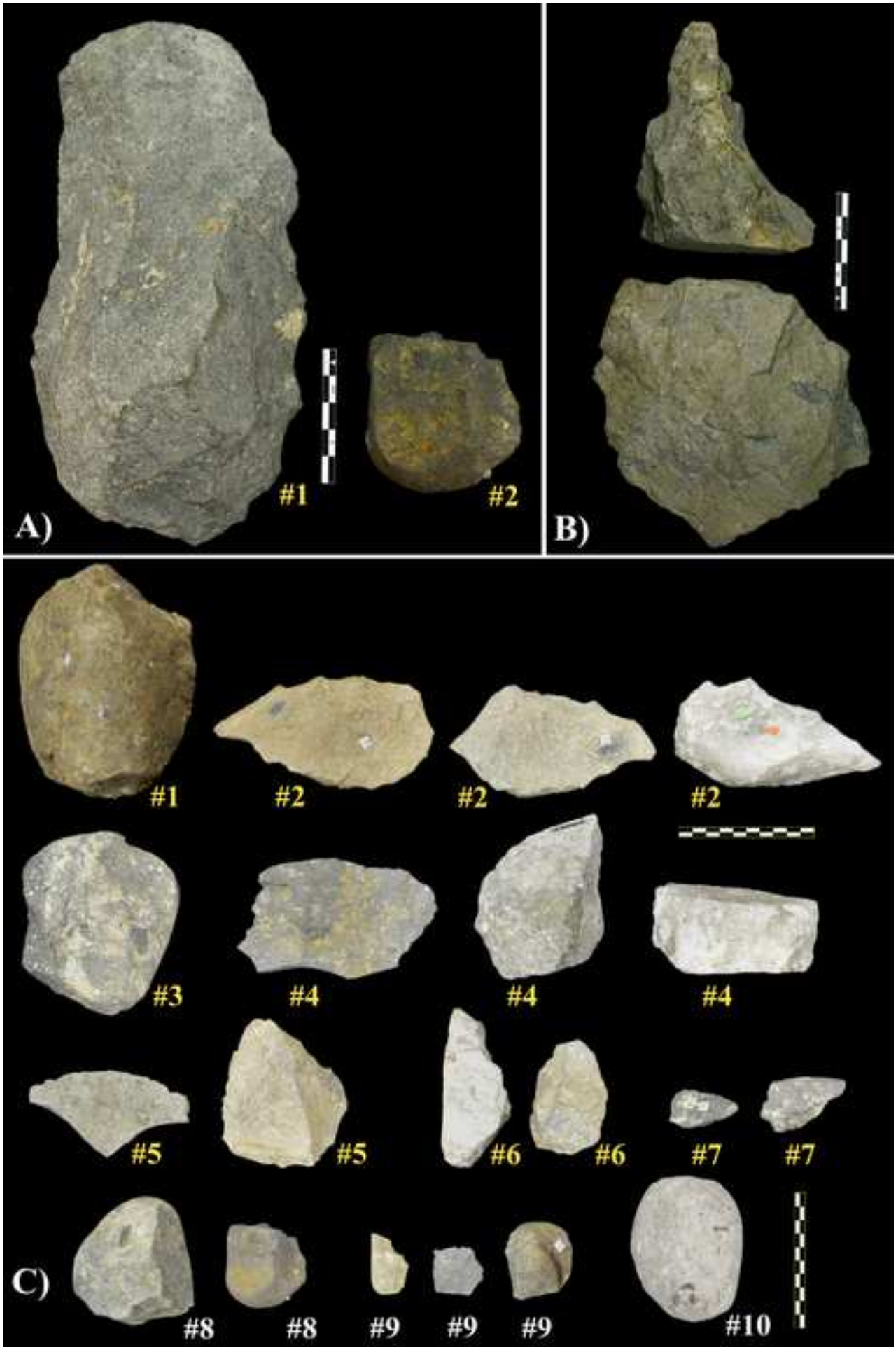

Figure_27

Click here to download high resolution image

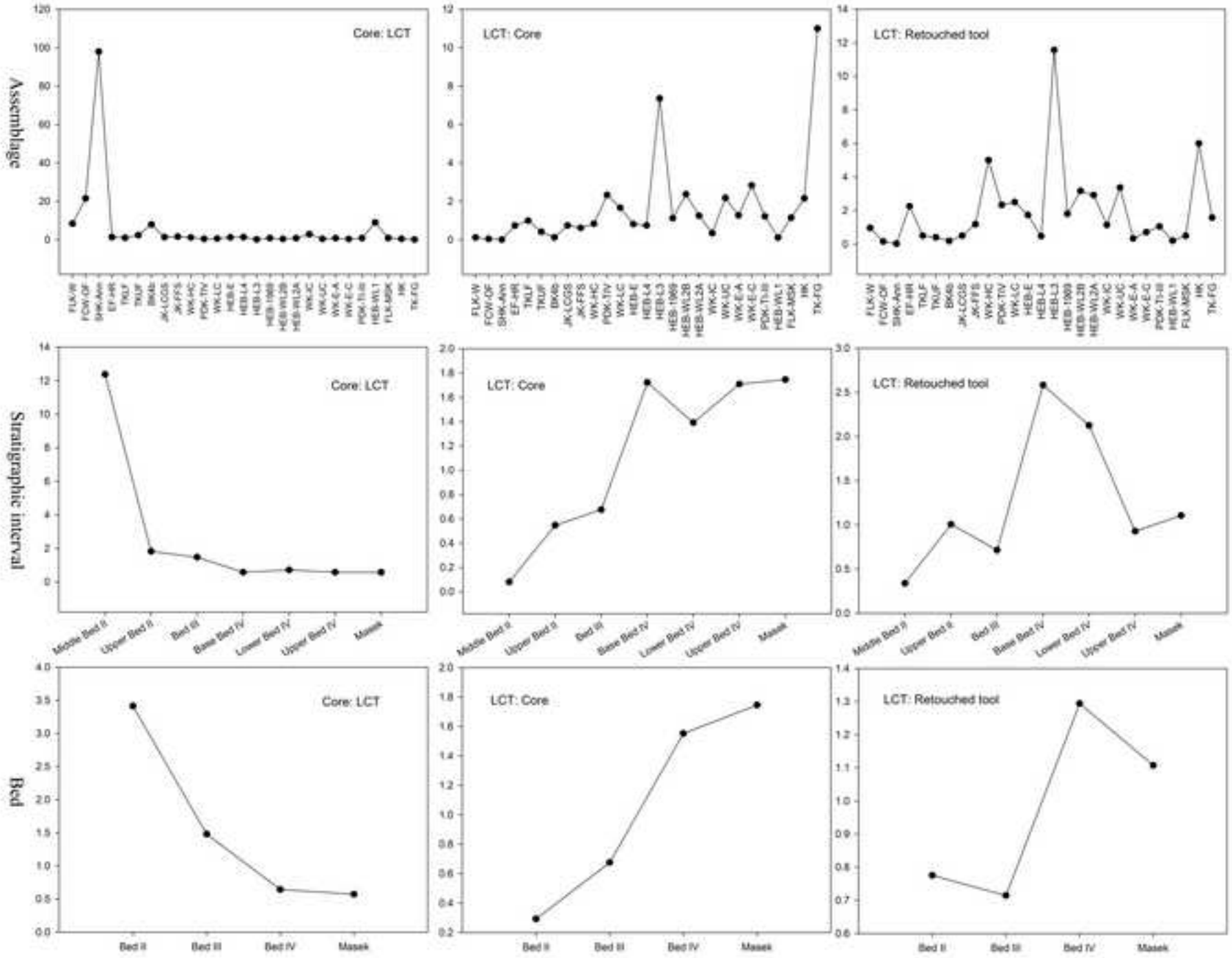

Supplementary Material

Click here to download Supplementary Material: Supplementary_Online_Material.pdf

Editorial Use: Not for Production

Click here to download Editorial Use: Not for Production: Figure_Instructions_for_Proofs.xlsx